Montana Tech Library
Digital Commons @ Montana Tech

Graduate Theses & Non-Theses | Student Scholarship

Summer 2019

INVESTIGATION OF THE TOPPLING OF RECTANGULAR RIGID BLOCKS USING A SHAKE TABLE AND DISTINCT ELEMENT MODELS

Sara Magallon

Follow this and additional works at: https://digitalcommons.mtech.edu/grad_rsch

 Part of the Geological Engineering Commons

INVESTIGATION OF THE TOPPLING OF RECTANGULAR RIGID BLOCKS USING A SHAKE TABLE AND DISTINCT ELEMENT MODELS

by

Sara Y. Magallón

A thesis submitted in partial fulfillment of the
requirements for the degree of

Master of Science in Geoscience:
Geological Engineering Option

Montana Tech
2019

Abstract

Understanding the engineering principles of failure modes in rock formations from seismic activity continues to be a challenging problem for engineers and geologists. The complexity of the geology, geometry, discontinuities, and earthquake ground motions contribute to the difficulty in estimating the stability of rock slopes. In this study, one classic rock slope failure mode is examined: the toppling behavior of a single rigid rectangular block under dynamic loading. An investigation employing experimental and numerical modeling techniques was performed to observe the response of wooden blocks with different aspect (width/height) ratios subjected to loading at the base and compared to established theoretical methods that use pseudostatic loads applied at the centroid. The physical experiments were conducted using a shake table with a data acquisition system consisting of accelerometers and a high-speed video camera. Because the shake table is a newly acquired research tool, a large component of the experimental program involved developing multiple calibration tests validated with mechanical engineering theory to verify the performance of the testing equipment and the experimental data. The link between the two loading scenarios (base and centroid) applied to the toppling block was accomplished using numerical modeling, with the simulations performed using Itasca's two-dimensional distinct element software UDEC. Results from the shake table and centroid loading scenario using UDEC matched theory. This study demonstrates the significance of understanding the fundamental rocking behavior of rigid blocks to better assess complicated toppling failures due to dynamic forces.

Keywords: shake table, distinct element models, rigid blocks, toppling, rocking motion, seismic, base excitations, rock slope, failure modes, dynamic loading, numerical modeling

Dedication

This thesis would not have been possible without the encouragement and support of a number of amazing faculty, staff, and other individuals. My thanks and appreciation goes out to all of them for being a part of this journey and making this thesis possible.

I am forever thankful to my friends, near and far, for their friendship, advice, and patience. Thank you for always listening to the good and bad, and reminding me it was all worth it. Your friendship makes my life a wonderful experience.

My deep and sincere gratitude goes to my family and best friends for their infinite and unparalleled love, help, and support. Thank you for understanding and accepting my crazy adventures. Every day I try to be a better human and become the role model my nieces and all young girls around the world deserve. I promise to keep trying, make noise, and brighten the path towards opportunity and equality.

Finally, I am forever indebted to my parents for selflessly giving me the opportunities and experiences that have made me who I am. This milestone would not have been possible without you, and I dedicate it to you. Gracias, Mami y Papi, “¡no me raje!”

“So often in life, things that you regard as an impediment turn out to be great, good fortune”
- Ruth Bader Ginsburg

Acknowledgements

Equipment and Research Funding:

- National Science Foundation (NSF) - 2014 Major Instrumentation Program (MRI): Acquisition of a Shake Table for Research on Seismic Stability of Rock Masses
- Montana Geological Society Scholarship
- Michael L. Condon Civil Engineering Scholarship, Deep Foundation Institute (DFI) Educational Fund
- Gary L. Grauberger Scholarship

I would like to sincerely thank my committee members:
Professor Mary MacLaughlin, Advisor, Geological Engineering
Professor Peter Lucon, Interim Department Head, Mechanical Engineering
Professor Larry Smith, Department Head, Geological Engineering

I would also like to extend my appreciation to:
Professor Josh Wold, Electrical Engineering
Steve Berry, GEOE Lab Technician
Scott Coguill, ME Lab Director
Nick Barney, Computer Support Specialist
Doug Weller, Shake Table Developer
Chris Clark, Software Developer
Donna Conrad, Administrative Associate
Electrical Engineering Senior Design Students: Chase Plum and Andrew Keele
Students: Marshall Metcalf, Thad Haines, Brent Sordo, and Garon Knudson

Table of Contents

ABSTRACT ..... **II**

DEDICATION ..... **III**

ACKNOWLEDGEMENTS ..... **IV**

LIST OF TABLES ..... **VII**

LIST OF FIGURES ..... **VIII**

LIST OF EQUATIONS ..... **XII**

1. INTRODUCTION 1
2. BACKGROUND: EARTHQUAKE GROUND MOTIONS & SEISMIC SLOPE STABILITY 4
   - *2.1. Earthquake Ground Motions* *4*
     - 2.1.1. Types of Seismic Waves 5
     - 2.1.2. Amplitude, Frequency, and Duration of Motion 5
   - *2.2. Effects of Geology on Ground Motions* *8*
   - *2.3. Failure Modes in Rock Slopes* *11*
   - *2.4. Development of Seismic Slope Stability Analysis* *13*
3. SHAKE TABLE OPERATION AND CALIBRATION 19
   - *3.1. Shake Table* *19*
   - *3.2. Shake Table Control Software* *21*
   - *3.3. Data Acquisition System and Accelerometers* *24*
   - *3.4. Shake Table Performance Testing and Calibration* *26*
     - 3.4.1. Voltage-Displacement Correlation 26
     - 3.4.2. Accelerometers, and Issues Identified 30
   - *3.5. Conclusions* *35*
4. TOPPLING BLOCK EXPERIMENTS & RESULTS 36

4.1. Toppling Block Analysis 36

4.2. Experimental Setup 38

4.3. Voltage Profiles 42

4.3.1. Sharp Step Profile 43

4.3.2. Parabolic Profile 44

4.3.3. Cycloidal Profile 46

4.4. Experiments 48

4.5. Data Processing 50

4.6. Results 52

5. Distinct Element Method Analysis and Results 54

5.1. Universal Distinct Element Code 54

5.2. Model Setup 57

5.3. Model Results 61

6. Conclusions and Recommendations 63

7. References Cited 65

8. Appendix A: Electrical Engineering Senior Design Report "Geological Engineering Shaker Table Characterization" 68

9. Appendix B: Accelerometer Specifications and Calibrations 82

10. Appendix C: PTC Mathcad and MATLAB Data 95

10.1. PTC Mathcad 95

10.2. MATLAB Script 99

11. Appendix D: Experimental Results Summary 104

12. Appendix E: Numerical Modeling Codes: UDEC & FISH functions 115

12.1. UDEC Model Setup 115

12.2. FISH Functions 121

13. Appendix F: Shake Table Standard Operation Procedure (SOP) 123

List of Tables

Table I: Rotational and translational quantities and relationship.....21

Table II: Voltage to displacement calibration.....29

Table III: Summary of block information.....39

Table IV: Calculated and experimental acceleration results.....52

Table V: UDEC results summary using loading scenario 1 (a and b).....62

Table VI: Observations during Block 2 testing 105

Table VII: Observations during Block 3 testing.....109

Table VIII: Observations during Block 4 testing.....112

List of Figures

Figure 1: Slope stability analysis: a. pseudostatic analysis, b. finite element modeling, c. permanent-displacement analysis (Jibson, 2011) 1

Figure 2: Types of seismic waves in earthquake ground motions ("Which seismic wave is the most dangerous? Why?," 2018).....5

Figure 3: General form of simple harmonic displacement function (Kramer, 1996) 6

Figure 4: Relation between acceleration, velocity, and displacement vs. time of strong ground motion data from El Centro, California earthquake on May 18, 1940 (Newmark, 1965) 8

Figure 5: East-west geologic profile showing variation between hard and soft/loose formations of the basin of Mexico City (Seed et al., 1987).....9

Figure 6: Failure modes of intact, discontinuous, and combination of both in rock slopes (Aydan, 2017) 12

Figure 7: Simplified rock slope failures: a. plane sliding; b. wedge sliding; and c. toppling (Hoek & Bray, 1981) 12

Figure 8: Dynamics of a single rocking block: sliding, toppling, and combination of both12

Figure 9: Diagram of rocking rigid block (Housner, 1963).....14

Figure 10: Kinematic conditions for toppling and sliding in base friction models (Bray & Goodman, 1981) 16

Figure 11: Modified kinematic chart for toppling and sliding (after Yeung, 1991).....16

Figure 12: Shake table and labeled components.....20

Figure 13: Relationship between rotational and translational properties ("College Physics," 2019) 21

Figure 14: LabVIEW software graphical user interface, test execution screen (main screen) 22

Figure 15: LabVIEW software graphical user interface, configuration screen 22

Figure 16: Relationship between acceleration, velocity, and position vs. time (Nave, 1998) 24

Figure 17: Dytran accelerometers used on shake table and blocks: series 3202 (left), series 3166 (middle), and series 3055 (right) (Dytran, 2019).....25

Figure 18: Diagram of IEPE accelerometer (National Instruments, 2019) 26

Figure 19: Hand sketch of shake table with physically measured parts for PTC Mathcad model 28

Figure 20: Portion of code and diagram of the PTC Mathcad model.....28

Figure 21: Oscilloscope (left) and function generator (right) used for calibrations 29

Figure 22: Idle system where the spikes are the reduced arbitrary noise 30

Figure 23: Low frequency response for single-axis, 3055 series IEPE accelerometer (Dytran, 2019) 31

Figure 24: Comparison between vibration profile and accelerometer response to profiles of 2, 3, and 10 Hz (left to right) 32

Figure 25: Custom built aluminum bracket used to mount multiple accelerometers at once on shake table.....32

Figure 26: Non-smooth behavior of shake table motion during dynamic profile recorded with 3166 accelerometers.....33

Figure 27: Example of free-body diagram for block on horizontal plane 37

Figure 28: Rectangular prismatic wooden blocks used for experiments 39

Figure 29: Experimental block setup on shake table 40

Figure 30: Progression of accelerometer configuration on blocks for experimental tests.41

Figure 31: Accelerometer configuration on blocks 42

Figure 32: 3055 and 3056 series Dytran accelerometers (“Dytran,” 2019).....42

Figure 33: Voltage profile for step function showing instantaneous application of voltage (displacement) with gradual unloading.....43

Figure 34: LabVIEW real-time plot of step function on Block 4 with four 3166 accelerometers mounted on the shake table and one 3055 accelerometer mounted on the block..44

Figure 35: LabVIEW real-time plot of parabolic function on Block 3, where input voltage is white and measured table accelerations are in color.....46

Figure 36: Cycloidal rise motion; displacement, velocity, and acceleration with corresponding equations (Myszka, 2012).....47

Figure 37: LabVIEW real-time plot of cycloidal function on Block 3, where input voltage is white and measured table accelerations are in color.....48

Figure 38: Voltage profile used on the shake table from cycloidal equations.....49

Figure 39: Displacement profile derived from cycloidal equations used to convert to voltage 49

Figure 40: Velocity profile derived from cycloidal equations.....50

Figure 41: Acceleration profile derived from cycloidal equations 50

Figure 42: Identifying start of vibration profile when LED light goes from on to off from images recorded by high-speed camera 51

Figure 43: Identifying the onset toppling acceleration from images recorded by high-speed camera 51

Figure 44: Examples of rigid/discontinuous (left) and deformable/continuous (right) blocks (Itasca, 2019; Bagi, 2012;).....55

Figure 45: Corner and edge interactions of blocks in UDEC (Itasca, 2019) 56

Figure 46: Rounding of corners of blocks in UDEC (Bagi, 2012) 56

Figure 47: Explicit solution flow chart for rigid blocks in UDEC (Thoraval, 1991) 58

Figure 48: General UDEC model setup indicating two loading scenarios 59

Figure 49: Velocity profile of loading scenario 1a, centroid loading of the block with applied force command.....62

List of Equations

Equation (1) 6

Equation (2) 6

Equation (3) 6

Equation (4) 37

Equation (5) 37

Equation (6) 38

Equation (7) 47

Equation (8) 47

Equation (9) 47

1. Introduction

Evaluating the stability of a rock slope often requires dissecting the problem into fundamental concepts. Determining the type of rock failure, whether plane sliding, wedge sliding, or toppling, allows for the application of proper analysis methods. Under static conditions, the stability of rock slopes is better understood and a variety of analysis methods are available such as rock mass classification, stereonets, kinematic analysis, and limit equilibrium-based equations.

The behavior of rock slopes under seismic loading is more complicated and less well understood. The stability of a rock slope depends on but is not limited to the rock type, geometry, discontinuities, weathering, groundwater, surcharge conditions, and dynamic loading. These conditions may be present simply and uniformly, or there may be complex settings depending on the heterogeneity of the rock slope. Methods for assessing slope stability or performance during earthquakes have evolved steadily since the early twentieth century, and generally fall into three categories: 1. pseudostatic analysis (Terzaghi, 1950); 2. finite element and finite difference modeling, a type of stress-deformation analysis (Clough, 1960; Clough and Chopra, 1966); and 3. permanent-displacement analysis (Newmark, 1965). Figure 1 contains an example for each category introduced. For sliding, the pseudostatic (rigid block) analysis method is oversimplified for the intricacies in rock slope stability, but it is a good

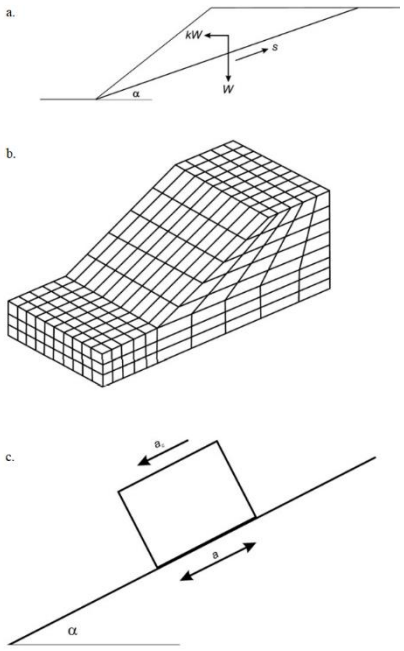

Figure 1: Slope stability analysis: a. pseudostatic analysis, b. finite element modeling, c. permanent-displacement analysis (Jibson, 2011)

starting point when other information is lacking. Naturally, with the practice of any analysis method, each of these techniques has their advantages and limitations depending on slope conditions and application requirements.

For seismically induced toppling failures, the most fundamental and highly studied concept is that of a freestanding rigid block resting on a perfectly rigid horizontal plane, subjected to an idealized ground acceleration acting parallel to the plane. Early references cited in the literature date back to 1885. Using examples of inverted pendulums, Housner (1963) was able to derive a systematic analytical approach to the study of the rocking response of a rigid body. Owing to the highly nonlinear nature of the problem, due to frictional forces and block impact with the base, a variety of rocking response modes can exist even when the input excitation is relatively simple (Tso & Wong, 1989). Before instrumentation had been developed to record strong ground motions, procedures were proposed to estimate the intensity of ground shaking from its observed effects on tombstones and monumental columns, whether they overturned or remained standing (Yim et al., 1980). The most common procedure used to estimate the "seismic intensity" at a site, derived from the equations of statics, is to assume that the peak acceleration was larger than the breadth-height ratio of an overturned body multiplied by the gravitational acceleration (Ishiyama, 1980).

Considering the various characteristics and scenarios that contribute to rock slope instabilities and methods to analyze them, it becomes easy to overlook the fundamental behavior. The purpose of this study is to investigate and verify the basic principles of the toppling behavior of a rigid block. Therefore, a basic example of a rigid block on a flat surface is used to estimate the magnitude of the onset toppling acceleration required to initiate toppling.

A simple experimental test plan modeled after the classical overturned tombstone and peak ground acceleration relationship was created consisting of three wooden blocks of known dimensions and mass. The blocks were individually placed on a unidirectional shake table and a range of accelerations, in the form of a pulse, were applied. The range of onset toppling accelerations for each block was identified using accelerometers mounted on the shake table, and a high-speed camera recorded images and video of the experiments. Data from the instrumentation were sent to a data acquisition system (DAQ) and was processed using a MATLAB script developed specifically for the project. The range of accelerations obtained from the shake table experiments was compared to pseudostatic accelerations derived from static equilibrium force and moment equations. In a parallel component of the study, block information was used to develop models using the two-dimensional, 6.0 version of the Universal Distinct Element Code (UDEC). Finally, experimental and numerical results of the onset toppling accelerations obtain from each methodology were compared and discussed.

The purpose of this study is twofold: 1. to investigate the range of the onset toppling acceleration of a rigid block starting at rest experimentally using a shake table and numerically using distinct element methods (DEM); and 2. to quantitatively compare two loading scenarios, one applied at the base of the block representing realistic earthquake base excitations and the other corresponding to traditional slope stability analysis with centroid loading. It is anticipated that the results of this study will allow engineers and geologists to be more confident regarding the results obtained from various slope stability analyses. The combination of analytical, experimental, and professional judgment with the understanding of complex geology provides a framework in which all of the most critical factors can be accounted for in earthquake engineering designs.

2. Background: Earthquake Ground Motions & Seismic Slope Stability

The earliest earthquake for which descriptive information was collected occurred in China in 1177 B.C., while Europeans mentioned them as early as 580 B.C. (USGS, 2019). Even though earthquake phenomena had been established, it was not until the mid 19th century that the roles of soil or rock type were considered in terms of their contribution to the magnitude and pattern of ground motions. Following damaging earthquakes in the early 1960's and the increasing development of slope stability analysis, the field of geotechnical earthquake engineering grew rapidly. Although much remains to be learned and understood, the field has matured to the point where generally accepted theories and analytical procedures now exist for many important problems (Kramer, 1996). Additionally, with high quality instrumentation, the recording of strong earthquake ground motion provides the basic data for earthquake engineering and the growing database has facilitated development of appropriate methods of rational hazard assessment and seismic design (National Research Council, 1982).

To understand the conceptually simple problem of rigid block motion, more than just the analytical derivation needs to be explored. This chapter begins with a short overview of earthquake ground motions and the effects of geology on ground motions. It then briefly summarizes the development of seismic slope stability analysis focusing on the toppling mode of failure.

2.1. Earthquake Ground Motions

Ground motions produced by earthquakes are erratic and can be difficult to characterize. They are propagating vibrations that carry energy from the source of the shaking outward in all directions. To simplify analysis, the vibrations are often represented as harmonic waves. For

engineering purposes, three characteristics of earthquake motion are of primary significance: 1. amplitude, 2. frequency content, and 3. duration of the motion (Kramer, 1996).

2.1.1. Types of Seismic Waves

Earthquakes radiate seismic energy as both body and surface waves. Traveling through the interior of the earth, body waves arrive before the surface waves. Body waves are of a higher frequency and are classified as either compressional (P-waves) or transverse shear (S-waves). Surface waves, known as Love and Rayleigh waves, are of a lower frequency. Figure 2 shows the characteristics of all four seismic waves; note that S-waves can have both vertical and horizontal components.

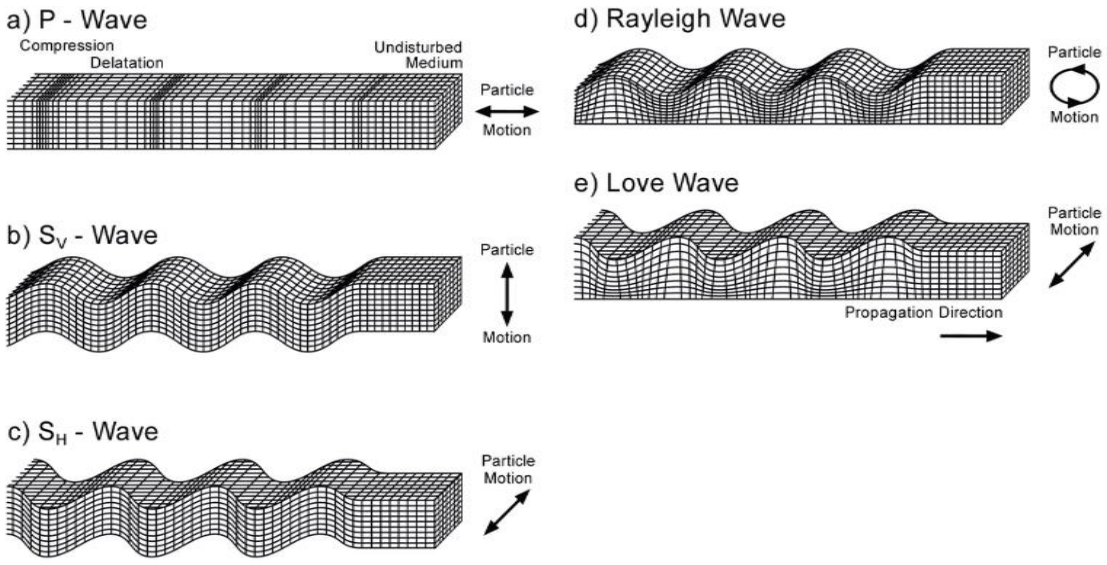

Figure 2: Types of seismic waves in earthquake ground motions
("Which seismic wave is the most dangerous? Why?," 2018)

2.1.2. Amplitude, Frequency, and Duration of Motion

Earthquake ground motions are multifaceted and there is not a single parameter that can be used to characterize them. The ground motion is often represented as a simple harmonic function as shown in Figure 3. Kramer (1996) shows that by differentiating the function of a

simple harmonic displacement equation (Eqn. 1) once and twice with respect to time, both velocity (Eqn. 2) and acceleration (Eqn. 3) expressions can be produced.

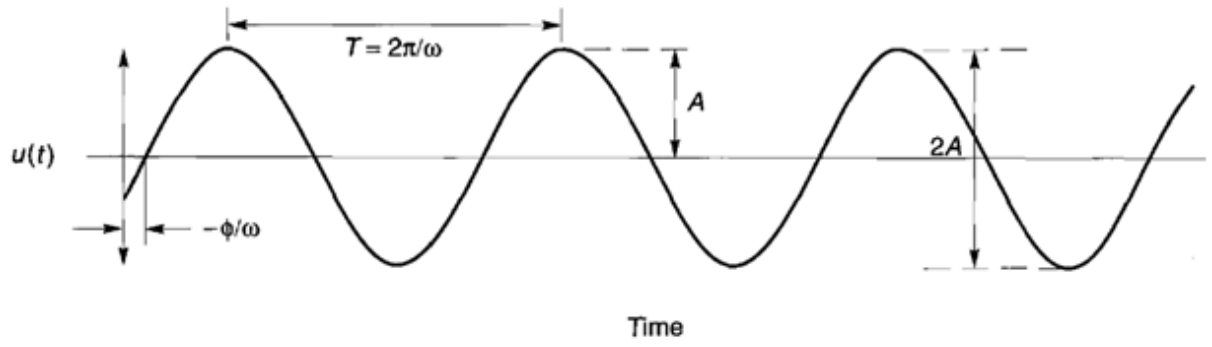

Figure 3: General form of simple harmonic displacement function (Kramer, 1996)

$$\mathrm{u}(t) = A\sin(\omega t + \varphi) \quad \textbf{(1)}$$

$$\dot{\mathrm{u}}(t) = \frac{du}{dt} = \omega A\cos(\omega t + \varphi) \quad \textbf{(2)}$$

$$\ddot{\mathrm{u}}(t) = \frac{d^2u}{dt^2} = -\omega^2 A\sin(\omega t + \varphi) = -\omega^2 u \quad \textbf{(3)}$$

where A is amplitude, T is the period, 1/T is the frequency, ω is the circular frequency, t is time, and φ is the phase angle. Similarly, u̇ and u may be derived from acceleration time histories by integrating.

The peak horizontal acceleration (PHA) is the most commonly used measure of the amplitude of a particular ground motion. The PHA for a given component of motion is simply the largest (absolute) value of horizontal acceleration obtained from the accelerogram of that component (Kramer, 1996). Vertical accelerations have received less attention in earthquake engineering than horizontal accelerations, primarily because the margins of safety against gravity-induced static vertical forces in constructed works usually provide adequate resistance to dynamic forces induced by vertical accelerations during earthquakes (Kramer, 1996).

Regardless, a general rule of thumb has been used where the peak vertical acceleration (PVA) is assumed to be two-thirds of the PHA (Newmark & Hall, 1982).

Earthquakes produce complicated vibrations with components of motion that span a broad range of frequencies. Frequency is defined as the number of occurrences of a repeating event per unit of time. As seismic waves travel away from a fault, their higher-frequency components are scattered and absorbed more rapidly than are their lower-frequency components (Vallejo & Ferrer, 2011). This also means that the frequency content changes with distance. Additionally, frequencies may change pending on the soil or rock type present, as described in Section 2.2.

Figure 4 shows the strong motion record for the north-south component data from the May 18, 1940, earthquake in El Centro, California. The acceleration data shown in part “a” was obtained from a strong motion accelerograph and the velocity and displacement profiles were derived through integration. The El Centro record is typical of a nearly periodic response of moderately low intensity combined with one very large displacement peak. It is noted that the highest intensity peaks of acceleration have a relatively short period or a relatively high frequency. The most important peaks in the velocity, however, have a longer period, which corresponds to a lower frequency, and the important peaks in the ground displacement have an even longer period (Newmark, 1965).

The duration of strong ground motion increases with increasing earthquake magnitude and decreases with distance from the source. The total duration and the total number of ‘spikes’ or peaks of velocity, and the reversals of velocity, are of importance in determining the response of a structure (Newmark, 1965).

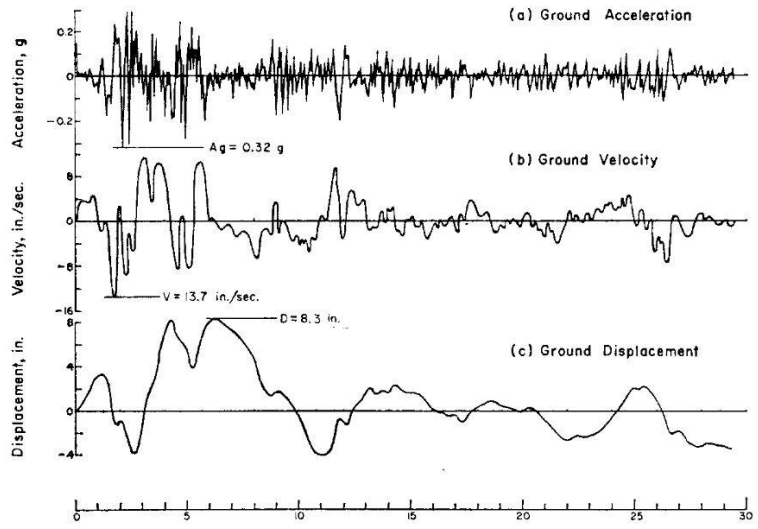

Figure 4: Relation between acceleration, velocity, and displacement vs. time of strong ground motion data from El Centro, California earthquake on May 18, 1940 (Newmark, 1965)

2.2. Effects of Geology on Ground Motions

Soil and rock conditions significantly contribute to the overall behavior of earthquake ground motions. Because heterogeneity and homogeneity of surrounding geology in a seismically active area can vary in small or large scales, it can be challenging to characterize a single site based on regional seismic hazard maps. Earthquakes generate larger shear waves than compressional waves and much of the damage close to an earthquake is the result of strong shaking caused by shear waves. Understanding the physical properties of geologic materials present at a site, particularly their shear strength, along with the surrounding geology, the response to earthquake ground motions can be better anticipated and incorporated into designs.

The strength and duration of ground shaking depends on the magnitude and location of the earthquake and physical characteristics of the site. Soil deposits tend to act as "filters" to seismic waves by attenuating motion at certain frequencies and amplifying it at others (Gohil, Solanki, & Desai, 2010). Since soil conditions have the potential to vary dramatically, both vertically and laterally, levels of ground shaking can also vary significantly. Common

failures associated with ground shaking in areas with soil include liquefaction, lateral spreading, settlement, piping, and landslides.

One of the most critical geologic conditions existing at some sites is a relatively soft sedimentary deposit with large thickness and lateral extents. When such a soil deposit is set in motion at its contact with bedrock, there is a tendency for the resultant motions of the soil to reflect the natural frequency of the sedimentary basin. This has the effect of increasing the magnitude of surface displacements and velocities, and would likely generate a larger ground motion than solid bedrock (Newmark, 1965). An example of such a geologic effect exists in Mexico City and was most notably seen on September 19, 1985, when a moment magnitude 8.0 earthquake struck the region. Figure 5 shows that the western part of Mexico City is underlain by rock and hard soil deposits, while the eastern part of the city is underlain by soft clay, silt, and sand filling the former lake bed (Seed, Idriss, & Dezfulian, 1987). The most damage occurred in regions of soft clay with great depths, damaging structures with heights ranging from 6 to 18 stories whose natural period resonated with the amplified long period waves.

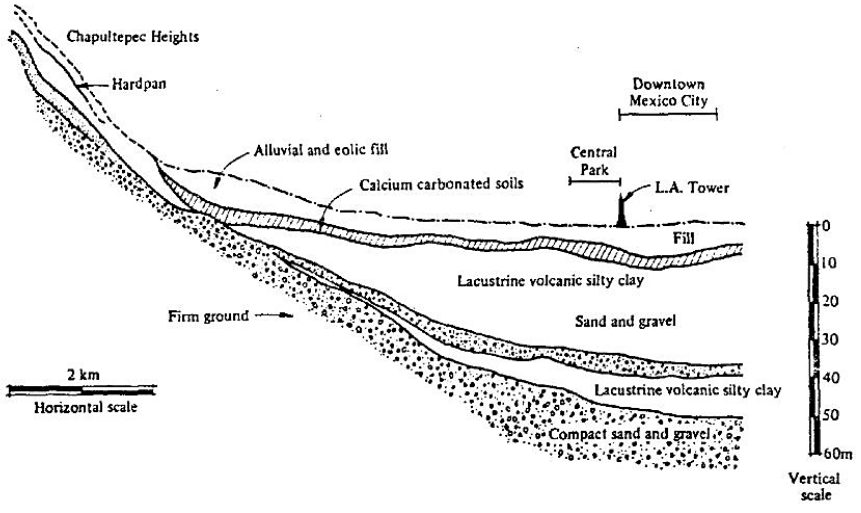

Figure 5: East-west geologic profile showing variation between hard and soft/loose formations of the basin of Mexico City (Seed et al., 1987)

Weak ground shaking typically initiates four types of internally disrupted landslides: rock falls, rock slides, soil falls, and disrupted soil slides. Stronger shaking impacts more coherent, deeper-seated slides, while shaking that is still stronger induces lateral spreads and flows. The strongest shaking is probably required for very highly disrupted rock avalanches and soil avalanches (Keefer, 1984).

Data from 40 historical worldwide earthquakes were studied to determine the characteristics, geologic environments, and hazards of landslides caused by seismic events (Keefer, 1984). This sample of 40 events was supplemented with intensity data from several hundred United States earthquakes to study relations between landslide distribution and seismic parameters. The most abundant of these were rock falls, disrupted soil slides, and rock slides. The greatest losses of human life were due to rock avalanches, rapid soil flows, and rock falls (Keefer, 1984).

There is much more information regarding the response of soil during earthquakes than the response of rock material. But similarly to soils, rock slope dynamic responses are affected by geomechanical parameters, seismic parameters and slope geometry. Young's modulus (E), Poisson's ratio (ν) and density (ρ) are the basic elastic material parameters that contribute to the behavior of intact rock during an earthquake. For instance, very solid granites will transmit energy better than highly weathered and soft rocks found in fault zones. Energy and high frequencies are dissipated when traveling through soft rock (USGS, 2019). Heavily fractured and jointed rock masses also absorb earthquake energy.

2.3. Failure Modes in Rock Slopes

Goodman and Kieffer (2000) describe a long but not exhaustive list of common failure styles, highlighting observable characteristics that distinguish one from another. The variety of geological materials and discontinuities present in rock masses lead to a corresponding variety of failure modes (as shown in Figure 6) but they generally are classified into several simplified categories: plane sliding, wedge sliding, or toppling failures (as shown in Figure 7). Block sliding and toppling is analyzed by studying the equilibrium conditions for each block in the slope. More complex cases cannot be represented by simple models and cannot be analyzed with limit equilibrium methods (Vallejo & Ferrer, 2011). For dynamic loads, even the simple case of a single block can display sliding, toppling, or a combination of sliding and toppling, as shown in Figure 8, and sustained back-and-forth rocking can also be observed. Most of the studies performed on rock slopes have been completed under static conditions, therefore, there is a gap in research regarding the dynamic response of blocky, rock slopes.

Typically, toppling occurs when geologic formations create columns through regular bedding planes, cleavage, or joints that strike parallel to the slope crest and dip into the rock mass (Goodman & Bray, 1976). These types of characteristics commonly occur in slates and schists, in steeply dipping thin-bedded sediments, in columnar-jointed volcanics, and in regularly-jointed granitics. Toppling mode of failure was not recognized until the 1960's and has been less studies than plane and wedge sliding. Goodman and Bray (1976) and Hoek and Bray (1981) developed an analytical method for straightforward cases and for slopes with schematic blocks. Although rock slope toppling does not usually produce high velocities, like some rock slides, if uncontrolled, retrogressive failure can encompass a large volume of rock, with deep tension cracks and considerable rock breakage (Goodman & Bray, 1976).

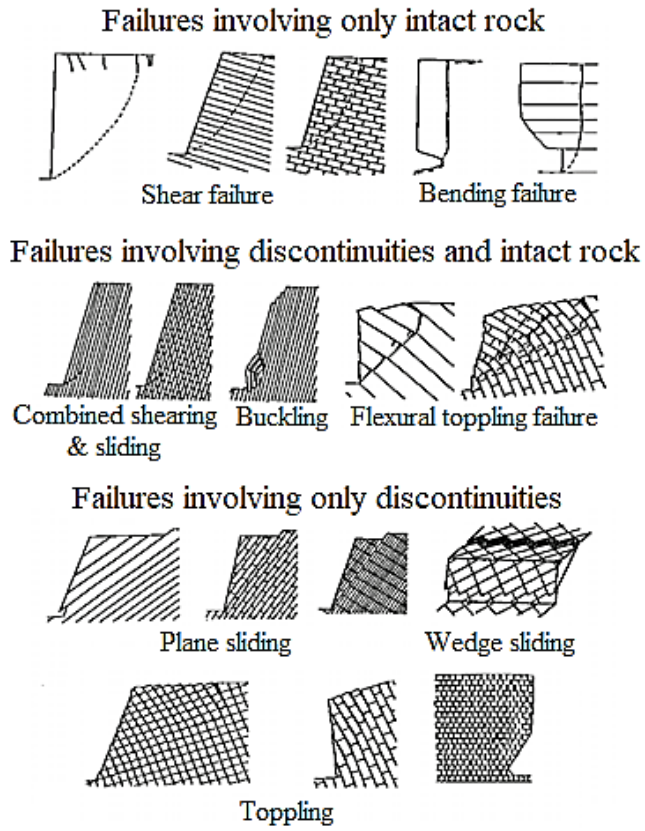

Figure 6: Failure modes of intact, discontinuous, and combination of both in rock slopes (Aydan, 2017)

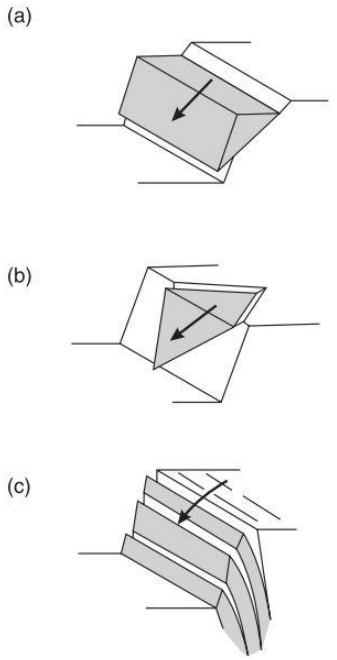

Figure 7: Simplified rock slope failures: a. plane sliding; b. wedge sliding; and c. toppling
(Hoek & Bray, 1981)

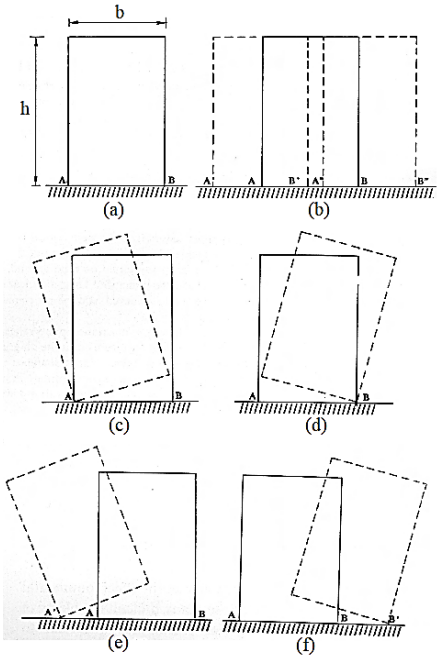

Figure 8: Dynamics of a single rocking block: sliding, toppling, and combination of both
(Augusti & Sinopoli, 1992)

2.4. Development of Seismic Slope Stability Analysis

Methods for assessing seismic slope stability or performance during earthquakes have evolved since the early twentieth century, and generally fall into three categories. The earliest and first category is the pseudostatic analysis for soil, rock, and structures (Terzaghi, 1950). It has been implemented in standard limit equilibrium-based analysis software such as SLIDE and SLOPE/W for its straightforward approach in modeling the seismic shaking as a permanent body force that is added to the force-diagram of a conventional static limit equilibrium analysis. The second category is fully dynamic stress-deformation analysis accomplished with finite element (FE) and finite difference (FD) modeling that is applicable for soil, rock, and structures (Clough, 1960; Clough and Chopra, 1966). It uses a mesh to model deformable systems and requires a high density of high-quality data and sophisticated soil-constitutive models to predict the stress-strain behavior of the model. DEM methods are newer methods typically used for rock material. The third and final category is the permanent-displacement analysis for soil and rock that models a landslide as a rigid block that slides on an inclined plane (Newmark, 1965). The block has a known yield or critical acceleration, which is the acceleration, required to overcome base resistance and initiate sliding, and the permanent displacement is the sum of the displacement increments that occur during segments of the ground shaking that exceed the critical acceleration.

Traditional seismic analyses, whether for toppling or sliding, include seismic coefficients for pseudostatic slope analysis and are used to account for the destabilizing effects of seismic forces that must be resisted by the slope (Melo & Sharma, 2004). The concept of transforming dynamic motion to a pseudostatic constant horizontal acceleration that initiates rocking overshadows the idea that the dynamic behavior of the earthquake can actually assist in stabilizing tall slender blocks (Housner, 1963). The traditional rocking block analysis has also

shown an unexpected scaling effect, which makes larger of two geometrically similar blocks more stable than the smaller block (Housner, 1963). Therefore, it is important to not only use the rigid block analysis, but also implement other analysis methods that account for the dynamic earthquake contribution towards loads that may destabilize a stable slope or vice versa.

Figure 9 contains a diagram of the rocking response of a rigid block. The rigid block is characterized by its weight, W, and its moment of inertia about the pivoting point, I_0. The location of the mass center of the block with respect to the pivotal base points, 0 and 0', is defined by the distance $R = \sqrt{h^2 + b^2}$, and the angle α. The displaced position of the block from its equilibrium position and measured from the horizontal base is represented by the angle θ (Housner, 1963; Tso & Wong, 1989).

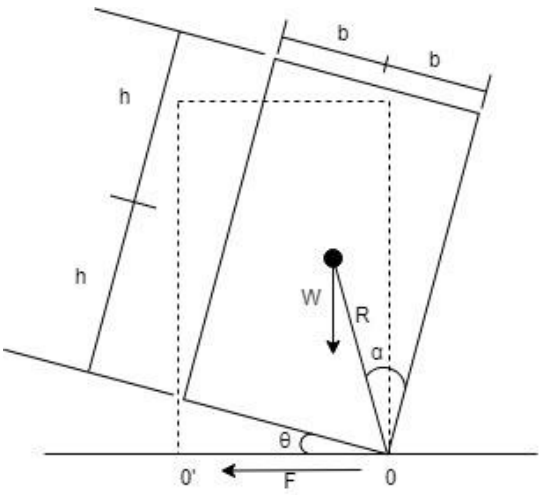

Figure 9: Diagram of rocking rigid block (Housner, 1963)

The derivations of the equations of a rocking block were made assuming no energy loss, but during real rock motion, a dissipation of energy occurs at the base. Housner (1963) made further derivations taking into account the incremental decrease in the energy of vibration. He concluded that for large amplitudes, the energy of vibration decreases rapidly, but for small oscillations, the energy decreases slowly. Furthermore, Housner (1963) realized that smaller

accelerations than are specified by the equations he derived may set the block to rocking but will not overturn it. However, it is possible to overturn the block with smaller accelerations if a number of pulses act successively. This is the case of earthquake ground accelerations, which tend to have short periods compared to the rocking periods of structures. Overall, his research demonstrated that there is an unexpected scaling effect, which makes the larger of two geometrically similar blocks more stable than the smaller block. It was also shown that the stability of a tall slender block subjected to earthquake motion is much greater than would be inferred from its stability against a constant horizontal force. After Housner's initial investigation of the rocking behavior of rigid blocks due to seismic loading, research on rock toppling behaviors increased.

In 1971, Cundall developed the distinct element method, introduced the two-dimensional Universal Distinct Element Code (UDEC), and provided the numerical modeling platform to replicate slope stability models. It was intended to simulate the behavior of fractured rocks around tunnels, excavations, landslides, and was the first member of a family of methods later given the name "discrete element methods". The software uses deformable contacts and an explicit, time-domain solution of the original equations of motion, further described in Chapter 5 (Itasca, 2019).

In 1980, Yim, Chopra, and Penzien investigated the rocking response of rigid blocks subjected to earthquake ground motions and developed numerical and computational procedures to solve the nonlinear equations of motion governing the rocking motion of the blocks. Their results found that the response of the block is very sensitive to small changes in its size and slenderness ratio and ground motion. A larger ground motion intensity than that required to overturn a block does not necessarily mean that that same block will overturn.

In 1981, Bray and Goodman developed the base friction principle, which permits the replacement of gravity in the plane of a two-dimensional physical model by drag forces acting along its base. Using the example of a rigid block on an incline plane, they adjusted a chart showing the kinematic conditions governing the modes of behavior of the block that had previously been derived by Ashby (1971). Figure 10 shows an example of the conditions for sliding and toppling of a block on a horizontal plane where the y-axis is the aspect ratio δ (b/h) of the block and the x-axis is the dip angle α of the inclined surface. Even if the block is on a horizontal plane, the relationship between the friction angle φ, aspect ratio, and inclination allows the chart to work because $\delta = \Delta x/\Delta y = \tan^{-1}(b/h)$ and $\alpha = \tan^{-1}(b/h)$. When $\delta < \tan \alpha$ the center of gravity of the block will lie beyond the pivot point and toppling about this point will occur (Ashby, 1971). Although a useful tool at the time, base friction models are constant velocity, and are not a good representation of real conditions in slopes subjected to constant acceleration (gravity). The chart was later adjusted by others (Sagaseta, 1986; Aydan et al., 1989; Yeung, 1991) to fully account for dynamics and block acceleration, shown in Figure 11.

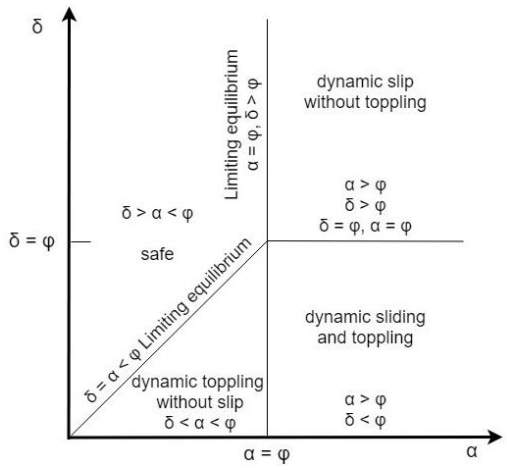

Figure 10: Kinematic conditions for toppling and sliding in base friction models
(Bray & Goodman, 1981)

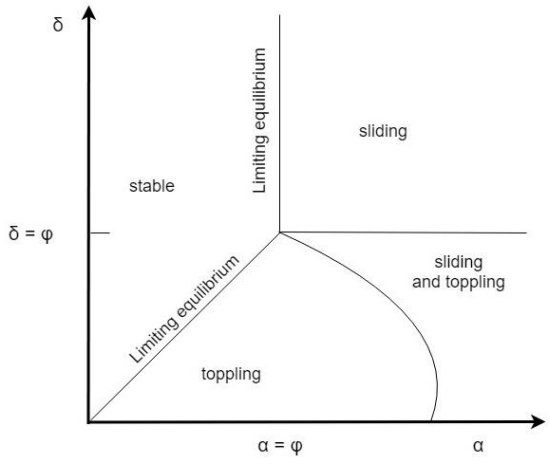

Figure 11: Modified kinematic chart for toppling and sliding (after Yeung, 1991)

Seismic slope stability analysis developed from the basic aim of estimating a minimum and maximum level of ground shaking intensities required to effect the stability of freestanding, slender bodies during strong earthquakes. Despite the apparent simplicity of the problem, tackling analytically the equations of motion, even for simple waveforms, was not an easy task due to the nonlinear geometric effects, the non-conservative nature of the impact, and the exponential character of the response functions (Voyagaki et al., 2013).

Since the early 1980's, with the improvement of numerical modeling software and numerous studies that continued analyzing the response of rigid blocks under dynamic earthquake loading, the once thought to be simple problem remains of interest. As Terzaghi recognized in 1950, the pseudostatic approach is a crude representation of the complex, transient, dynamic effects of earthquake shaking by a single constant unidirectional pseudostatic acceleration (Kramer, 1996). Therefore, it is common for researchers to use a combination of experimental and numerical models in order to develop better conclusions regarding the over or under conservatism of traditional slope stability analysis methods for various scenarios. Updated experimental equipment, such as elaborate shake tables, accelerometers, high-speed cameras, lasers, and Linear Variable Differential Transformer (LVDT) sensors, to name a few, are readily available to improve existing research or investigate various problems that have not been feasible.

The design of the project described in this thesis was prompted from one parametric study which showed that steady rocking response amplitude is highly sensitive to the size of the block and the excitation frequency in the low frequency range (Wong & Tso, 1989). Thus, low frequency base excitations were applied to three different sized wooden blocks. The goal was to observe the block behavior and have a better understanding of the lowest range of acceleration

required to ensue initial signs of block instability and develop conclusions regarding the difference between loading at the base and the centroid. The following chapters explain the equipment used, experimental procedures, numerical models, and results.

3. Shake Table Operation and Calibration

The shake table at Montana Tech is a custom-built system with a broad scope of requirements. The general specifications of the shake table were to have the capability to produce vibration oscillations from frequencies of 0 – 20 Hz, with a maximum frequency response between 35 – 40 Hz, and be able to carry a maximum load of approximately 2,000 lbs. The shake table is driven with a custom LabVIEW software called *MT Earthquake Monitor and National Instruments (NI) hardware* data acquisition system (DAQ) that sends a user-defined voltage profile to the shake table motor controller, initiates high-speed camera recording, receives instrumentation data through the DAQ, and produces multiple types of data files saved onto the workstation. This chapter contains descriptions of: 1. initial conditions of the shake table equipment, software, DAQ, and accelerometers; 2. shake table performance testing and calibration procedures that were designed and implemented; and 3. issues that were identified and mitigated.

3.1. Shake Table

The shake table was custom designed and built for Montana Tech. A Synchronous Servo Torque Motor connected to a crank arm using a Polytetrafluoroethylene (PTFE) ball joint swivel drives the shake table. The crank arm is attached to a table rod, which is linked to an aluminum 3-foot by 5-foot by 1-inch-thick table with linear bearings mounted on a steel frame. The motion of the table is unidirectional (north-south) and purely translational in the horizontal direction. All motions of the shake table were recorded using single-axis Dytran accelerometers and a high-speed camera. Figure 12 shows the shake table, servo motor, cooling system, high-speed camera, breaker panel, and control panel.

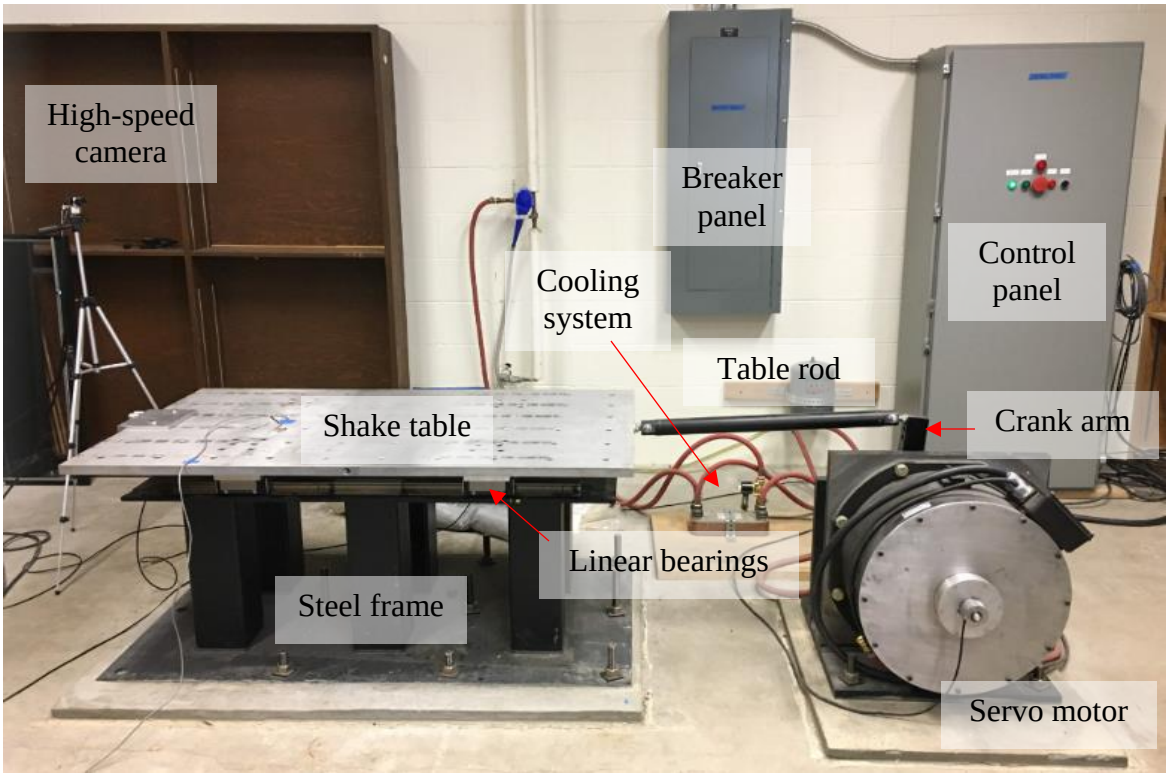

Figure 12: Shake table and labeled components

The displacement of the shake table is directly correlated to the analog voltage inputs (+/- 10 V) to the shake table system. According to the manufacturer, the maximum load rating for the table is 2,000 pounds and the stroke length of the motor arm is +/- 6 inches (which corresponds to +/- 22° on the crank arm). Note that linear and angular accelerations are directly proportional and the shake table uses a voltage input to create linear displacement. Figure 13 and Table I show the relationship between rotational and translational quantities associated with motion along an arc. Note that the tangential acceleration a_t is associated with the change in magnitude of velocity, but not its direction. Also note that the translational motion of the shake table is more complicated because it is connected to the rotating motor arm with mechanical components.

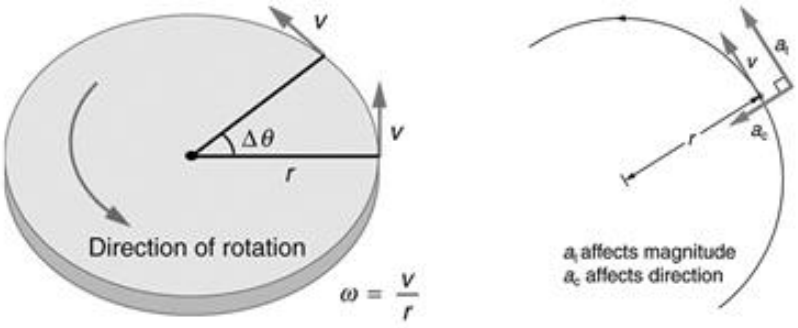

Figure 13: Relationship between rotational and translational properties ("College Physics," 2019)

Table I: Rotational and translational quantities and relationship

Rotational	Translational	Relationship
Angle of rotation, θ	Displacement, x	θ = x/r
Angular velocity, ω	Velocity, v	ω = v/r
Angular acceleration, α	Acceleration, a	α = a_t/r

where: r = radius of curvature, a_t = tangential acceleration

3.2. Shake Table Control Software

The shake table is operated by executing a computer program called *MT Earthquake Monitor*, specifically designed for the equipment. The software was developed using the visual programming language Laboratory Virtual Instrument Engineering Workbench (LabVIEW) and a multifunction I/O device (PCI-6229) from National Instruments. "LabVIEW is a systems engineering software for applications that require test, measurement, and control with rapid access to hardware and data insights" (National Instruments, 2019). "The PCI-6229 provides a combination of analog I/O, digital I/O, and counter/timer functionality in a single device for computer-based systems" (National Instruments, 2019).

The *MT Earthquake Monitor* software outputs an arbitrary waveform on one analog output (AO) channel to the shake table system, acquires up to 32 channels of input (AI) data at

800 samples per second (sps) on the DAQ, and acquires images at 340 frames per second (fps) with a high-speed Basler camera. The shake table system's design functionality involves outputting, configuring, and acquiring data, logging data to disk, and displaying data (Clark, 2016). Figures 14 and 15 show the graphical user interfaces (GUIs) of the software.

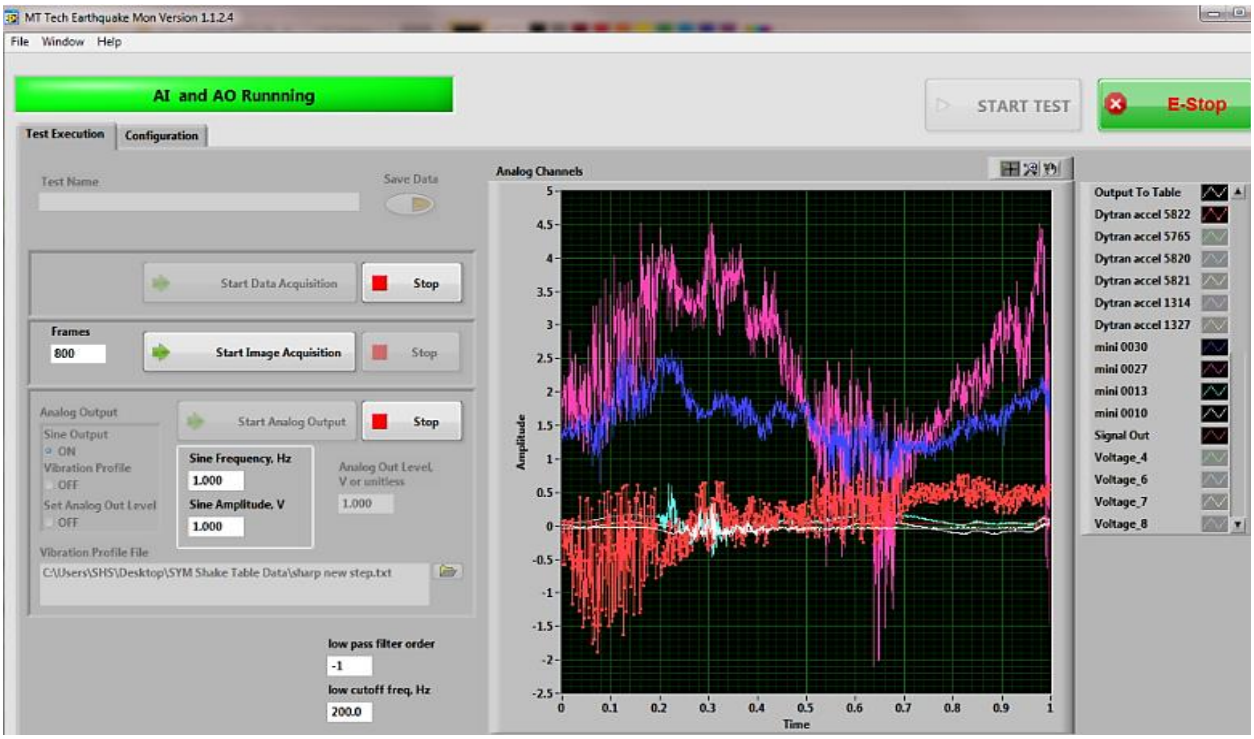

Figure 14: LabVIEW software graphical user interface, test execution screen (main screen)

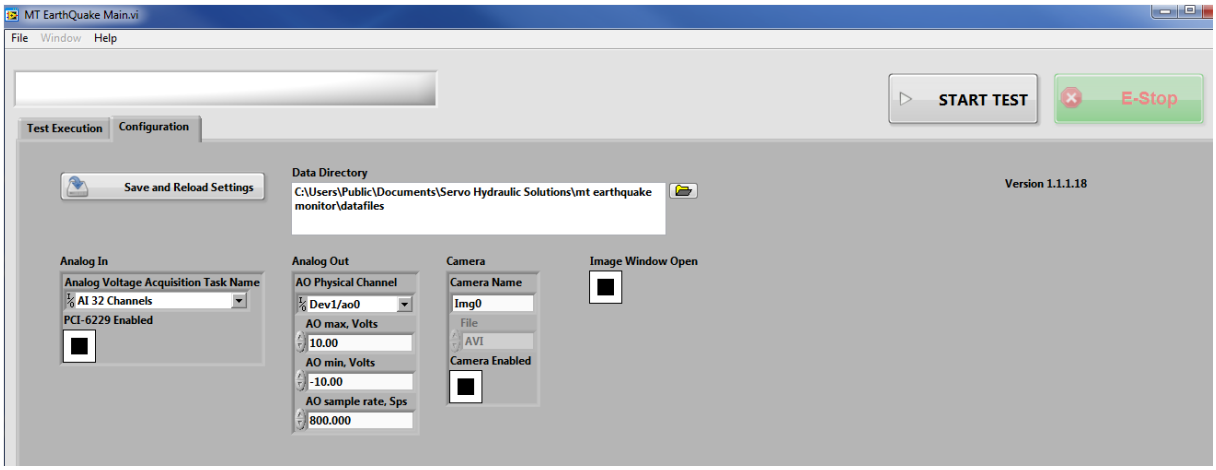

Figure 15: LabVIEW software graphical user interface, configuration screen

The software controls the shake table system using one of the three configuration methods known as the set analog out level, sine output, or vibration profile. With the set analog out level method, the table moves to a position that corresponds to the voltage manually selected by the user. With the sine output method, the user can choose frequency and amplitude values while the AO is operating, and once the sine output is applied, the table motion continues according to the specified sine function until it is manually stopped.

The vibration profile is the most commonly used method of operation. The vibration profile requires a data input file in the form of a text file (.txt), which consists of a string of numbers representing voltage values applied over time increments of 1/800 of a second. Vibration profiles are interpreted by the system as voltage output to be sent to the table. In this mode, an array of voltage values is output by the digital-to-analog converter (DAC) at a rate of 800 sps. A correlation between voltage and displacement was established to facilitate development of vibration profiles, further explained in Section 3.3. Because earthquake ground motions are often recorded or specified as values of acceleration, the process to develop these profiles typically begins with a desired acceleration, which is integrated twice to obtain position (displacement), and then a voltage-displacement calibration is applied to identify the corresponding voltage needed to achieve the desired acceleration. Figure 16 displays the motion relationships in one-dimension.

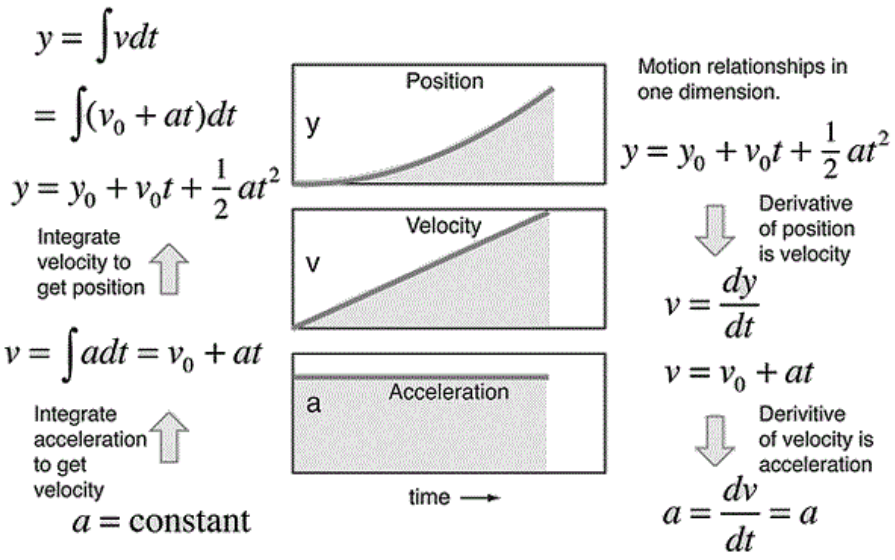

Figure 16: Relationship between acceleration, velocity, and position vs. time (Nave, 1998)

In the Fall of 2018 and Spring of 2019, two electrical engineering students performed an evaluation of the shake table and developed a program to facilitate this process. The program uses the relationships shown in Figure 16 to convert from acceleration data, the most common form in which earthquake ground motions are recorded, to voltage, the format needed for the vibration profile. They also observed that the shake table displays a resonant peak between 5 and 6 Hz. Their full report is found in Appendix A.

3.3. Data Acquisition System and Accelerometers

The shake table's main data acquisition system has 32 channels designed to be compatible with integrated electronic piezoelectric (IEPE) accelerometers and a high-speed Basler camera to collect data. The Basler camera acquires images at 340 fps and the software compiles the images to create a slow-motion video. The camera runs at default settings of exposure time of 2ms to allow for the full 340fps and does not work well with images with a high dynamic range or bright spots. The frame rate of the Basler is set only indirectly by changing related attributes such as exposure time (Clark, 2016).

The shake table is equipped with four Dytran series 3166 and two series 3202 industrial accelerometers with mass and sensitivities of 228 grams, 500 mV/*g* and 160 grams, 100 mV/*g*, respectively. In general, a low sensitivity accelerometer (fewer mV/*g*) is used to measure high amplitude signals and a high sensitivity accelerometer is used to measure low amplitude signals (National Instruments, 2019). The accelerometers provided use IEPE technology, ideal for higher frequencies (above 20 Hz). To accommodate the lower frequency range of the experimental test plan (below 5 Hz) and allow the use of the accelerometer on block specimens, a small mass Dytran series 3055 IEPE accelerometer was purchased. The 3055 accelerometer weighs 10 grams and has a sensitivity of 500 mV/*g*. The series 3202 and series 3166 industrial accelerometers were mounted on the table while the smaller series 3055 general purpose accelerometers were mounted on the blocks. Figure 17 shows the three different accelerometers used in the experiments. The specifications and calibration certificates of each accelerometer used during testing are located in Appendix B.

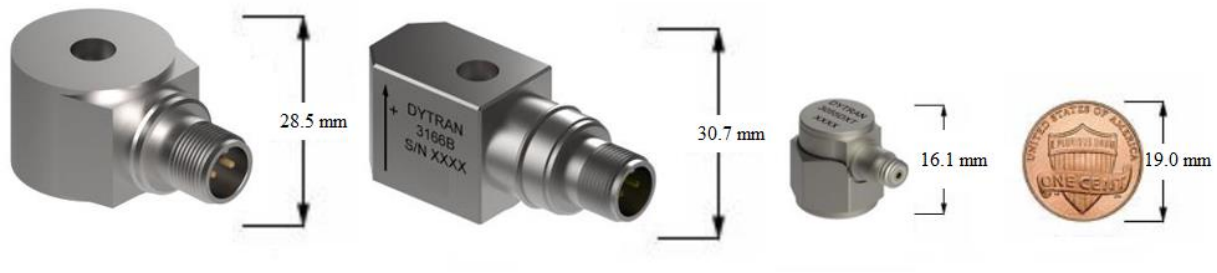

Figure 17: Dytran accelerometers used on shake table and blocks: series 3202 (left), series 3166 (middle), and series 3055 (right) (Dytran, 2019)

Figure 18 shows an IEPE accelerometer that uses a mass attached to a piezoelectric material (usually quartz, tourmaline, or a ferroelectric ceramic) to sense accelerations. When accelerated, the inertial force of the mass strains the piezoelectric material, which develops an electrical charge between the two surfaces being strained. The resulting voltage or displacement

is proportional to acceleration if the dielectric constant does not vary with charge. Because piezoelectric materials are stiff, their natural frequencies are high, so they are particularly useful for high-frequency measurements. The IEPE accelerometer response at low frequencies can be strongly influenced by signal conditioning system characteristics (Kramer, 1996).

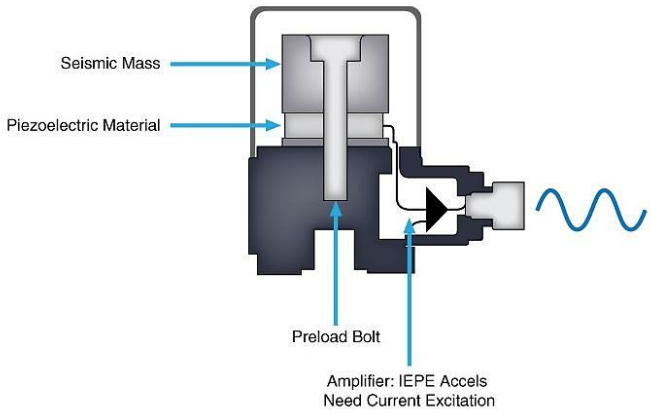

Figure 18: Diagram of IEPE accelerometer (National Instruments, 2019)

3.4. Shake Table Performance Testing and Calibration

Being a unique and one-of-a-kind research tool, the shake table system was delivered without calibration certificates or standard operating procedure (SOP) documents. Before performing experiments, the shake table required calibration and validation of performance. Additionally, although a set of harmonic motion voltage vibration profiles was included with the shake table, a process to develop new vibration profiles needed to be established.

3.4.1. Voltage-Displacement Correlation

To develop a level of confidence for the performance of the shake table and establish a voltage to displacement correlation, in-house calibrations were performed using basic physical measurements, engineering software, an oscilloscope, and a function generator. Figure 19 shows a hand sketch with measurements required to interpret the shake table as a common kinematic mechanism known as the “crank and slider” using PTC Mathcad, as shown in Figure 20.

PTC Mathcad is computer software used for the verification, validation, documentation, and re-use of engineering calculations. The shake table's design parameters of +/- 6 inches of displacement were verified using the model. The results were used to determine that the shake table had a maximum displacement in the positive direction (south) of about 4.83 inches and in the negative direction (north) of about 5.35 inches at the maximum and minimum voltage inputs of +/-10 V.

Manually increasing voltage inputs on the shake table by 1 V increments and physically measuring the displacement further verified the system model in PTC Mathcad. This was performed using both the "set analog out level" method on the *MT Earthquake Monitor* software and with an electronic test instrument that graphically displays varying signal voltages (oscilloscope) and an independent voltage source known as a function generator. Figure 21 shows the oscilloscope (left) and function generator (right) used in the calibration process. Results of the calibration are presented in Table II. The table calibration results were directly compared with the PTC Mathcad predicted displacement and an average percent difference of 1.1% was found between the model and the system displacement response. Because the model results are within the acceptable 95% confidence level range, the model built in PTC Mathcad was considered validated. All recorded calibration results are presented in Appendix C.

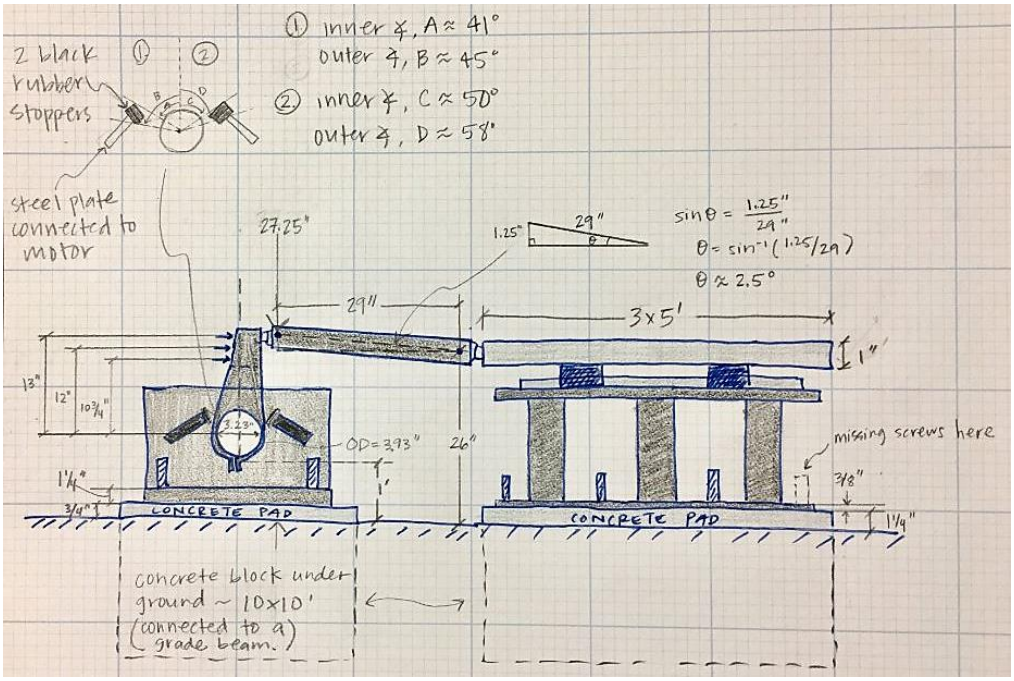

Figure 19: Hand sketch of shake table with physically measured parts for PTC Mathcad model

Shake Table Model

Created 11/15/2018 by Peter Lucon
Modified 06//2018 by Peter Lucon

File Name: Shaker_Model_r00.xmcd
Current File Name: Shaker_Model_r00.xmcd

Description:

The program calculates the angles for the 4 bar linkage (offset crank) given a driven angle.

System Variables:

Length of the Base Member 'L1': $L_1 := (26\text{in} - 14\cdot\text{in}) = 12\cdot\text{in}$

Length of the Left Member 'L2': $L_2 := 14\cdot\text{in}$

Length of the Coupler Linkage 'L3': $L_3 := 29\cdot\text{in}$

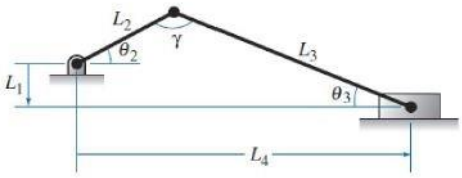

Driving Angle by the Motor 'Theta2': $\theta_2 := -75\text{deg}$

Single Solution Given above Angle:

Theta 3: $\theta_3 := \left(\text{asin}\left(\frac{L_1 + L_2\cdot\sin(\theta_2)}{L_3}\right)\right) = -3.01\cdot\text{deg}$

Length of the Right Linkage 'L4': $L_4 := L_2\cdot\cos(\theta_2) + L_3\cdot\cos(\theta_3) = 32.583\cdot\text{in}$

Angle Between R_{CD} and R_{CB}: $\gamma := 180\text{deg} - (\theta_2 + \theta_3) = 258.01\cdot\text{deg}$

Figure 20: Portion of code and diagram of the PTC Mathcad model

An observation made while conducting the voltage-displacement calibration, was that when the step function was applied, as the table reached the maximum voltage it appeared to

slightly exceed the voltage and create a jerking motion as it retracted to the proposed voltage. The jerking motion was associated with the tuning of the Bosch Rexroth drive in which the drive was commanding the motor to follow the voltage profile as tightly as possible. The lack of flexibility created oscillations at the end of the step function. Section 4.3 explains the process taken in choosing a better motion response to overcome extra vibrations.

Figure 21: Oscilloscope (left) and function generator (right) used for calibrations

Table II: Voltage to displacement calibration

Voltage to Table (V)	Displacement measured (in)	Displacement in PTC Mathcad (in)	% Difference
-10	5.3	5.4	1.3
-9	4.8	4.8	0.2
-8	4.3	4.3	0.1
-7	3.7	3.8	0.8
-6	3.2	3.2	0.8
-5	2.7	2.7	0.6
-4	2.1	2.1	0.5
-3	1.6	1.6	2.2
-2	1.1	1.1	-0.1
-1	0.5	0.5	-0.4
0	0.0	0.0	0.0
1	0.5	0.5	-1.2
2	1.1	1.0	-1.9
3	1.6	1.6	-2.6
4	2.1	2.1	-1.8
5	2.6	2.5	-1.7
6	3.1	3.0	-3.0
7	3.6	3.5	-1.7
8	4.0	4.0	-1.8
9	4.5	4.4	-1.5
10	4.9	4.8	-0.9

3.4.2. Accelerometers, and Issues Identified

During normal operation of the shake table, an arbitrary noise of about 3V in amplitude was observed in the measurement signals. To verify that the noise was not from the accelerometers, the accelerometers were tested with the function generator and oscilloscope, which have independent voltage sources. No irregular noise was observed from the accelerometers. In order to reduce the noise, the signal input and all accelerometers were passed through an anti-alias (AA) filter. The AA filter is an active, low pass filter that blocks high frequencies, but will not attenuate the signal into the shake table. A passive filter known as a capacitor with a capacitance of 0.068 microfarads (µF) was soldered on the drive input in the control panel to help reduce the noise to acceptable levels below 200 mV. The noise was reduced to about 200 mV in amplitude but is still present. Figure 22 shows an idle system marking approximately 0.2 on the y-axis representing amplitude.

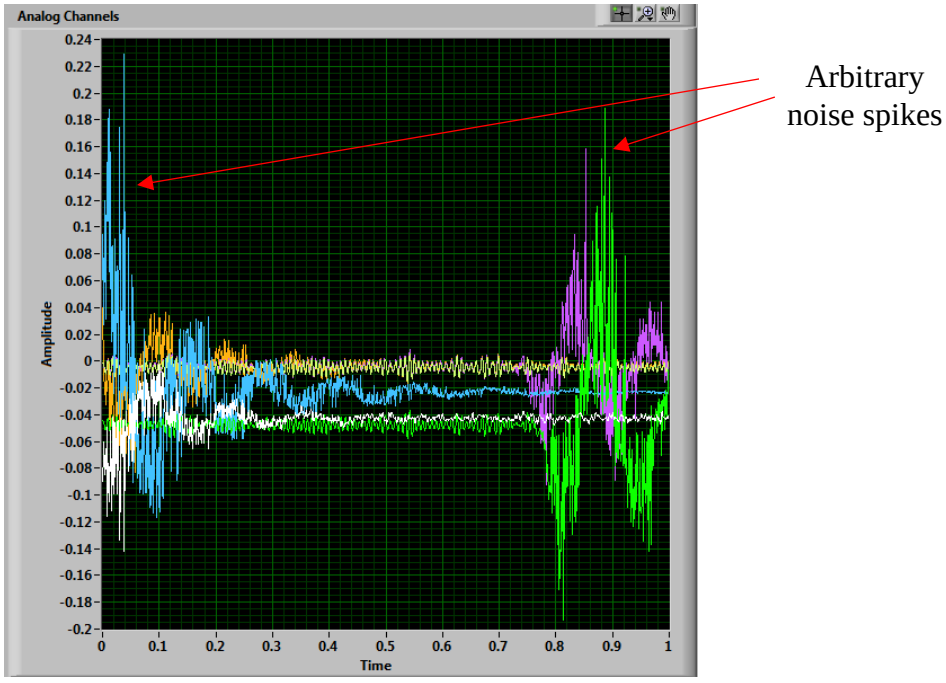

Figure 22: Idle system where the spikes are the reduced arbitrary noise

Calibrations were performed using a simple frequency sine sweep test to observe the response of the accelerometers at various frequencies. From the frequency response plot shown in Figure 23 and frequency sweep tests shown in Figure 24, it was determined that acceleration profiles with frequencies between 0 – 3 Hz were not be recognized by the IEPE accelerometers. Research was conducted to investigate the type of accelerometers that would perform well in a lower frequency range. Although microelectromechanical system (MEMS) accelerometers were the best option for low frequency performance due to their small size and ability to measure static (constant) acceleration, the technology was not compatible with the DAQ system without modifications. Therefore, the series 3055 general-purpose IEPE accelerometer with 500 mV/*g* sensitivity was purchased and in addition to the standard calibration at 100 Hz, a low frequency calibration at 2 Hz was performed by Dytran. The 3055 accelerometer has a frequency response of +/- 5 % in the frequency range of 2 – 5000 Hz and begins to drop around 1 – 3 Hz. In general, a low sensitivity accelerometer is used to measure high amplitude signals and a high sensitivity accelerometer is used to measure low amplitude signals (National Instruments, 2019).

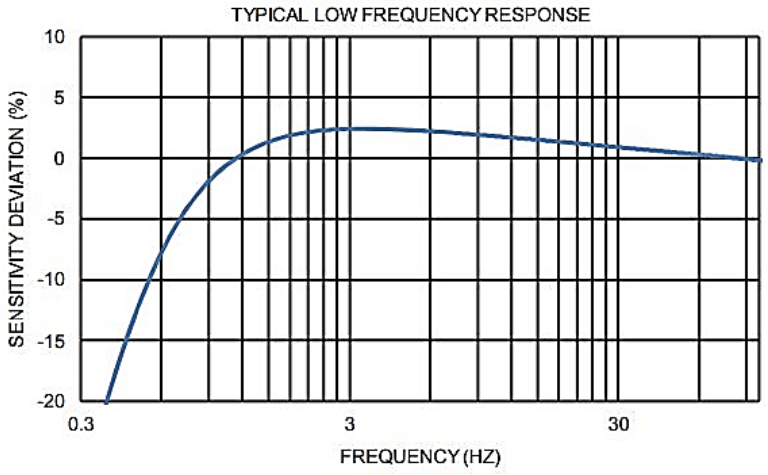

Figure 23: Low frequency response for single-axis, 3055 series IEPE accelerometer (Dytran, 2019)

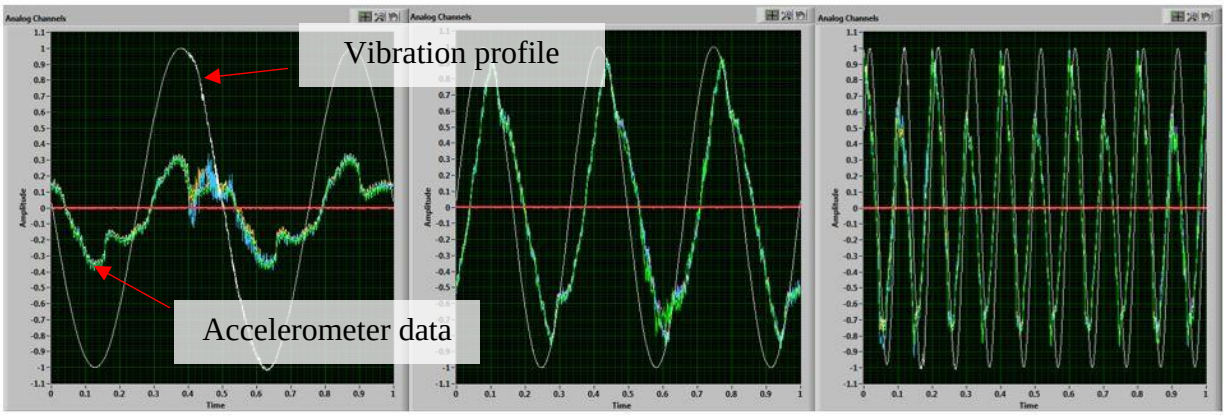

Figure 24: Comparison between vibration profile and accelerometer response to profiles of 2, 3, and 10 Hz (left to right)

To allow direct comparison of data from multiple accelerometers, the aluminum bracket shown in Figure 25 was designed. Performing multiple tests on all accelerometers with the same vibration profile resulted in identical plots. The aluminum bracket with four accelerometers provided the ability to collect redundant accelerometer data. Due to the arbitrary noise in the system that travels through various channels at different times, it was determined that a best practice was to collect data from as many channels as possible. By using redundant measurements it is more likely that at least one channel will be noise-free during critical segments of time.

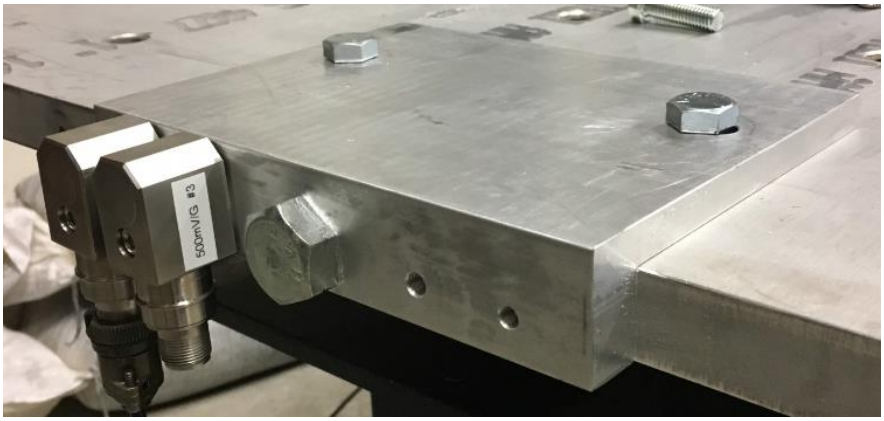

Figure 25: Custom built aluminum bracket used to mount multiple accelerometers at once on shake table

While performing low frequency vibration profiles, not only was it observed that the accelerometers did not perform well at these low frequencies, but the shake table's behavior was not smooth. Figure 26 shows a 1 V at 2 Hz profile which is below detection range for the accelerometers and shows distinct non-smooth behavior in the accelerometer data, depicted by the thicker plot line. Using the oscilloscope and function generator from Figure 21, multiple low frequency vibration profiles were implemented to test that the non-smooth response was not an error from the accelerometers, but that it was poor dynamic performance from the shake table.

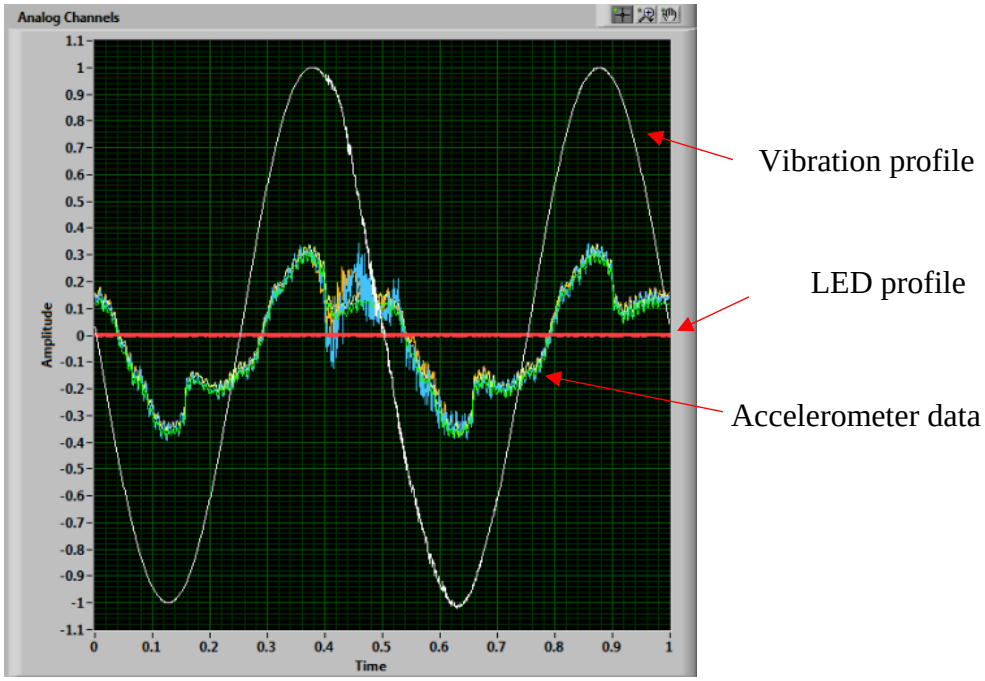

Figure 26: Non-smooth behavior of shake table motion during dynamic profile recorded with 3166 accelerometers

The primary purpose of the DAQ system is to record data from all accelerometers and, simultaneously, record imagery with the high-speed camera. When the user clicks on the "Start Test" button in the *MT Earthquake Monitor* software, it initiates the DAQ system and the high-speed camera recording, and sends vibration profile after a short delay. The purpose of the delay is to allow data and images to be captured prior to the arrival of the vibration profile to be

sure to capture the initial response. The goal was to produce data files of different types (.csv, .bmp, and .avi), but having the same timestamp. Unfortunately, there were significant difficulties in achieving the synchronization between the data types, because of the different initiation and rates for the measurements of acceleration and camera images. Furthermore, although the image titles contain the timestamp of when the image was taken, the values are misleading because the delay causes alternating positive and negative image timestamps.

Through numerous equipment setup configurations and software updates, the most recent (11^{th}) version of the *MT Earthquake Monitor* software implemented a mitigation based upon monitoring light emission diode systems (LEDs) that would allow the user to identify the beginning and end of the vibration profile in the data and image files. The LED light is placed on the shake table within view of the camera. When there is no other signal being sent to the table, the system sends a 4 V signal to the LED light, illuminating it. When the vibration profile is sent through the AO, the 4 V signal is removed and the LED turns off; the LED turns back on as the 4 V signal is reinstated after the vibration profile is completed. Hence, the LED provides a visual indication of the duration of the vibration profile and may be used to identify the timing of the high-speed images. Correspondingly, the 4 V signal is observable in the datafiles, changing to the initial value in the input voltage profile (usually zero) when the profile is sent to the table, and returning to 4 V at the end of the profile. While not perfect, this system allows identification of the initiation of the profile in the .csv files and the video files. The *MT Earthquake Monitor* software still needs improvement to overcome a system lag between the time when the vibration profile is sent, when the high-speed camera begins to record, and when the DAQ starts recording data.

3.5. Conclusions

Although many issues became apparent during testing and calibration of the shake table, the mitigations implemented have greatly enhanced the quality of the data, allowing experiments to be conducted with reasonable confidence. Some issues that have not been completely addressed include the synchronized timestamp on all data types while using the “Start Test” button, DAQ compatibility with MEMS accelerometers, and the use of low frequency IEPE accelerometers. Appendices A, B, C, and F include all of the calibration details along with an SOP for operating the shake table.

4. Toppling Block Experiments & Results

To understand the fundamental rocking behavior, a series of physical tests were conducted on a unidirectional shaking table to investigate the effects of external loading along the base of a rigid block from an at rest position on a horizontal plane. Blocks consisting of different geometric characteristics were placed on a shake table and accelerations to mimic pseudostatic forces derived from static equilibrium force and moment equations were applied. Additionally, data were collected using accelerometers and a high-speed camera. This experimental setup and process provides a realistic representation of how a rock block would behave when introduced to various seismic intensities at the base of the rock block.

The purpose of the experimental tests were to confirm the results from theoretical analysis using static equilibrium force and moment equations by experimentally determining the onset toppling acceleration, which is the minimum acceleration required to initiate toppling of a rigid block from a horizontal at rest position. Although the theoretical analysis is based on pseudostatic loading applied at the block centroid and the loading in the shake table is due to forces created by movement of the base of the block, it was anticipated that the results would match. Developing the experimental tests, optimized for the constraints of the shake table and accelerometers, was an iterative process. This chapter contains sections describing the quantitative analysis of toppling blocks, experiment setup, development of voltage profiles, experimental trials, data processing, and results.

4.1. Toppling Block Analysis

Although many solutions have been derived for pendulums and rocking blocks and columns, the simplest approach is the static equilibrium force and moment analysis (Housner, 1963). The standard solution is derived using Newton's 2nd Law of Motion.

Figure 27 contains a free-body diagram of the block with dimensions indicated and external forces labeled. Note that the external force F is assumed to be the pseudostatic inertial force replacing the dynamic earthquake force and is acting horizontally at the centroid of the block, in the direction opposite to the ground motion.

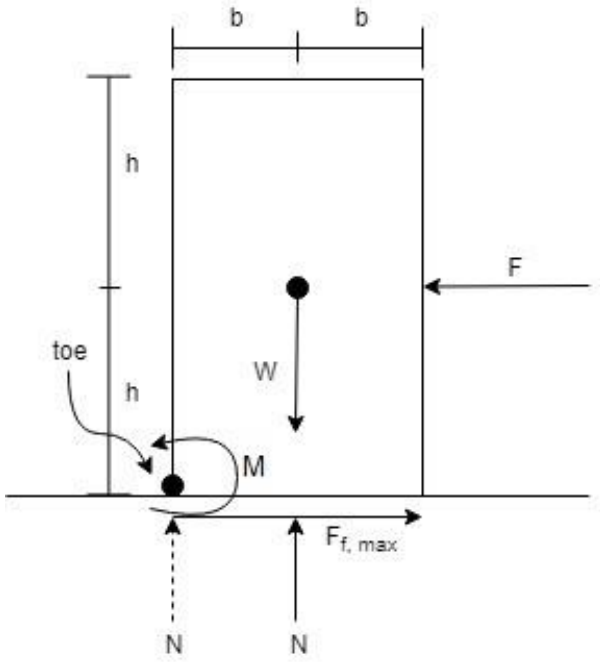

Figure 27: Example of free-body diagram for block on horizontal plane

Assuming no motion in the x- or y-directions, the sum of the forces in each direction is zero:

$$\sum F_x = 0: F - F_f \;\therefore F = F_f \quad \textbf{(4)}$$

$$\sum F_y = 0: W - N \;\therefore W = N \quad \textbf{(5)}$$

where W=mg, F=ma, $F_{f,max}$=μN.

Note that to prevent sliding in the x-direction requires $F \leq \mu N = F_{f,max}$. At the point that toppling initiates, the normal force N moves to the toe, as indicated by the dashed line in Figure 27.

$$\sum M_{toe} = 0: -W(b) + F(h) + N(0) + F_f(0) = 0 \quad \textbf{(6)}$$

$$\Longrightarrow -mg(b) + ma(h) = 0$$

$$\Longrightarrow -g(b) + a(h) = 0$$

Solving for "a", the minimum acceleration to make the block topple:

$$\Longrightarrow a = g\left(\frac{b}{h}\right) \; ; general\ acceleration\ equation$$

In summary, the horizontal earthquake acceleration required to make the block topple is equal to the acceleration of gravity multiplied by the aspect ratio (width/height) of the block.

4.2. Experimental Setup

Rectangular prismatic wooden blocks were used because wood can be manipulated into a well defined shape that is easily modeled. A set of four blocks was prepared using a wood planer, jointer planer, and table saw. The edges of the blocks were lightly sanded to prevent splintering. The blocks were dimensioned to have aspect ratios of 1:1.8, 1:3.0, 1:4.1, and 1:5.4. The masses and dimensions of the blocks, calculated mass density values, and pseudostatic accelerations required for toppling are presented in Table III. The experimental test plan was initially developed to use four blocks, but the shortest block labeled “Block 1” was damaged during preparation and was not used. The three blocks used in the experiments are shown in Figure 28.

Figure 28: Rectangular prismatic wooden blocks used for experiments

Table III: Summary of block information

Block #	Height (m)	Length (m)	Width (m)	Mass (kg)	Volume (m^3)	Density (kg/m^3)	Static Acceleration (m/s^2)	Static Acceleration (g)
2	0.25	0.081	0.083	0.79	0.0017	470	3.25	0.33
3	0.34	0.079	0.083	1.10	0.0023	488	2.27	0.23
4	0.45	0.081	0.083	1.44	0.0030	475	1.77	0.18

The blocks were placed individually on the shake table as shown in Figure 29. The shake table operates in the south to north direction, south being positive and north being negative (south is left in Figure 29). To maintain consistency throughout the experimental test plan, the shake table was marked with a test location and each side of the blocks was labeled with a cardinal direction, allowing the block to be placed on the table with the same orientation for every trial.

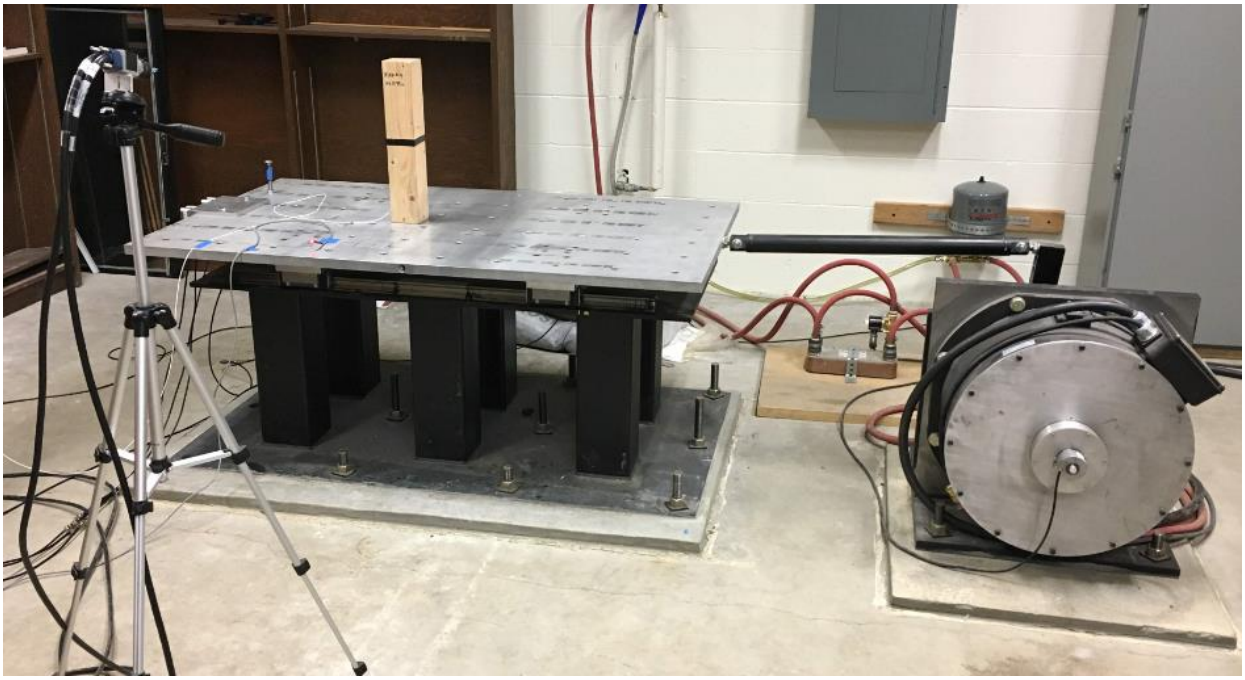

Figure 29: Experimental block setup on shake table

As the experimental test plan was implemented, modifications were made and new tests were performed, the accelerometer configuration modified as shown in Figure 30. By the end of the study, three configurations using various combinations of accelerometers had been used. All accelerometers used for the experimental test plan were single-axis IEPE accelerometers. Four 3166 industrial accelerometers with a sensitivity of 500 mV/*g* remained mounted on the shake table with the aluminum bracket described in Section 3.4.2, during all experiments. Multiple acceleration measurements allowed for data recording in multiple channels in the DAQ system in an attempt to avoid the arbitrary electrical noise in the equipment, as described in Section 3.4.2 above. The noise occurred in various channels, at seemingly random times. Having multiple sources of data increased the likelihood of obtaining one set of useable data that was free of noise in critical segments of time.

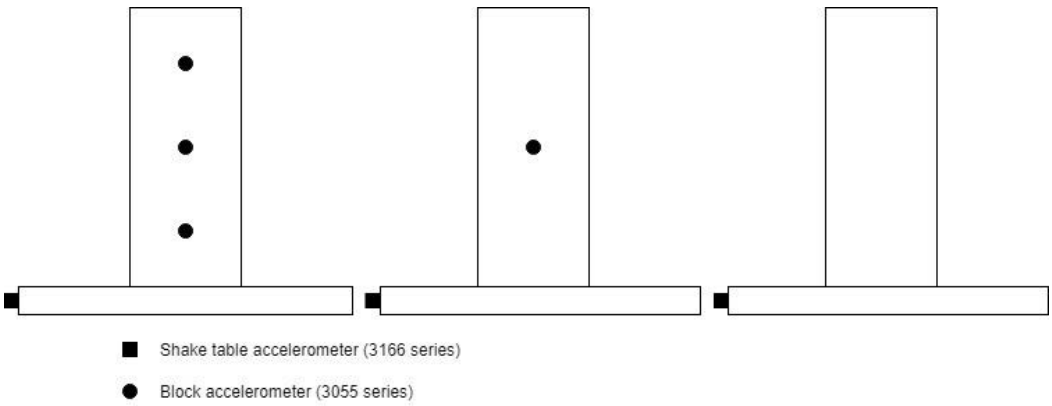

Figure 30: Progression of accelerometer configuration on blocks for experimental tests

Initially, three miniature accelerometers with a sensitivity of 10 mV/*g* were externally mounted near the top, middle, and bottom of the block, as shown in the leftmost diagram in Figure 30. The purpose of this configuration was to collect as much data as possible from the block and compare with numerical modeling data for validation of both methodologies. During the experiments, it was observed that the accelerometers were not able to detect block accelerations at the low frequencies induced in the experiments, and this configuration was removed from the experimental test plan.

The second configuration consisted of one 3055 general purpose accelerometer with sensitivity of 500 mV/*g*, externally mounted near the centroid of the block, as depicted in the middle diagram of Figure 30. While testing the smallest of the three blocks, Block 2, it was observed that the 10 gram mass accelerometer affected the toppling behavior. When the accelerometer was placed on the "front" of the block (in the direction of positive loading, as shown in Figure 31, left), the block toppled at much lower accelerations than when the accelerometer was placed on the "side" of the block (perpendicular to loading, as shown in Figure 31, right). Furthermore, the accelerometer had unfavorable mounting and cable connections making it difficult to recess it into the center of the blocks to prevent toppling from

initiating at artificially low values. Figure 32 shows the mounting and coaxial cable configurations where both accelerometers are mounted with a stud on the mounting surface, but connection outlet varies in location and direction. The second configuration was eventually removed from the experimental test plan, as well.

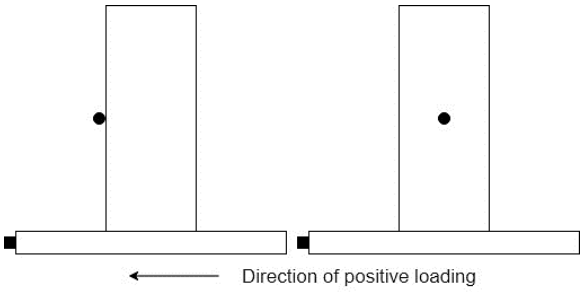

Figure 31: Accelerometer configuration on blocks

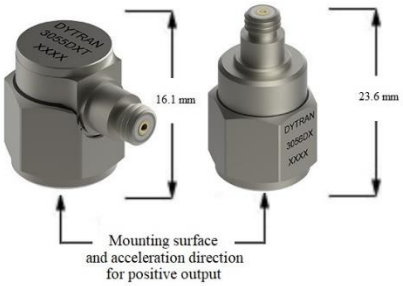

Figure 32: 3055 and 3056 series Dytran accelerometers (“Dytran,” 2019)

After some experimentation, it was concluded that data regarding the shake table acceleration was of more value for the concept of base excitation of rigid bodies than the actual acceleration of the block. Correspondingly, in the final configuration (shown in the rightmost diagram in Figure 30), no accelerometers were placed on the blocks and only table accelerations were recorded.

4.3. Voltage Profiles

The voltage profile controls the displacement and ultimately the acceleration used in the experimental test plan. Therefore, various voltage profiles were investigated in order to obtain consistent and quantifiable acceleration of the shake table. A voltage profile with a segment of constant acceleration was necessary to quantify the level of acceleration required for the initiation of toppling of the wooden specimens as described in Table III. Satisfying the constraints of the shake table and accelerometers described in Chapter 3 led to the trial of three

types of motion equations in order to create a constant acceleration segment: sharp step, parabolic, and cycloidal motions.

4.3.1. Sharp Step Profile

Initially, a sharp step function with slow unloading, similar to the voltage vs. time profile shown in Figure 33, was used to develop pulse-like loading behavior that would initiate uplift, leading to toppling of the block. In theory, an acceleration slightly higher than the static acceleration calculated for each block should initiate toppling and if large enough would ensue toppling. The step function could be scaled to produce various acceleration values, as measured by the accelerometers attached to the table.

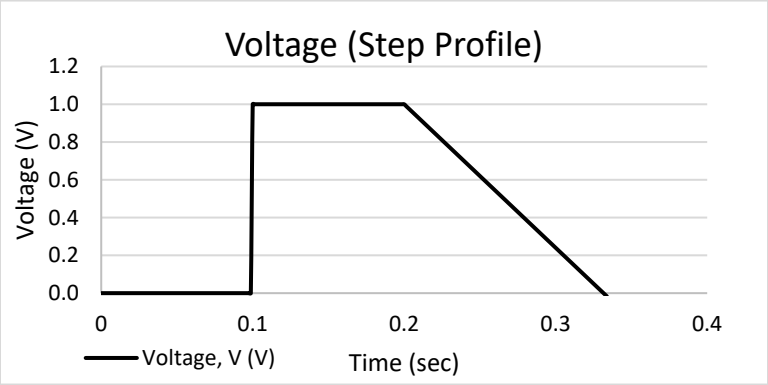

Figure 33: Voltage profile for step function showing instantaneous application of voltage (displacement) with gradual unloading

Figure 34 is a plot from the LabVIEW software for one of the early tests performed using the step function with the 3055 accelerometer (blue plot) mounted on the exterior of the centroid of Block 4. The white plot is the scaled vibration profile and the initial acceleration is estimated from reading the maximum negative inflection point on the cleanest source of data between the yellow, pink, or green plots, which represent the redundant accelerometers on the shake table. All brightened categories on the right of the real-time plot are the activated data channels that are recording data. During the use of the step function, it was observed that the shake table could not

properly perform the sharp nature of the voltage profile. While attempting to reach the maximum displacement correlating to the input voltage signal, the table would exceed this displacement and jolt back to the proposed displacement, creating an additional sharp reversal in the acceleration profile and affecting the behavior of the block. It was also observed that the step function was not applying a constant acceleration. The sharp step vibration profile was eliminated from the experimental test plan and two other options were investigated.

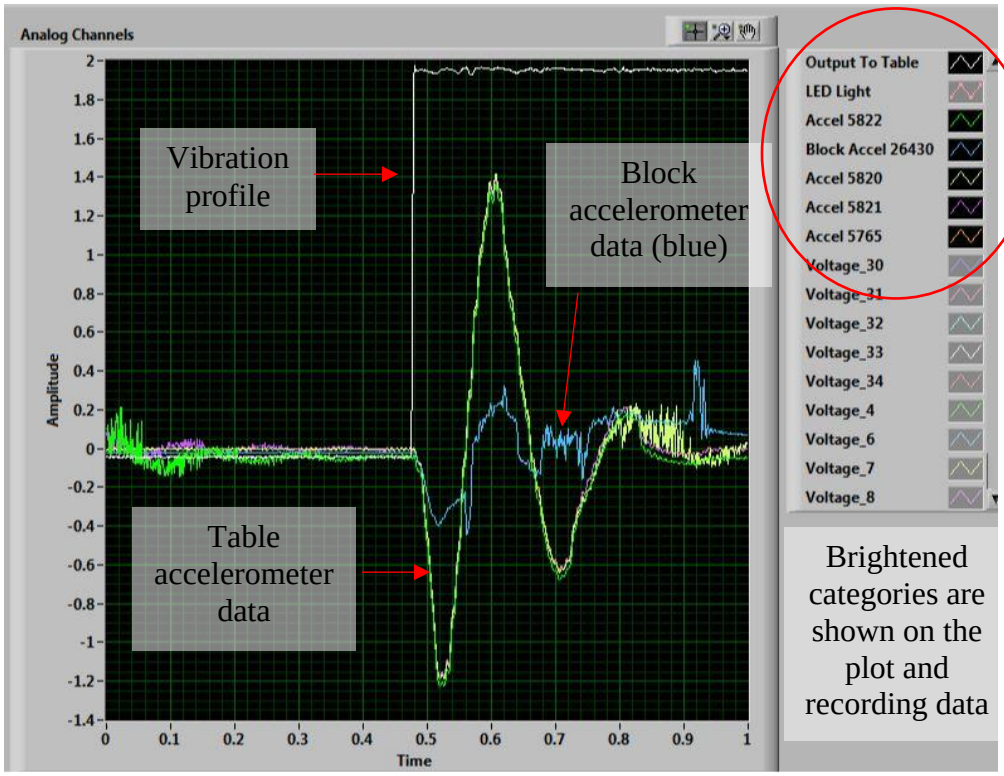

Figure 34: LabVIEW real-time plot of step function on Block 4 with four 3166 accelerometers mounted on the shake table and one 3055 accelerometer mounted on the block

4.3.2. Parabolic Profile

After observing that the sharp step profile was not resulting in constant acceleration, an investigation was performed to explore the best equations to use in order to produce a displacement profile that reasonably simulated constant acceleration. Before choosing an equation of motion, two parameters were established in order to develop the appropriate

displacement profile: 1. the acceleration had to be achieved in a segment of time that was compatible with the 3 Hz lower limit of the accelerometers; and 2. a frequency greater than 2 Hz but less than 5 Hz had to be used because the accelerometers were not designed to respond well below 2 Hz and a resonant peak occurred between 5 and 6 Hz, as discussed in Section 3.2. Frequencies above 6 Hz were too high for the experimental test plan. With the parameters set, a displacement profile consisting of a 3 Hz frequency at 1 V displacement was the ideal "Test Profile." Using the voltage-displacement calibration mentioned in Section 3.4.1, it was established that 1 V corresponded to 0.531 inches of displacement and would be relatively easy to scale. Additionally, the test profile was intended to be small enough that when applied to all three blocks of varying dimensions, toppling would not be induced, allowing positive increases in scaling of the Test Profile to be required to initiate toppling.

The second type of equation of motion considered for pseudostatic loading was a parabolic function. Theoretically, the parabolic function provides constant acceleration as shown in Figure 16. Unfortunately, the function is discontinuous at the maximum acceleration making it less than ideal for moderate or high speeds (Söylemez, 1999). Figure 35 shows the acceleration versus time profile recorded (colored lines) for the parabolic input (white line). It may be observed that the achieved acceleration (colored lines) is not constant on the entire time interval, and that constant acceleration was only achieved over a segment of time equal to about 0.1 s (from about 0.65 to 075 s).

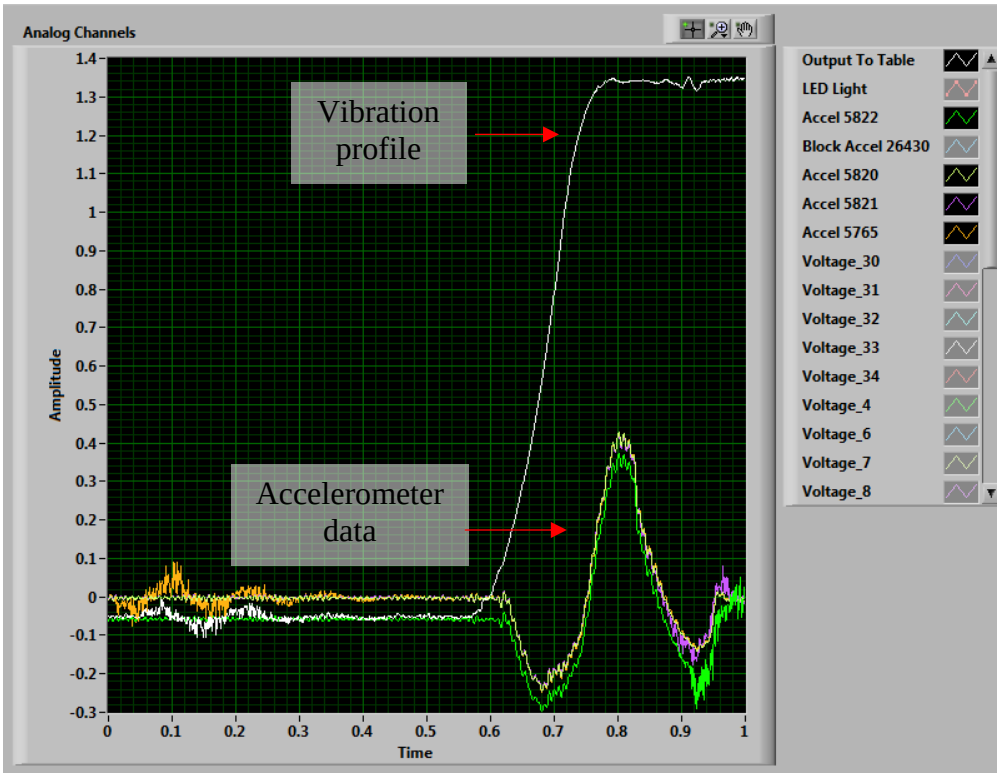

Figure 35: LabVIEW real-time plot of parabolic function on Block 3, where input voltage is white and measured table accelerations are in color

4.3.3. Cycloidal Profile

Although simple harmonic functions, such as sine and cosine functions, are often used in the study of the dynamic behavior of rigid bodies, they may not express the realistic nonlinear motion rigid blocks experience during earthquakes. Zhang and Makris (2001) examined in depth the transient rocking response of free-standing rigid blocks subjected to physically realizable trigonometric pulses, including a cycloidal pulse. Using cycloidal functions, studies show that acceleration is finite at all times and the starting and ending acceleration is zero. Therefore, the cycloidal function generates the lowest jerk compared to other equations of motion, producing the lowest vibrations, stress, noise, and shock characteristics (Söylemez, 1999). It is particularly ideal for cyclic (back and forth) loading. Equations 9, 10, and 11 were used to develop displacement, velocity, and acceleration profiles, respectively (Figure 36). The displacement

profile of the cycloidal motion was converted to voltage and used as the main vibration profile for the experimental test plan (Myszka, 2012).

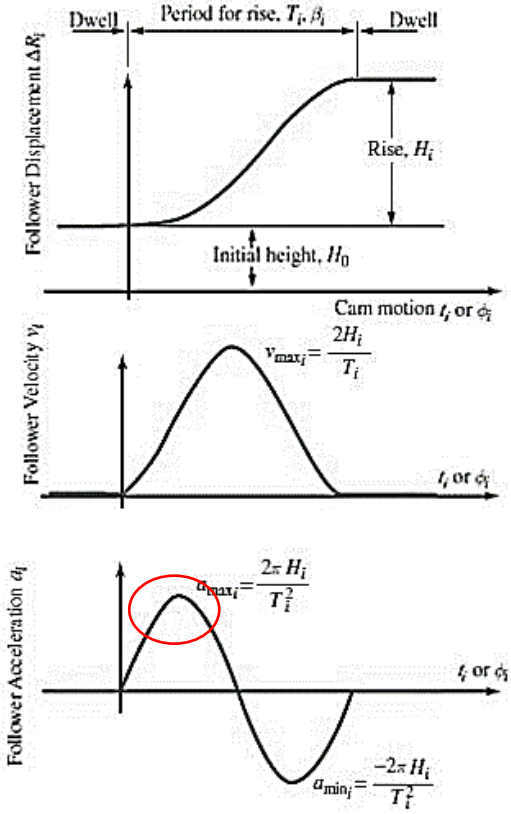

$$\Delta R_i = H_0 + H_i\left[\frac{t_i}{T_i} - \frac{1}{2\pi}\sin\left(\frac{2\pi t_i}{T_i}\right)\right] \quad \textbf{(7)}$$

$$v_i = \frac{H_i}{T_i}\left[1 - cos\left(\frac{2\pi t_i}{T_i}\right)\right] \quad \textbf{(8)}$$

$$a_i = \frac{2\pi H_i}{{T_i}^2}\left[sin\left(\frac{2\pi t_i}{T_i}\right)\right] \quad \textbf{(9)}$$

Figure 36: Cycloidal rise motion; displacement, velocity, and acceleration with corresponding equations (Myszka, 2012)

The disadvantage of the cycloidal function is that the acceleration is not constant, as shown in the bottom diagram of Figure 36. It was observed during the experiments, however, that the segment near the maximum acceleration (in red in Figure 36) that is approximately horizontal was of sufficient length that this approach was judged to be the best possible solution. Figure 37 depicts the acceleration versus time profile for the cycloidal function, with input signal in white and measured table accelerations in color. The cycloid function also achieved approximately constant acceleration over a segment of time of 0.1 s (from 0.65 to 0.75 s), but with a smaller "return" peak after the constant segment as compared to the parabolic function.

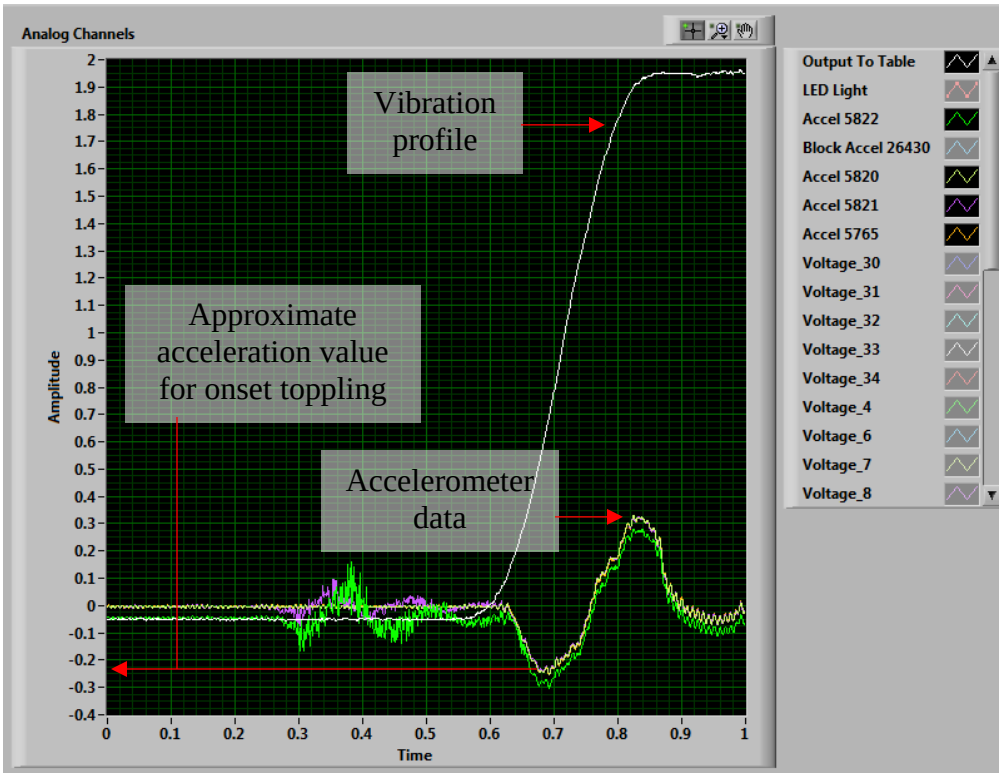

Figure 37: LabVIEW real-time plot of cycloidal function on Block 3, where input voltage is white and measured table accelerations are in color

4.4. Experiments

To begin each test, one of the blocks was placed on the shake table and set into motion using the Test Profile. The voltage of the Test Profile corresponds to displacement of the table and represents the amplitude of the input shaking profile. The Test Profile was scaled up increasing the amplitude (acceleration) while keeping the frequency constant, until a response in the rigid block was detected with visual observations and high-speed camera recordings. Multiple trials were performed at the critical scale factor for which initial toppling of the block was detected. Additionally, several trials were performed at scaled levels just above and below the critical acceleration to better pinpoint the range of accelerations that induced toppling behavior.

Different states of the vibration profile used for the experimental test plan of the study are shown in Figures 38 through 41; note that the voltage and displacement plots shown in Figures 38 and 39 have the same shape but different values on the y-axis. In order to achieve an acceleration that was observable within the calibrated range of the accelerometers (3 Hz frequency) the voltage profile was applied over a segment of time equal to one third of a second.

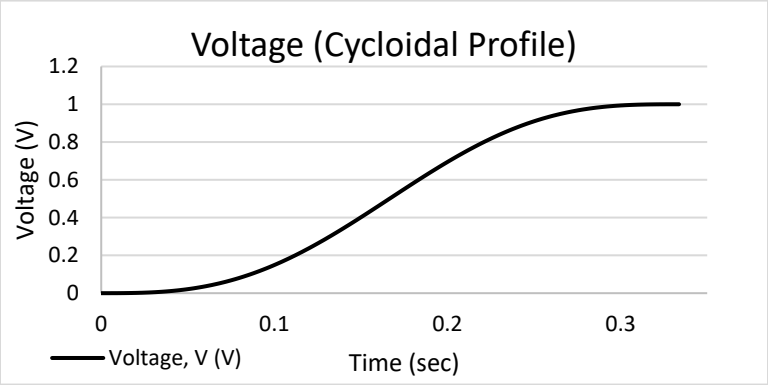

Figure 38: Voltage profile used on the shake table from cycloidal equations

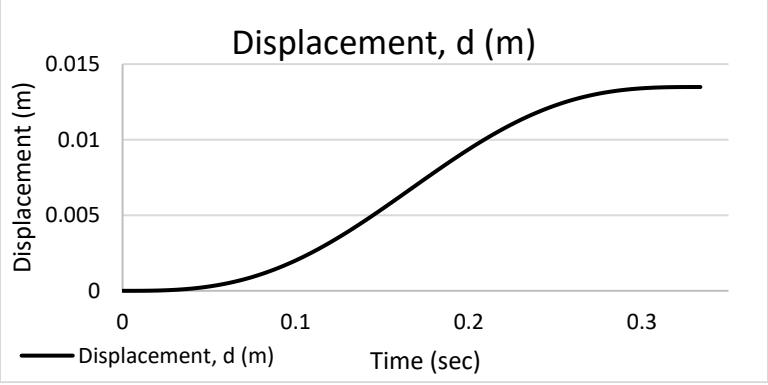

Figure 39: Displacement profile derived from cycloidal equations used to convert to voltage

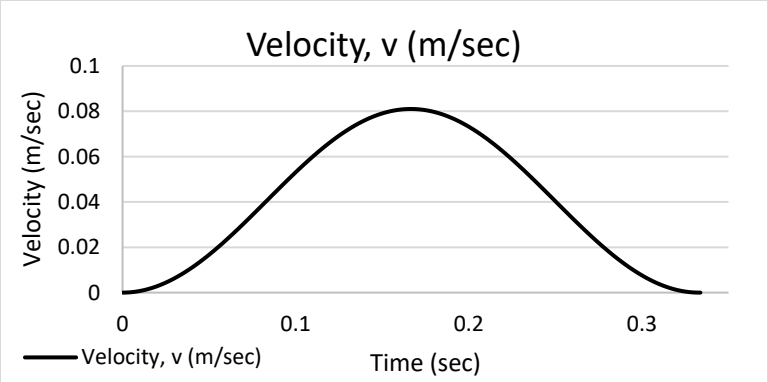

Figure 40: Velocity profile derived from cycloidal equations

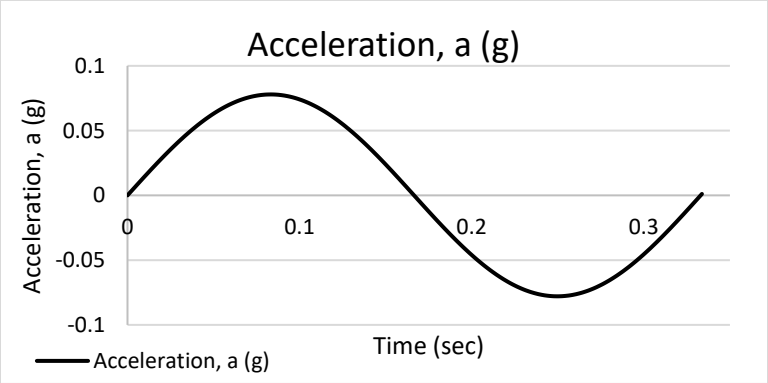

Figure 41: Acceleration profile derived from cycloidal equations

4.5. Data Processing

Approximately 200 trials were performed during the experimental component of this study. Most trials produced a data file (.csv) with accelerometer data, a folder with hundreds to thousands of image frames (.bmp) collected by the high-speed camera, and a slow-motion video (.avi). Using the LED's 4 V signal recorded in the data file, explained in Section 3.4.2, the start of the vibration profile was found. The start of the vibration profile is found in the image frames by organizing the name of the pictures in chronological order within the folder they are in. The set of alternating positive and negative titles (Section 3.4.2) in the images is the time right before the vibration profile begins and can be deleted from the data set. The start of the

vibration profile is then found in the images by going through each image and finding the one where the light is first on and then off, as shown in Figure 42. After finding the image of the block where the light is first on and then off, scrolling through images to find the moment where the block corner begins to lift and reaches a point before toppling indicates the onset toppling acceleration. Figure 43 shows the moment where the block lifts and toppling ensues. This was not as trivial as anticipated, and further verification was done by comparing frames showing toppling with the slow-motion videos to further pinpoint the onset toppling acceleration.

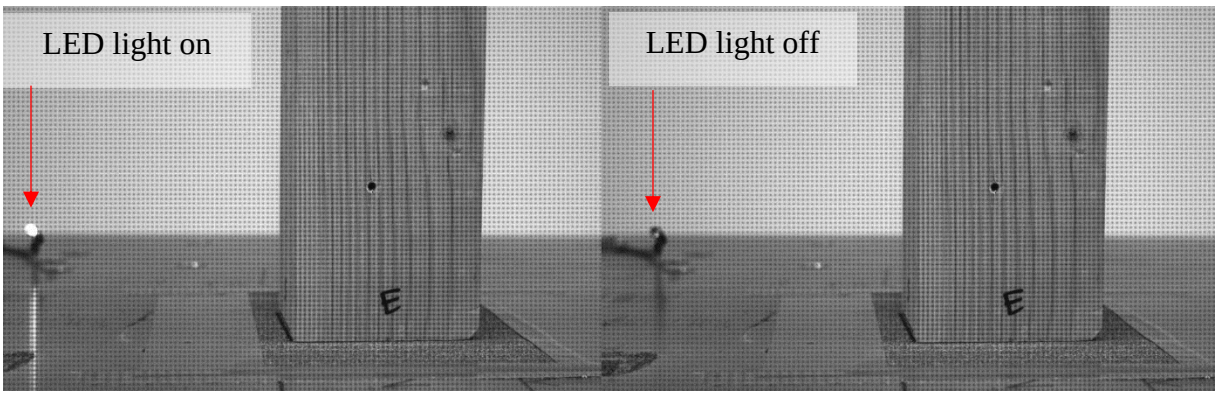

Figure 42: Identifying start of vibration profile when LED light goes from on to off from images recorded by high-speed camera

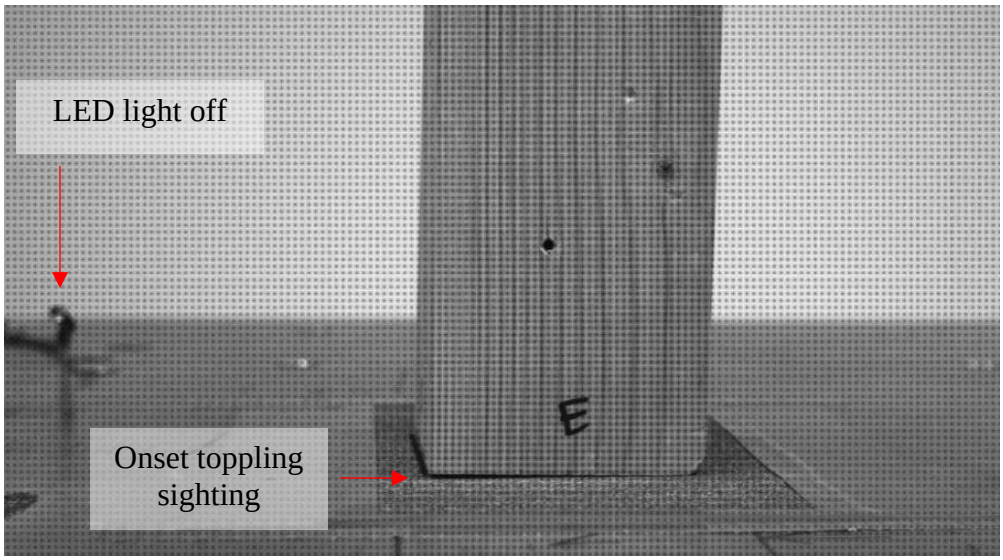

Figure 43: Identifying the onset toppling acceleration from images recorded by high-speed camera

The acceleration values also required interpretation, as they were not constant and only approximately constant over a short segment of time. In order to obtain maximum acceleration values, plots such as the one shown in Figure 37, presenting real-time data, were produced by using the “print screen” button on the keyboard as the Test Profile started. The software does not record the plot shown on the screen; therefore, it had to be manually recorded. Using Excel to plot the data recorded in the .csv files did not show the noise as distinctly as the on screen, real-time plots. After recording the plot on screen, the negative approximately horizontal “plateau” acceleration value on the colored lines was interpreted from the channel with the least noise, as indicated on Figure 37. This was considered to be the “constant” acceleration value induced during the test. Occasionally, noise occurred on multiple channels near the acceleration “plateau” and the test was repeated.

4.6. Results

Table IV displays the results from the shake table experiments. The shake table results matched theory for Blocks 3 and 4, but not for Block 2. Block 2 unintentionally had an aspect ratio (0.33), which was too close to the tangent of the 20° friction angle (0.36), and often failed by sliding rather than toppling when the accelerations were applied. To mitigate this problem, the friction angle for Block 2 was increased to 46° by applying sandpaper to the bottom of the block, and additional trials were performed that were in much better agreement with theory.

Table IV: Calculated and experimental acceleration results

Block #	Friction angle (deg)	Calculated acceleration (g)	Shake Table acceleration range (g)
4	20	0.18	0.17 – 0.19
3	20	0.23	0.22 – 0.24
2	20	0.33	> 0.55
2	46	0.33	0.31 – 0.32

Appendix D contains tables VI, VII, and VIII, which provide detailed observations of block behavior for each trial test performed. Overall, the experimental results matched the analytical results within 3 to 6 % error and were further validated using numerical modeling techniques explained in Chapter 5.

5. Distinct Element Method Analysis and Results

Numerical models provide a means to rapidly investigate various scenarios and conditions that cannot be otherwise easily evaluated. In this study, numerical models were used to simulate two loading scenarios: pseudostatic loading of blocks at the centroid, and dynamic loads applied at the base. This allowed independent verification of the shake table results. Compared to physical experiments, using the numerical models allowed for quicker reproduction and repetition of tests and the ability to perform sensitivity analyses by varying one input parameter at a time. Being unable to physically replicate centroid loading of the block with the shake table, having a validated numerical model allowed for a certain level of confidence with the second loading scenario.

A variety of numerical analyses methods are available for continuum and discontinuum systems. Choosing the correct analysis method is critical for ensuring the model in question is treated under the proper conditions and results are realistic. For this research, the Universal Distinct Element Code (UDEC), a member of the Discrete Element Method (DEM) family was selected to analyze the behavior of rigid blocks under dynamic loading because detachment of rock blocks during shaking is anticipated. In contrast, continuum methods (such as finite difference and finite element methods) were designed to model the behavior of irregularly shaped objects containing multiple materials, but not containing pre-existing discontinuities or detachments that occur during analysis.

5.1. Universal Distinct Element Code

UDEC is a two-dimensional numerical software used to simulate the static or dynamic response to loading of discontinuous media (Itasca, 2019), with an explicit time-marching solution of the full equations of motion facilitating the analysis of progressive, large-scale

movements of slopes in blocky rock (Itasca, 2019) . As a member of the DEM family, UDEC models a discontinuous medium as a system of individual blocks interacting along their boundaries, thereby allowing blocks to disconnect from neighboring blocks (Itasca, 2019). This enables the software to simulate complex, non-linear behaviors, and determine large displacements and rotations along discontinuities of deformable or rigid blocks (Itasca, 2019).

Models in UDEC may contain a combination of both deformable and rigid blocks because each body communicates with surrounding bodies via boundary contacts which may change as a function of time (Pande, Beer, & Williams, 1990). Rigid and deformable blocks are assigned reference points at corners, as shown in Figure 44 (left), so the degrees of freedom and equations of motion are satisfied. Deformable blocks are subdivided into triangular finite-difference zones (Figure 44, right), and calculations of internal stress and strain are performed within each zone. In this project, it was decided to use rigid blocks because the block material was relatively stiff and the anticipated displacements due to translation and rotation were much larger than displacements due to internal strain or deformation.

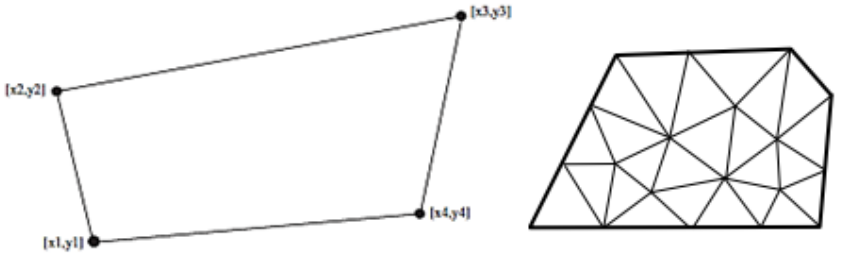

Figure 44: Examples of rigid/discontinuous (left) and deformable/continuous (right) blocks
(Itasca, 2019; Bagi, 2012;)

In UDEC, contacts are created at each block corner that interacts with a corner or edge of an adjacent block, depicted in Figure 45. All contacts are assigned normal and shear stiffness values, and contact forces are directly related to the deformation or overlap at contacts and the

contact stiffness. Joint constitutive models are designed to be representative of the physical response of rock joints, therefore making UDEC the ideal software for modeling blocks of rock or other similar materials.

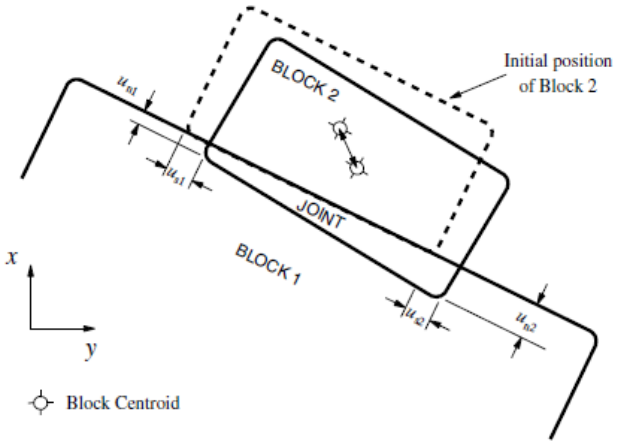

Figure 45: Corner and edge interactions of blocks in UDEC (Itasca, 2019)

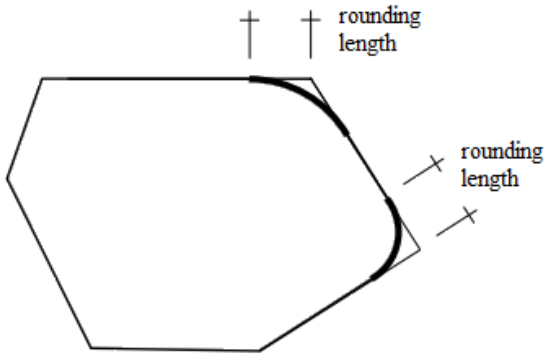

Figure 46: Rounding of corners of blocks in UDEC (Bagi, 2012)

In order to avoid unrealistic behavior associated with interlocking of sharp corners, the corners of the blocks are rounded. In UDEC, this is accomplished by applying the same rounding length to all corners in the model as shown in Figure 46. The rounding length should be selected taking into consideration the size of the smallest block or zone so that only corners are affected and not the entire block shape. As block motion occurs, contact points are automatically updated using computationally efficient algorithms. Boundary conditions are implemented by specified velocity (usually zero) of an entire block in one or more directions, and by applied force or stress at one or more edges of a block.

The explicit algorithm used in the UDEC code is based on the use of force-displacement laws which specify the interactions between a block and its surrounding neighbors at the contacts, and a law of motion that governs the displacements of the blocks as they are subjected to forces which are not in balance (Thoraval, 1991). The explicit solution requires a time-

stepping solution of the same basic equations until equilibrium or steady state is reached, or the simulation is ended. The method assumes that the selected time step is sufficiently small that accelerations and velocities are considered constant within a step. The flow chart in Figure 47 shows a graphical representation of the solution process, beginning with the initialization. During the initialization, the critical time step is determined based on the block masses and contact stiffnesses. The law of motion is then applied to each block using the known force sums derived from gravity, contacts, boundary conditions, structural elements, etc., to determine its acceleration which is then integrated to determine its velocity components. Using the velocities previously calculated, the block corner positions are updated. There is no limitation in the deformation or motion of the blocks because the entire UDEC code is a large strain model. After applying the displacements, the normal and shear forces at each contact are determined from the joint constitutive law and the process is repeated. This process is repeated until the user-defined "cycle time" or total number of "cycles" has been reached. Joint constitutive models are designed to be representative of the physical response of rock joints, therefore making UDEC the ideal software for modeling rigid blocks.

5.2. Model Setup

Three rigid block models were developed using UDEC's version 6.0 software to represent the three wooden blocks tested with the shake table. Figure 48 shows an example of the block setup. Each model was simulated using two external force loading scenarios: one at the centroid of the block and the other on the shake table. The purpose of these models was to replicate the shake table experiments, primarily through base loading, and have correlating data between experimental and numerical results.

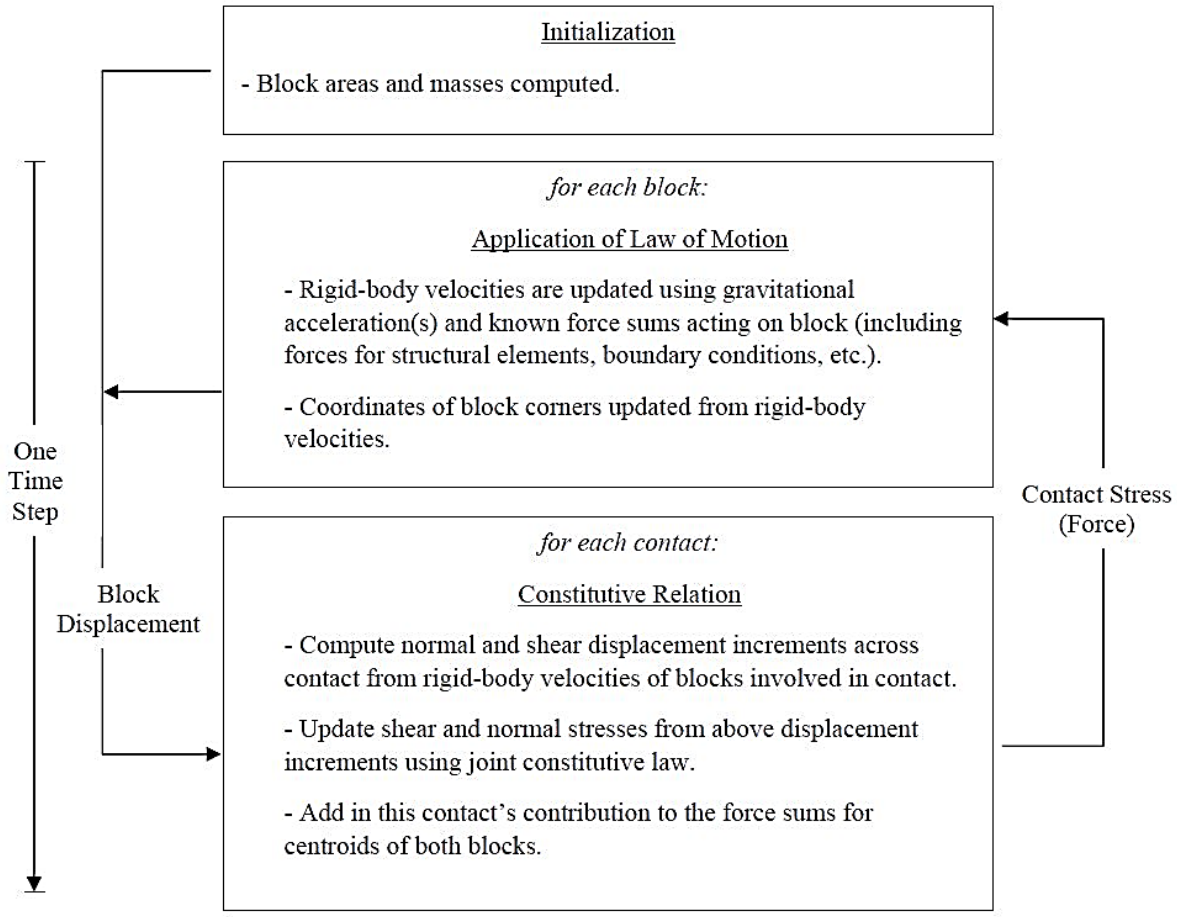

Figure 47: Explicit solution flow chart for rigid blocks in UDEC (Thoraval, 1991)

Each model consisted of three blocks: the rigid wooden block, the moveable shake table block below it, and a stabilization block below the shake table to support it. Table III (Section 4.2) lists the dimensions and density values of the blocks. The shake table dimensions used for the model were 1.5 m in length and 0.025 m in thickness. The two-dimensional UDEC version applies a unit width to all elements in the model. Finally, material properties were implemented for both the wooden block and aluminum shake table. Density was calculated for each of the wooden blocks and a density of 2700 kg/m^3 was used for the aluminum shake table (The Engineering Toolbox, 2019).

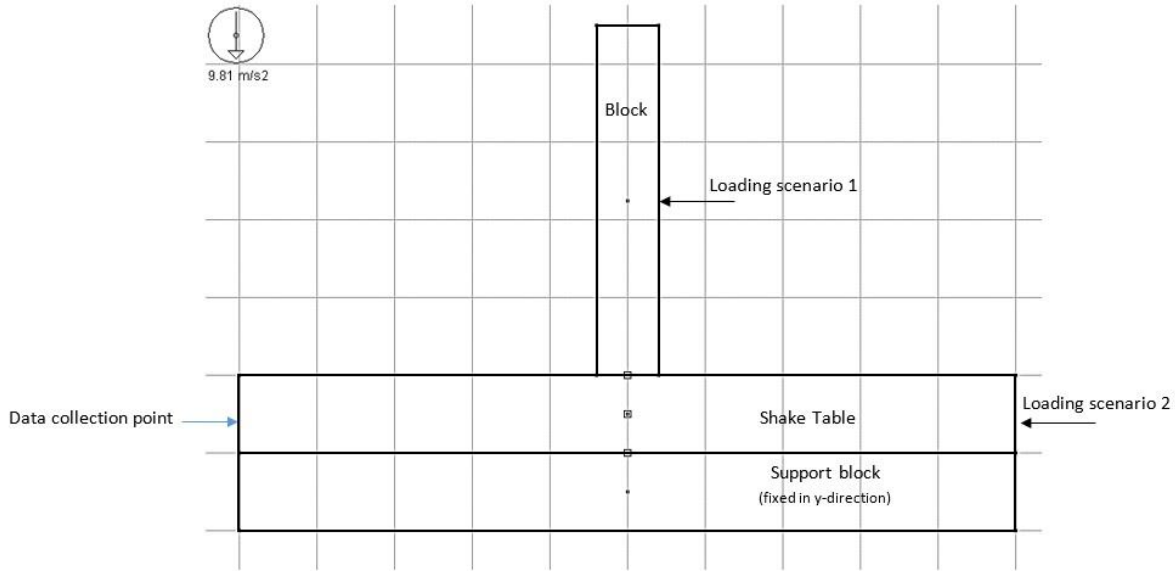

Figure 48: General UDEC model setup indicating two loading scenarios

The Coulomb slip model was selected to model the block interfaces. The interface between the block and shake table was assigned a friction angle of 20°, which was measured by performing multiple tilt tests between the wooden blocks and a block of aluminum similar to the shake table. The interface between the shake table and stabilization block was assigned a friction angle of 0° to allow for unrestricted motion between the two blocks. The Coulomb slip model also requires values of shear and normal joint stiffness at the interface, although it is rare to have quantitative data for these parameters. The available guidance (Itasca, 1989) suggests the use of values high enough such that penetration between blocks is not observed, but not too high or the corresponding time step size is too small and the simulations take too long. A value of $1x10^{11}$ N/m was selected for the shear and normal stiffnesses and appeared to satisfy the constraints.

Two other parameters that are not obtained from material properties and require engineering judgment include damping and rounding of corners. Mechanical damping is used in DEM to simulate real energy loss that is not represented by mathematically perfect material

models (Hoek & Bray, 1981). Being able to simulate the energy dissipation produces more realistic results. The default “local” damping condition was applied, and a value of 0.1 was initially used for the damping parameter. Too little rounding of corners can create problems during modeling and too much may not be realistic for blocks of rock. Therefore, picking the right amount of rounding for the entire model is important. The initial model used a rounding value of 0.001.

After setting up the model, the “solve” function was applied to establish an initial state that was both in equilibrium and not actively failing. At this point, FISH functions were set up to record velocity data. FISH is a programming language embedded within UDEC that enables the user to define new variables and functions. The functions are used to extend UDEC’s usefulness or add user defined features (Itasca, 2019). While modeling rigid bodies, UDEC only stores velocities for the block centroids and there is no history command defined to write the data to a file. In order to retrieve velocity data, a FISH function (FindBlocks) was written to collect the x- and y-velocity components at the centroid of the block and shake table. Another FISH function (make_array) was written to place all the history commands into one data file exported after each UDEC run. The FISH codes are included in Appendix E.

Once the model was in equilibrium and FISH functions were set to record and save data, the seismic load was applied. For the pseudostatic simulation (scenario 1), a horizontal force was accomplished with two methods: a. applying a horizontal force component at the centroid of the block; and b. applying a horizontal component of “gravity”, while fixing the shake table and restricting the horizontal acceleration to apply only to the block. Base loading (scenario 2) was accomplished by applying a horizontal force to the shake table block, causing motion of the shake table and producing an inertial force in the block.

5.3. Model Results

With each loading scenario, an iterative process was used to determine the values of acceleration and horizontal force that initiated the beginning of toppling. Acceleration values were adjusted in increments of 0.01 m/s^2 and force values were adjusted in increments of 1 N. Each model started with a specified "cycle time" of 0.5 seconds. Cycle times of 1.0 and 2.0 seconds were used to verify that the applied load was truly initiating toppling. Additionally, data saved regarding the block centroid were reviewed to confirm that the block had a positive non-zero y-component of velocity, indicating a toppling response. Figure 49 shows loading scenario 1a using the applied force command at the centroid of the block and the response of the block. For loading scenario 1a, after observing the initiation of toppling, the force value was used in the relationship F = ma to calculate the associated acceleration with the known block mass (a = F/m). Table V shows the results from pseudostatic loading at the centroid with the force command (scenario 1a) and loading with the horizontal gravity component (scenario 1b). The results are in good agreement with the theoretically calculated pseudostatic acceleration needed to initiate toppling. A sensitivity analysis was performed to investigate the influence of damping, rounding, and joint stiffness values on the results; only minimal changes in the results were observed even though the parameters were changed by as much as +/- one order of magnitude. It was identified, however, that some error was evident in the model results because the block widths had been specified as 8.0 cm rather than 8.3 cm. The bottom lines in Table V show the results of the simulations done using 8.3 cm for the block widths, and these match the theoretical values even more closely.

Table V: UDEC results summary using loading scenario 1 (a and b)

Block #	Block height (m)	Block width (m)	Block mass (kg)	Theoretically calculated pseudostatic acceleration needed to initiate toppling		Pseudostatic Loading Scenario 1a: applied force (N) needed to initiate toppling			Pseudostatic Loading Scenario 1b: horizontal component of acceleration applied by UDEC needed to initiate toppling	
				(m/s^2)	(g)	Force (N) applied by UDEC	Applied acceleration: a=F/m			
							(m/s^2)	(g)	(m/s^2)	(g)
4	0.45	0.08	17.1	1.77	0.18	30	1.75	0.18	1.71	0.17
3	0.34	0.08	13.3	2.27	0.23	30	2.26	0.23	2.25	0.23
2	0.25	0.08	9.4	3.25	0.33	29	3.09	0.31	3.06	0.31
4	0.45	0.083	17.7	1.77	0.18	32	1.80	0.18	1.76	0.18
3	0.34	0.083	13.8	2.27	0.23	33	2.40	0.24	2.33	0.24
2	0.25	0.083	9.8	3.25	0.33	31	3.18	0.32	3.17	0.32

The UDEC model for loading scenario 2, loading of the block via motion of the shake table block beneath it, did not yield results that matched anticipated theoretical values. The results for this loading scenario were much more difficult to interpret due to the need to calculate the movement of the block relative to the shake table, which was also in motion; the code developed to investigate this loading scenario needs refinement.

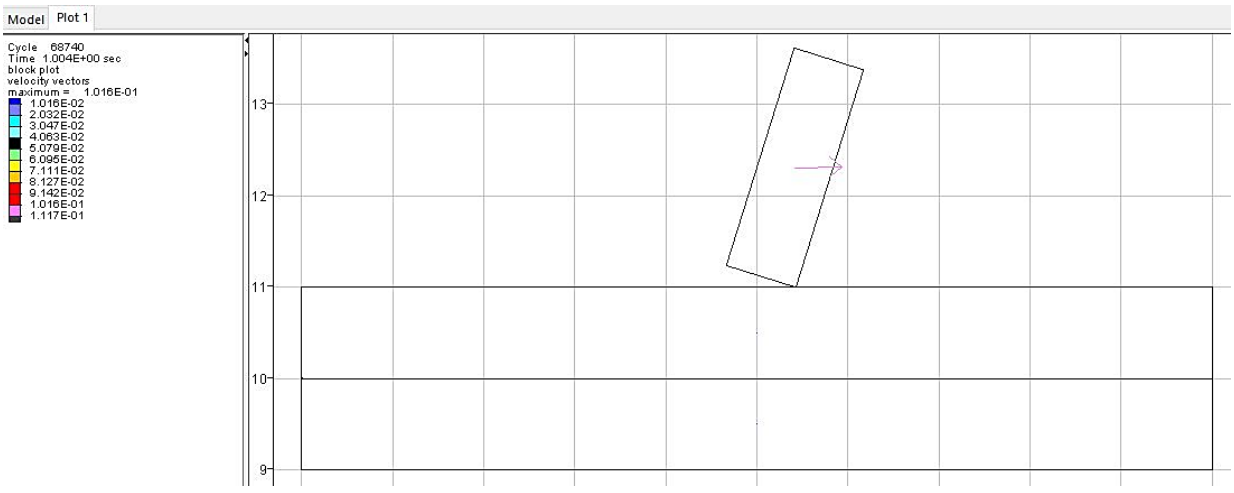

Figure 49: Velocity profile of loading scenario 1a, centroid loading of the block with applied force command

6. Conclusions and Recommendations

With a thorough understanding and appreciation of geology, earthquake ground motions, and rock mechanics, the limitations in the various methods of slope stability analysis are evident. Primarily, it is difficult to account for the complexity inherent in a rock slope. Secondly, most slope stability analyses use a single, constant, unidirectional inertial force to model the complex, transient, and dynamic nature of an earthquake. As a result, a slope could be unstable even if the computed pseudostatic calculation showed stable results. Furthermore, to satisfy the static equilibrium equations, the inertial force is assumed to act at the centroid of the rigid block when realistically the dynamic interaction of the earthquake force and a rigid body is experienced at the base. As Zhang and Makris (2001) conclude in their research, the sensitive nonlinear nature of the problem complicates further the task of estimating peak ground acceleration by only examining the geometry of free-standing objects that either overturned or survived a ground shaking event.

It is important to apply multiple slope stability approaches and engineering judgement into the evaluation of a rock slope. A combination of the pseudostatic approach and numerical modeling evaluating permanent-displacement under various force loading scenarios, i.e., loading at the centroid and loading at the base of a rigid block, are implemented in this study to investigate whether traditional methods are more or less conservative. By the end of this study, it was concluded that traditional methods, such as pseudo-static loading, are a proper representation of the initiation of toppling behavior of rigid blocks and base excitations.

There are several advantages and disadvantaged inherent in the use of the pseudostatic approach in limit equilibrium stability analysis. The pseudostatic approach is simple and straightforward; however, it should never be the sole method used in an analysis. With the

additional use of numerical analyses, clearer recommended guidelines could be developed based on characteristics of the design earthquake input acceleration, as well as the geometry and properties of the rock mass. Additionally, with the seismic database established today and the ability to identify potential toppling failures of rock slopes from geomorphic features, a proactive movement to mitigate these types of failures can possibly be achieved.

7. References Cited

Ashby, J. (1971). Sliding and toppling modes of failure in models and jointed rock slopes. M.Sc. Thesis, Department of Mining, Imperial College of Science & Technology, UK.

Augusti, G., & Sinopoli, A. (1992). Modelling the dynamics of large block structures. *Meccanica 27, 195-211*.

Aydan, Ö. (2017). *Rock Dynamics* (Volume 3 of ISRM Book Series). Taylor & Francis Group.

Aydan, O., Shimizu, Y., & Ichikawa, Y. (1989). The effective failure modes and stability of slopes in rock mass with two discontinuity sets. *Rock Mechanics and Rock Engineering*, *22*(3), 163–188.

Bagi, K. (2012). Fundamentals of the discrete element method, Secion 05: UDEC, Budapest University of Technology and Economics, 45-54.

Bray, J. W., & Goodman, R. E. (1981). The theory of base friction models. *International Journal of Rock Mechanics and Mining Sciences & Geomechanics Abstracts*, *18*(6), 453–468.

Clark, C. (2016). MT Earthquake Monitor System Software Design User's Manual, Bolder Software LLC, confidential document.

College Physics. (2019). Retrieved from https://courses.lumenlearning.com/physics/chapter/10-1-angular-acceleration/

Dytran. (2019). Retrieved from https://www.dytran.com/

Gohil, D., Solanki, C., & Desai, A. (2010). Earthquake Wave Energy Flow and Distribution. Indian Geotechnical Conference - 2010, December 16-18, 2010.

Goodman, R. E., & Bray, J. W. (1976). Toppling of Rock Slopes. *Specialty Conference on Rock Engineering for Foundations and Slopes,* ASCE, Boulder, CO.

Goodman, R. E., & Kieffer, D. S. (2000). Behavior of Rock in Slopes. *Journal of Geotechnical and Geoenvironmental Engineering*, 126.8 (2000): 675-684.

Hoek, E., & Bray, J. (1981). *Rock Slope Engineering, 3rd edition* (4th ed.). Taylor & Francis Group.

Housner, G. W. (1963). The Behavior of Inverted Pendulum Structures During Earthquakes. *Bulletin of the Seismological Society of America*, *53*(2), 403–417.

Ishiyama, Y. (1980). Motions of rigid bodies and criteria for overturning by earthquake excitations. *Building Research Institute, Ministry of Construction, Japan*, 24–37.

Itasca. (1989). UDEC Manual.

Itasca. (2019). Retrieved from https://www.itascacg.com/software/udec

Keefer, D. K. (1984). Landslides caused by earthquakes. *Geological Society of America Bulletin*, *95*, 406–421.

Kramer, S. L. (1996). *Geotechnical Earthquake Engineering*. (W. J. Hall, Ed.). Prentice-Hall International Series.

Melo, C., & Sharma, S. (2004). Seismic Coefficients for Pseudostatic Slope Analysis. *13th World Conference on Earthquake Engineering*, (369), 15.

Myszka, D. (2012). *Machines and Mechanism. Mechanical Linkages*. Prentice Hall, Chapter 9, 223-233.

National Instruments. (2019). Retrieved from https://www.ni.com/en-us/innovations/white-papers/06/measuring-vibration-with-accelerometers.html

National Research Council. (1982). *Earthquake Engineering Research, 1982*. Washington, DC: The National Academies Press

Nave, C. R. (1998). HyperPhysics. Retrieved from http://hyperphysics.phy-astr.gsu.edu/hbase/acons.html#c3

Newmark, N. (1965). Effects of Earthquakes on Dams and Embankments. *Géotechnique*, *15*(2), 139–160.

Newmark, N., & Hall, W. (1982). Earthquake Spectra and Design. *EERI Monographs*.

Pande, G. N., Beer, G., & Williams, J. R. (1990). *Numerical Methods in Rock Mechanics*. John Wiley & Sons Ltd.

Sagaseta, C. (1986). On the modes of instability of a rigid block on an inclined plane. *Rock Mechanics and Rock Engineering*, *19*(4), 261–266.

Seed, H. B., Idriss, I. M., & Dezfulian, H. (1987). Relationships Between Soil Conditions and Earthquake Ground Motions in Mexico City in the Earthquake of Sept. 19, 1985, (UCB/EERC-87-15).

Söylemez, E. (1999). Basic Cam Motion Curves. In *Mechanisms* (5th ed.). Middle East Technical University (1979). Retrieved from http://ocw.metu.edu.tr/pluginfile.php/6886/mod_resource/content/1/ch8/8-3.htm

The Engineering Toolbox. (2019). Retrieved from www.engineeringtoolbox.com

Thoraval, A. (1991). *Development of the UDEC software and verification against analytical solutions in the framework of a collaboration between CERCHAR (former name of*

INERIS), the Department of Civil, Environmental and Geotechnical Engineering of the University of Minnesota and ITASCA Consulting Group. Retrieved from https://www.researchgate.net/publication/325248360

Tso, W. K., & Wong, C. M. (1989). Steady state rocking response of rigid blocks part 1: Analysis. *Earthquake Engineering & Structural Dynamics*, *18*, 89–106.

USGS. (2019). "Soil Type and Shaking Hazard in the San Francisco Bay Area", retrieved from https://earthquake.usgs.gov/hazards/urban/sfbay/soiltype/

Vallejo, L. I. G. de, & Ferrer, M. (2011). *Geological Engineering*. CRC Press/Balkema.

Voyagaki, E., Psycharis, I. N., & Mylonakis, G. (2013). Rocking response and overturning criteria for free standing rigid blocks to single-lobe pulses. *Soil Dynamics and Earthquake Engineering*, *46*, 85–95.

Which seismic wave is the most dangerous? Why? (2018). Retrieved from https://www.quora.com/Which-seismic-wave-is-the-most-dangerous-Why

Wong, C. M., & Tso, W. K. (1989). Steady state rocking response part 2: Experiment. *Earthquake Engineering & Structural Dynamics*, *18*(December 1987), 107–120.

Yeung, M. (1991). *Application of Shi's discontinuous deformation analysis to the study of rock behavior*. PhD Dissertation, University of California at Berkeley.

Yim, C. -S, Chopra, A. K., & Penzien, J. (1980). Rocking response of rigid blocks to earthquakes. *Earthquake Engineering & Structural Dynamics*, 8.6 (1980): 565-587.

Zhang, J., & Makris, N. (2001). Rocking Response of Free-Standing Blocks under Cycloidal Pulses. *Journal of Engineering Mechanics*, *127*(5), 473–483.

8. Appendix A: Electrical Engineering Senior Design Report "Geological Engineering Shaker Table Characterization"

GEOLOGICAL ENGINEERING

SHAKER TABLE CHARACTERIZATION:

A Senior Design Project By:
Andrew Keele
&
Chase Plum

Appendix A: Geological Engineering Shaker Table Characterization by Keele & Plum, pg 1/13

Introduction:

The purpose of this document is to give an overview of how the Shaker Table works as well as help introduce the concepts needed to understand the usage of the table. Section one is a "How To" section that explores the information needed to make the shaker table function. Section two explores the testing and results that the Fall 2018/Spring 2019 senior design team performed. Section three goes over some helpful tips and tricks that the team encountered through general operation of the table.

The shaker table functions by sending a voltage to the motor controller. The motor controller attempts to move the motor arm to a particular angle. This angle translates through the motor arm to table movement. This moves the table to a position that corresponds to the voltage input. This position voltage relationship is further explored in the DC Linearity Testing section. It is very important to understand that the voltage input corresponds to a displacement and not an acceleration.

SECTION 1: "HOW TO"

Included in this section is information on how to use the Shaker Table. This includes turning the Shaker Table on, running tests using the MT EarthQuake Program, recording data, and how to analyze that data.

- **How to turn the shaker table on**:

To turn the table on first flip the Shaker Table breaker that can be seen in Figure 1. Once the breaker has been flipped to on you must wait approximately 30 seconds before the system can by enabled. Once the 30 seconds have passed it is time to press the green "Enable" button that can be seen in figure 2. Once this button has been pressed the system has been powered on.

Figure 1: Shaker Table Breaker Box

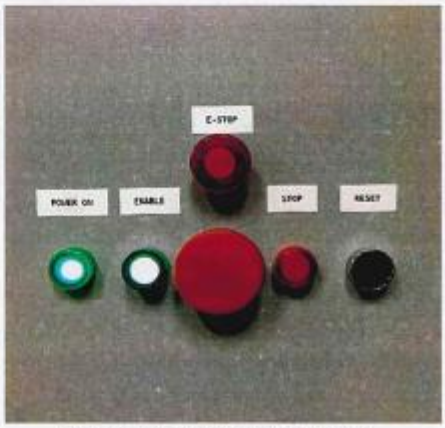

Figure 2: Shaker Table Enable Button

Appendix A: Geological Engineering Shaker Table Characterization by Keele & Plum, pg 2/13

- **Running Tests and Saving Data:**

To perform a test first launch the latest version of MT EarthQuake Monitor program. Once the program has been launched you will see the main screen shown below in Figure 3. There are several ways to perform tests using the three different analog output features. The first way is to use the "Sine Output" feature shown in Figure 3. If this is selected, you can set the sine frequency and amplitude and the program will generate that specific sine wave for you. However, this will only work for frequencies of integer values. Frequencies of non-integer values such as 4.5 Hz will produce a rectified sine wave. The next possible way to perform a test is to use the "Vibration Profile" feature. This feature allows users to input voltage profiles that are uploaded as ".txt." files. This is the feature you would use to model non-integer sine waves such as earthquake profiles to the table as text files. The final feature is the "Analog Out" level. This is used to send DC voltage profiles to the table. If analog out level is selected, you can set the DC voltage value that you want to send to the table.

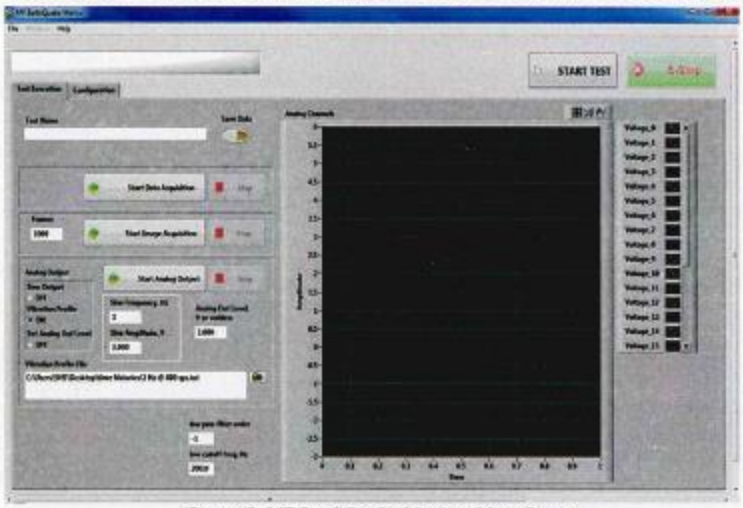

Figure 3: MT EarthQuake Monitor Main Screen

Now that the correct voltage profile is selected it is time to send it to the table. This is done but clicking on the "Start Analog Output". Once this is pressed the voltage profile will run until completion or until the "Stop" button is pressed. To view plots of the data being recoded simply press the "Start Data Acquisition" button. This data will only be saved if the "Save Data" button in Figure 3 is selected. When this is selected it will be bright yellow not the dim color shown in Figure 3. Data will be recorded and saved from the time "Start Data Acquisition" is pressed until the "Stop" button is pressed. The data will be saved under the name you desire by simply naming it in the "File Name" section.

- **Analyzing Data:**

Once a test has been performed and data has been recorded it is saved as an excel file. The destination you wish to save this excel file in can be set under the configuration tab shown in Figure 3. The top row in the excel file contains information as to what each column of data contains. The data can then further be analyzed by plotting the columns of the data in your preferred program.

Appendix A: Geological Engineering Shaker Table Characterization by Keele & Plum, pg 3/13

SECTION 2: "SUMMARIZATION OF TESTS AND RESULTS"

See Appendix A to show how voltage profiles were created

This section includes tests we performed and the results from these tests. We performed these tests to better understand how the Shaker Table operates. This was needed to work toward our task of generating voltage profiles that would accurately map real life earthquake acceleration profiles to the table.

- **DC Linearity**

During the DC Linearity testing we applied a constant voltage to the shaker table whereby the shaker table would be displaced by a distance from a set starting position corresponding to a 0-volt input. As voltage increased from zero the table would be displaced left, and as voltage decreased from zero the table would be displaced right. We found that the displacement of the table was proportional to the voltage applied.

$$D(V) = 0.5*V \text{ in.}$$

- **Sine Sweep 1**

The purpose of this test was to try and obtain an acceleration sine wave with a magnitude of 1 G from 2Hz to 10Hz in intervals of 0.5Hz. We created the voltage profiles using the physics relationships between displacement and acceleration. The voltage profiles needed to be scaled by the following scale factors:

  - 0.5: Voltage to displacement scale factor determined by the DC linearity test.
  - 0.00259: Unit conversion factor going from in/sec^2 to G's.
  - $(1/\omega)^2$: Scale factor to undo the ω^2 term that comes from taking the second derivate of displacement. Where ω is frequency of the sine wave.

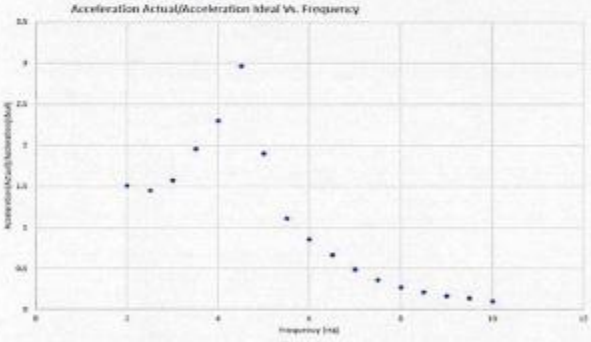

Figure 4: Magnitude plot of Measured/Expected Acceleration

The target acceleration outputs were sin waves of amplitude 1 G for all the frequencies tested. We were not able to achieve these using the method described above. Instead we found much higher G's in the 3.5Hz to 5.5Hz range and much lower G's in the range above 5.5Hz. A magnitude plot was developed from the data and the resulting plot was indicative of a second order transfer function shown in Figure 4.

- **Sine Sweep 2**

From the results of the first sine sweep tests we knew that the voltage profiles needed further scaling. We scaled the same voltage profiles by dividing them by the magnitude of the measured acceleration divided by the expected acceleration at the corresponding frequency. We then

Appendix A: Geological Engineering Shaker Table Characterization by Keele & Plum, pg 4/13

performed the tests from the first sine sweeps again and were able to achieve 1 G of acceleration for a majority of the frequencies we tested.

- **Generating a transfer function for the system**:

We found that the system has a frequency response that resembles a second order transfer function. This may seem confusing if you are not used to the terms frequency response and transfer function. The easiest way to explain this relationship is to give an example. Lets say you are inputting a voltage profile that is supposed to map an acceleration wave of 1 G at 4.5Hz on the table. The fact that the system has the frequency response shown in Figure 4 it means that instead of getting that 1 G acceleration sine wave you will get a scaled version. For this particular frequency response at 4.5Hz the magnitude is approximately 3. This means that the acceleration wave will have a magnitude of 3 G's instead of the 1 G we were expecting.

We could use this relationship to scale our voltage profiles by the inverse of the transfer function to get the desired acceleration profiles mapped to the table. Voltage profiles were created using an application created using MATLAB. *See appendix A for details on creating voltage profiles including creating an approximated transfer function from the data points we collected.*

- **Mapping sums of sine waves**:

These tests were performed to see if we could map sums of sine waves acceleration profiles to the Shaker Table. This would tell us if we were ready to map real life earthquake acceleration profiles to the table. Results from these tests can be seen in Figure 5. As you can see from the top graph, we were able to map a sum of two sine waves, one at 3Hz and the other at 6Hz, to the table. We then progressed to more complicated sine waves that can be seen in the middle and bottom graph of Figure 5. These results were not what we were expecting. The more complicated sine waves do not show the exact match we received when mapping the sum of 3Hz and 6Hz. This led us to believe that there may be some non-linearity in the system that we were not accounting for.

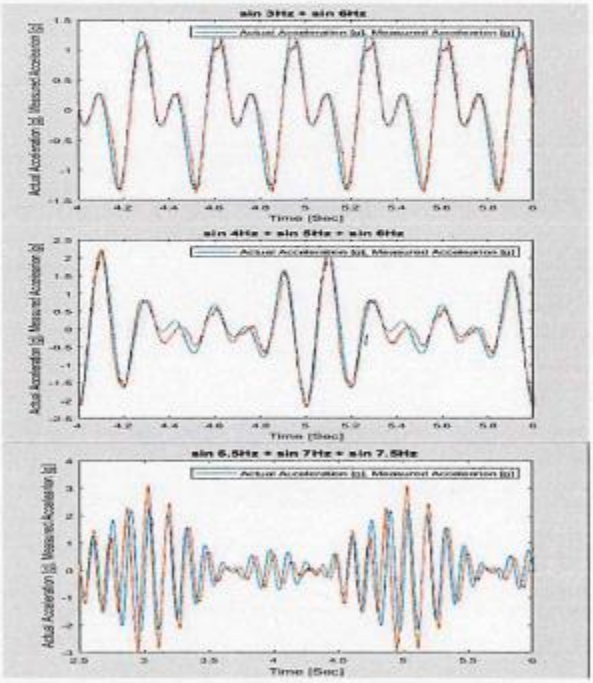

Figure 5: Mapping sums of acceleration sine waves

- **Proportional Voltage to Accelerations**

The next test we performed were to see if we could explore this non-linearity in the system. We performed tests by increasing the voltage by a certain percentage and seeing if that increase corresponded to the same percentage increase in acceleration.

Appendix A: Geological Engineering Shaker Table Characterization by Keele & Plum, pg 5/13

The results from these tests are shown in Figure 6. These test results showed that the acceleration has a non-linear relationship to changes in voltage. At 3Hz and 6Hz show more of a linear relationship and this explains why we were able to map these correctly to the table. Frequencies such as 5Hz shown in yellow showed a much more non-linear relationship. This explained why we were not able to map the more complicated sums of sine waves to the table.

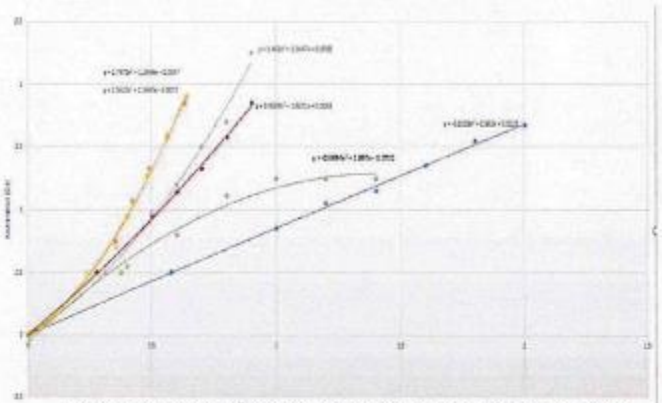

Figure 6: Linearity of Acceleration Testing: 3 Hz – Blue, 4 Hz – Gray, 4.5 Hz – Orange, 5 Hz – Yellow, 6 Hz – Red, 8 Hz – Green.

After the discovery of this non-linearity we moved to better characterizing the table for use by future students. We felt this would be much more beneficial rather than handing over an incomplete dynamic model for the system.

- **Low Frequency Tests**

The low frequency testing was done to see the quality of data recovered in the frequency range below 2 Hz. Pictured to the right is the resulting acceleration from a 4.5-volt amplitude sin wave at 1 Hz as can be seen the output from the accelerometer is less than ideal. The 500mV/G Accelerometers used are most likely not sensitive enough for use in the range under 2 Hz. For the acceleration achieved here we would expect about 0.225 G's which corresponds to about 113 mV from the accelerometer. Furthermore, the accelerometers used are only calibrated down to 2 Hz.

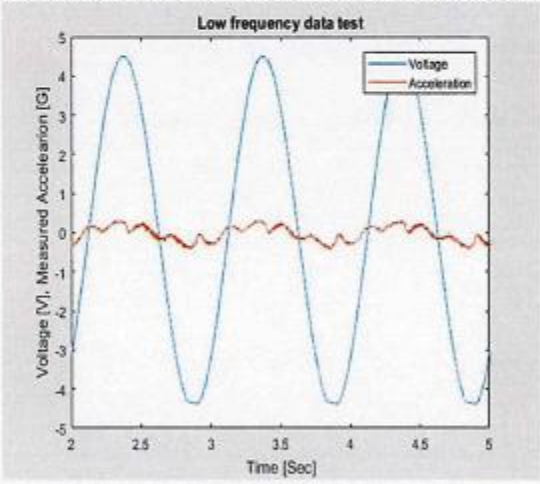

Figure 7: Low Frequency Result: 1 Hz sin wave input

More testing is advised with more sensitive accelerometers. The use of more sensitive accelerometers maybe be able to provide smoother looking acceleration readouts for the lower frequency range.

- **High Frequency Saturation Tests**

The purpose of the high frequency saturation testing was to see the limits of the accelerations that could be produced for all frequencies spanning the usable range of the table. The results of these tests indicated that at the upper range, around 7 Hz and above, saturation becomes an issue. Below this saturation is less of an issue due to unsafe acceleration levels being achieved prior to saturation. As frequency increases the maximum acceleration that can be achieved decreases. We expect this trend to extend past 10 Hz.

Appendix A: Geological Engineering Shaker Table Characterization by Keele & Plum, pg 6/13

Due to the fact that acceleration amplitudes decrease as you ask the table to move more quickly (i.e. higher frequencies), we believe that the saturation of acceleration is due to saturation of the controller output.

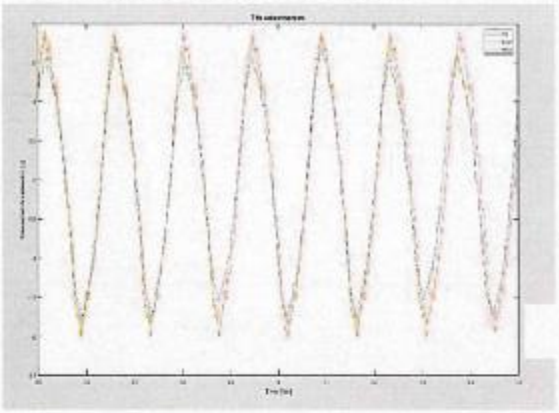

Figure 8: Example of high frequency saturation. Voltage continues to increase but amplitude of acceleration remains constant

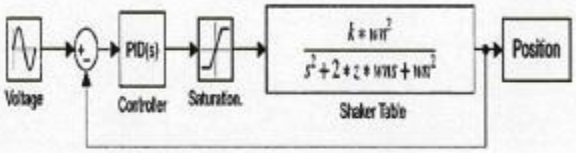

Figure 9: Block diagram of what we believe is causing the high frequency saturation

- **Loading Testing**

The purpose of the loading testing was to see if the acceleration of the table would be affected by the addition of loading. We applied loading to the table by adding sand bags in increments of 80 lbs. The table was loaded up to 240 lbs. From no load up to 160 lbs There was little variance in the amplitude of acceleration recorded. However, loading the table to 240 lbs resulted in a large jump in acceleration. This result suggests a dependence of amplitude on the loading. This large jump could indicate that we again have stressed the control system and it is having trouble keeping up.

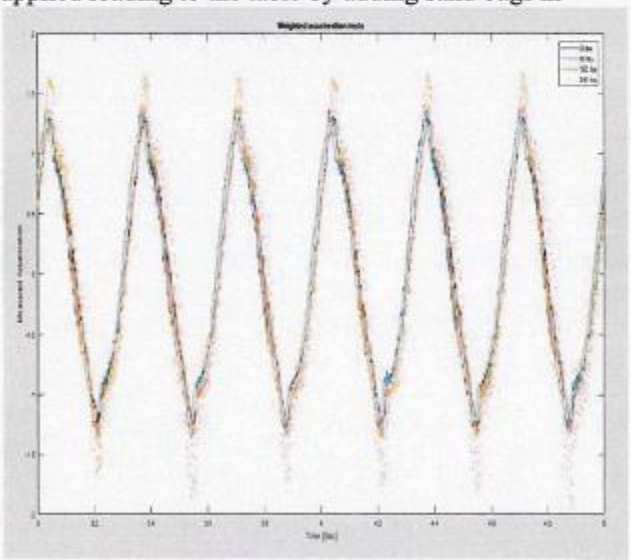

Figure 10: Weighted Acceleration Results for 3 Hz sin wave.

We only performed this testing at 3 Hz. Therefore, it is advised to complete this testing for the full range of useable frequency. This further testing would be very beneficial to understand further understanding the dynamics of the table. This will be especially enlightening if this data is compared to the initial amplitude variance results.

Appendix A: Geological Engineering Shaker Table Characterization by Keele & Plum, pg 7/13

SECTION 3: "HELPFUL TIPS AND TRICKS"

Included in this section is anything we found that may be useful in dealing with the Shaker Table. This includes anything from bugs we found in the MT EarthQuake program to helpful tips on using the table.

- **MT EarthQuake Monitor code bugs:**
  - Acceleration data is recorded as the negative of the actual data: This is helpful to know when analyzing the actual data recorded.
  - Voltage clipping for sine waves greater than 4.4V: When a voltage profile is inputted that is greater than 4.4V the negative portion of the sine wave will start to clip. This is however only in the code itself. The table does not see the physical clipping of the voltage profile.
  - Vibration profile generator: When using the vibration profile generator to create voltage profiles you are only able to create sine waves in integer frequencies. If you do non integer instead of getting a full peak to peak sine wave it will create a rectified sine wave with only positive portions of the wave.

- **Zeroing the table**

Before any test is performed the table should always be set to the zero position. This can be done in a couple of ways. The first of which is just inputting a voltage profile of all zeros to the table. The other way is to use the analog out level function of the table and set the level to zero. Both ways will zero the table so that you are able to perform tests.

- **Viewable plots**

The MT EarthQuake Monitor program has a multitude of visible plots that can be displayed. Most of these plots do not show information of any importance. The program starts up with all plots on. To only display the plots you are looking for it can be done from the main page of the program. Shown in Figure 3 there is a list of the plots on the right hand side. To turn the plots on or off simple right click on the plot and click on the "Plot Visible" button. This will turn that specific on/off.

Appendix A: Geological Engineering Shaker Table Characterization by Keele & Plum, pg 8/13

APPENDIX A:

- **Acceleration Conversion tool**:

The acceleration conversion tool is a graphical user interface that allows for the easy conversion of accelerations to voltages which can be sent to the Shaker Table. This application was developed during the fall 2018/spring 2019 senior design project.

- **How to use the Application**:

The application requires a MATLAB installation to work. If '.mlapp' files extensions are set up on your computer to open automatically with MATLAB then simply double click on the file 'AccelerationApp.mlapp', otherwise start up MATLAB. While in MATLAB change your working directory to the folder with the file 'AccelerationApp.mlapp' in it. From here all you need to do is type 'AccelerationApp' and the following GUI should appear.

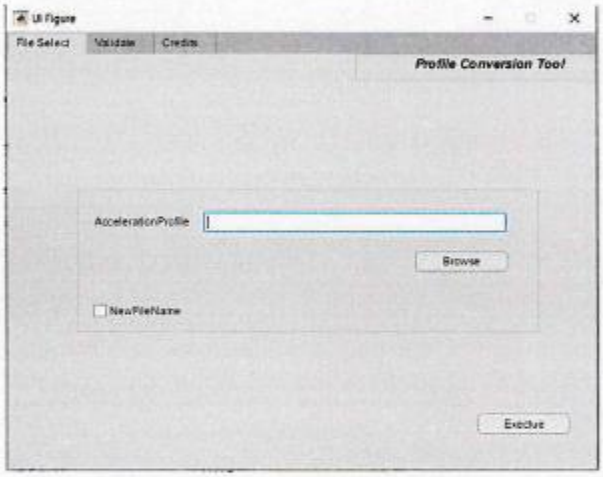

Figure 1: Acceleration to Voltage App Overview

Pressing the browse function will open the file explorer from here simply go into the folder named 'Acceleration' and select the Acceleration Profile you need.

* Earthquake Profiles should be set up as a single column of numbers in a .txt file.

Simply press execute after you've selected the desired Acceleration Profile. The voltage profile will be saved into the folder named 'Voltage'. The name of the voltage profile will default to 'voltage.txt' unless the 'NewFileName' box is checked.

The validate tab plots the voltage profile and acceleration profile for a quick double check to make sure you get the profiles you were expecting.

- **Overview of how Application works**:

The Application functions by use of signals and systems concepts. Using the Fast Fourier Transform we were able to find the spectra (magnitude a phase information) associated with desired Accelerations Profiles. We used the inverse of our transfer function we developed to scale our desired Accelerations to the required Accelerations. We then used the Inverse Fourier Transform to get a time domain required Acceleration and integrated this twice to get displacement. A unit conversion term to get from g's to inches per second as well as a factor to get from in to volts was then applied to achieve a time domain voltage profile that would produce the desired Acceleration.

Appendix A: Geological Engineering Shaker Table Characterization by Keele & Plum, pg 9/13

- **Method for Interpolation**:

A transfer function is a model of a devices outputs for given inputs. Using data gathered during the senior design project we created a base for our transfer function. We filled out our transfer function fully using linear interpolation by means of the interp1() function. Due to the fact that we only had a single sided transfer function we mirrored it using the fliplr() function and concatenated the reflection and original. We did a similar procedure with the phase and frequencies.

- **Method for Fourier Transform**:

The MATLAB code makes use of the function fft() to take the Fourier transform of desired accelerations. To convert our required acceleration back to the time domain we used the function ifft(). Due to the fact that our interpolated function is centered about zero we used fftshift() to move our fft() data to be centered about zero as well. At the end we performed another fftshift() of our altered Acceleration to shift it back and used the ifft() to get the Acceleration back to the as a time domain vector.

- **Method of integration**:

We used the trapezoid rule to integrate our new Acceleration. This was done by using the cumtrapz() function in MATLAB. The mean was subtracted off each integration due to the nature of integrated sinusoids.

- **Helper Functions**:

A few helper functions were written to clean up the main code.

  - 'toText.m' writes data to text files.
  - 'fromText.m' reads data in from text files.
  - 'Widthof.m' calculates the average spacing of vectors.

These files should be in the Dependencies folder for function of the application.

* toText and fromText only write and read to and from single columnated text files and therefore inputs files must be formatted as such.

- **Notes**:
  - **Sampling Frequency**

Much of the operation of the application is dependent on the sampling frequency being 800 samples per second. If a different sampling frequency was used for Acceleration profiles the variable 'Fs' must be changed in 'Convert.m' and if possible the sampling rate of the table should be adjusted as well.

If a sampling frequency is unknown but a time vector is associated with the Acceleration Profile, then you can simply find the sampling frequency by getting the sampling period and taking the reciprocal of this as your sampling frequency. The sampling period will be the mean spacing of the time vector.

Appendix A: Geological Engineering Shaker Table Characterization by Keele & Plum, pg 10/13

- **Acceleration Profile Formatting**

Due to some variance in formatting of acceleration profiles it may be necessary to edit time histories to remove a column of data associated with the time vector. It is suggested to use a text editor like notepad++ because it has a columnal selection feature which will make the conversion of time histories to acceleration profiles much less tedious.

Appendix A: Geological Engineering Shaker Table Characterization by Keele & Plum, pg 11/13

APPENDIX B: MATLAB CODE

```
function [t Voltage Acc_t] = Convert_array(AccelerationProfile,DesiredName)

%This function converts acceleration profiles to voltage profiles
%for input to the geological shaker table

% Dependencies :
%           Widthof.m          | Calculates average spacing of vector
%           toText.m           | Writes data to text file
%           fromText.m         |reads data from text file

addpath('Dependencies');
for(i = 1:length(AccelerationProfile))
%%
%%%%%%%%%%%%%%%%%%%%%%%%%%%% Acceleration Data %%%%%%%%%%%%%%%%%%%%%%%%%%%%
[Acc_t, time] = fromText(strcat('Acceleration/',AccelerationProfile(i)));


A = fftshift(fft(Acc_t));                              % Moving fft to center
around 0

Fs = 800; Ts = 1/Fs; END = time; t = (0:END-1)*Ts'; % need to change time for
                                                     % actual time vector
                                                     % eventually
N = length(A);No = length(Acc_t);
to = t;

Ts_AP = Widthof(t); Fs_AP = 1/Ts_AP; % calculating average spacing of the
time vector read in

%%
%%%%%%%%%%%%%%%%%%%%%%%%%%%% Interpolation %%%%%%%%%%%%%%%%%%%%%%%%%%%%%%%%

 %   Using acceleration data collected from shaker table
 %   a frequency response is created by interpolating the
 %   rough data to curve fit for All the frequencies required
 %   for Acceleration inputs

f = (0:N-1)*Fs/N-Fs/2;      % Shifting frequency vector to +_Nyquist
figure;plot(f,abs(A))

n=N/2; fp = (0:(n-1))'*(Fs/(2*n));

f_tp = [0.0 2.0 2.5 3.0...
        3.5 4.0 4.5 5.0...
        5.5 6.0 6.5 7.0...
        7.5 8.0 8.5 9.0...
        9.5 10.0 Fs/2];

M_tp = [.9235 .9235  (1.44*1.2) (1.8424) ... 0.0 2.0 2.5 3.0
        (2.2207) (2.5403) (2.7489) (2.1883) ... 3.5 4.0 4.5 5.0
        (1.5586) (1.0755) (.8071) (0.5405)...  5.5 6.0 6.5 7.0 (over at 1.75
but under at 1)
```

Appendix A: Geological Engineering Shaker Table Characterization by Keele & Plum, pg 12/13

```
        (.3507*1.4) (.2626*1.25) (.2051*1.1) (.1565) ...  7.5 8.0 8.5 9.0
        (.1297*.85) (.09574*.8) (.09574*.8)]; ... 9.5 10.0 Fs/2

P_tp = [  0    -28.26 -34.72 -38.07 ...
        -45.04 -57.96 -74.52 -127.3 ...
        -150.5 -170.6 -190.7 -194.7 ...
        -196   -196   -197   -197   ...
        -197   -197   -197 ]*pi/180;

%fliplr reverses the vector so we get symetric reflection about 0hz
fn = (-n:-1)'*(Fs/(2*n));

f_tn = -fliplr(f_tp);
M_tn = fliplr(M_tp);
P_tn = fliplr(P_tp);

Mip = interp1(f_tp,M_tp,fp);
Pip = interp1(f_tp,P_tp,fp);
Min = interp1(f_tn,M_tn,fn);
Pin = interp1(f_tn,P_tn,fn);

X=[Min.*exp(-1i*Pin);Mip.*exp(1i*Pip)]; % frequency response of
                                        % Shaker Table about 0Hz
                                        %-1i is conjugation to maintain
%%

%plots response of shake table
figure(77); plot(f_tp,M_tp,'ob',fp(1:N/2),Mip,'.r');
title('Acc/Acc(Volt) Vs. Frequency');
legend('Real Values','Interpolated')
xlabel('Frequency [Hz]'); ylabel('Magnitude [abs]')
xlim([0 20])

% figure; plot(f_tp,P_tp,fp(1:N/2),Pip);
% legend('Real Values','Interpolated')
% xlim([0 20])

V = A./X; %Conversion of acceleration Desired to acceleration needed

a_t = ifft(fftshift(V)); %accleration after tf
a_t = a_t(1:No);
% figure; plot(to,a_t)
% title('Voltage, time (TF output)')

%%
%%%%%%%%%%%%%%%%%%%%%%%%%%%%%% cumtrapz Integration %%%%%%%%%%%%%%%%%%%%%%%%%
I = cumtrapz(to,a_t); %integration using cumtrapz
Avg = mean(I);
I = I - Avg;

II = cumtrapz(t,I); %second integration using cumtrapz
Avg2 = mean(II);
II = II - Avg2;
```

Appendix A: Geological Engineering Shaker Table Characterization by Keele & Plum, pg 13/13

```
%%
%conversion factors g's to in/s^2 ; in to volts
Kg = 1/.00259; Kd = 1/.5;

Voltage = II*Kg*Kd; %II is the 2nd integral of a_t
figure; plot(to,Voltage)
title('Voltage Profile')

toText(strcat('Voltage/',DesiredName(i)),Voltage);
toText('Log/Log.txt','Convert did its job') %put these in for easier
troubleshooting

end
end
```

9. Appendix B: Accelerometer Specifications and Calibrations

DYTRAN INSTRUMENTS, INC.
Dynamic Transducers and Systems
21592 Marilla St. • Chatsworth, CA 91311 • Phone 818-700-7818
www.dytran.com • e-mail: info@dytran.com

SPECIFICATIONS

MODEL 3202A LIVM ACCELEROMETER

SPECIFICATION	VALUE	UNITS
PHYSICAL		
WEIGHT	160	GRAMS
SIZE, L x D x H	2.26 x 1.44 x 1.12	IN
MOUNTING PROVISION, (MOD 6523 SCREW PROVIDED)	THRU HOLE, CAPTIVE 1/4-28 SCREW	
ELECTRICAL CONNECTOR, RADIAL (MIL-C-5015)	2-PIN MILITARY 10SL-4P, HERMETIC	
MATERIAL CASE/CONNECTOR	316L	ST. STEEL
PERFORMANCE		
SENSITIVITY, ± 5% [1]	100	mV/G
RANGE FOR ± 5 VOLTS OUT	±50	G
FREQUENCY RESPONSE, ± 5%	.5 - 5,000	Hz
MOUNTED RESONANT FREQUENCY	>25	kHz
EQUIV. ELECTRICAL NOISE FLOOR, (RESOLUTION)	.0002	G RMS
AMPLITUDE NON-LINEARITY (ZERO BASED BEST FIT ST.LINE METHOD)	2.0	% F.S., MAX.
TRANSVERSE SENSITIVITY, MAX.	5	PERCENT
STRAIN SENSITIVITY	.0015	G's PER MICROSTRAIN @ 250/με
ENVIRONMENTAL		
MAXIMUM VIBRATION	350	G's, RMS
MAXIMUM SHOCK	3000	G's, PEAK
TEMPERATURE RANGE	-60 TO +250	°F
ENVIRONMENTAL SEAL	GLASS TO METAL/WELDED, HERMETIC	
ELECTRICAL		
COMPLIANCE (SUPPLY) VOLTAGE RANGE [2]	+20 to +30	VDC
EXCITATION CURRENT RANGE	2 to 20	mA
OUTPUT IMPEDANCE, NOM.	200	OHMS
OUTPUT BIAS VOLTAGE RANGE	11 to 13.0	VDC
DISCHARGE TIME CONSTANT	1.0 to 2.0	SEC.
OUTPUT SIGNAL POLARITY FOR ACCELERATION TOWARD TOP	POSITIVE GOING	
POWER/SIGNAL GROUND to CASE ISOLATION, MIN.	10	GΩ

SUPPLIED ACCESSORIES:

(1) Model 6523, 1/4-28 MOUNTING SCREW

[1] MEASURED AT 100 Hz, 1 G RMS. A CALIBRATION CERTIFICATE TRACEABLE TO **NIST** IS SUPPLIED WITH EACH INSTRUMENT.

[2] THE USE OF DYTRAN LIVM CURRENT SOURCE POWER UNITS IS RECOMMENDED. **DO NOT CONNECT THIS INSTRUMENT TO A SOURCE OF DC VOLTAGE WITHOUT CURRENT LIMITING PROTECTION, 20 mA MAX.** TO DO SO WILL DESTROY THE INTERNAL AMPLIFIER AND VOID THE WARRANTY.

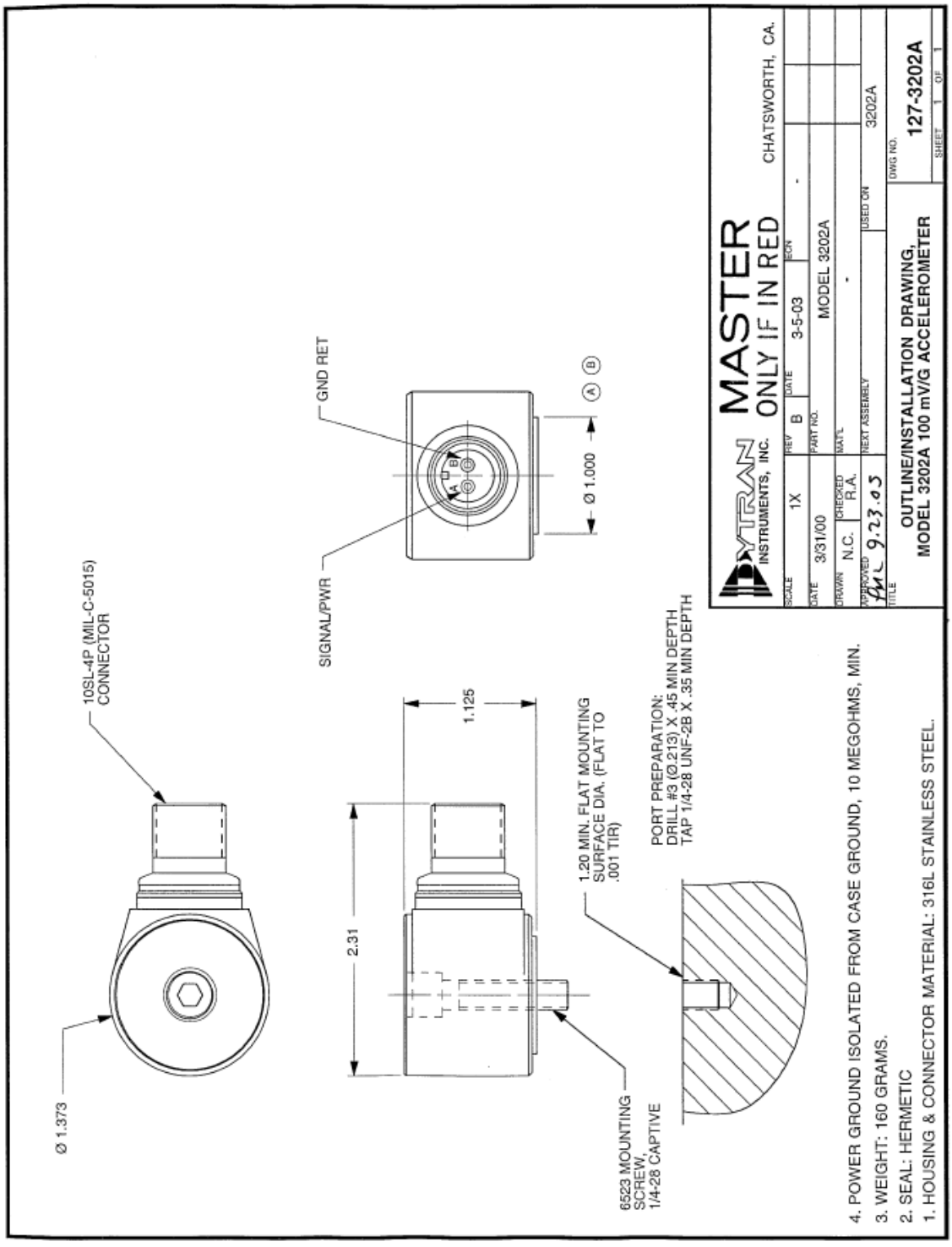
10SL-4P (MIL-C-5015)
CONNECTOR
Ø 1.373
GND RET
SIGNAL/PWR
Ø 1.000
A B
1.125
2.31
1.20 MIN. FLAT MOUNTING
SURFACE DIA. (FLAT TO
.001 TIR)
PORT PREPARATION:
DRILL #3 (Ø.213) X .45 MIN DEPTH
TAP 1/4-28 UNF-2B X .35 MIN DEPTH
6523 MOUNTING
SCREW,
1/4-28 CAPTIVE
4. POWER GROUND ISOLATED FROM CASE GROUND, 10 MEGOHMS, MIN.
3. WEIGHT: 160 GRAMS.
2. SEAL: HERMETIC
1. HOUSING & CONNECTOR MATERIAL: 316L STAINLESS STEEL.
MASTER
ONLY IF IN RED
DYTRAN INSTRUMENTS, INC.
CHATSWORTH, CA.
SCALE 1X
REV B
DATE 3-5-03
ECN -
DATE 3/31/00
PART NO. MODEL 3202A
DRAWN N.C.
CHECKED R.A.
MAT'L -
APPROVED 9.23.05
NEXT ASSEMBLY
USED ON 3202A
TITLE
OUTLINE/INSTALLATION DRAWING,
MODEL 3202A 100 mV/G ACCELEROMETER
DWG NO. 127-3202A
SHEET 1 OF 1

SPECIFICATIONS

MODELS 3166B, 3166B1 & 3166B2 LIVM ACCELEROMETER

SPECIFICATION	VALUE	UNITS
PHYSICAL		
WEIGHT	228	GRAMS
SIZE, L x W x H	2.90 x 1.00 x 1.21	IN
MOUNTING PROVISION, (MOD 6523 SCREW PROVIDED)	THRU HOLE, CAPTIVE 1/4-28 SCREW	
ELECTRICAL CONNECTOR, RADIAL	2-PIN MILITARY 10SL-4P, HERMETIC	
MATERIAL CASE/CONNECTOR	316L	ST. STEEL
ELEMENT STYLE	CERAMIC PLANAR SHEAR	
PERFORMANCE		
SENSITIVITY, ± 5% 3166B/3166B1/B2 [1]	100/500/10	mV/G
RANGE FOR ± 5 VOLTS OUT, 3166B/ 3166B1/ 3166B2	±50/ ±10/ ±500	G
FREQUENCY RESPONSE, ± 10%, 3166B/ 3166B1/ 3166B2	0.3 – 5,000	Hz
MOUNTED RESONANT FREQUENCY	>21	kHz
EQUIV. ELECT. NOISE FLOOR, (RESOLUTION) 3166B/ 3166B1/ 3166B2	.00006/ .00008/ .001	G RMS
AMPLITUDE NON-LINEARITY (ZERO BASED BEST FIT ST.LINE METHOD)	2.0	% F.S., MAX.
TRANSVERSE SENSITIVITY, MAX.	5	PERCENT
STRAIN SENSITIVITY	0.0001	G/με @ 250/με
ENVIRONMENTAL		
MAXIMUM VIBRATION	350	G's, RMS
MAXIMUM SHOCK	3000	G's, PEAK
TEMPERATURE RANGE	-60 TO +250	°F
ENVIRONMENTAL SEAL	GLASS TO METAL/WELDED,HERMETIC	
ELECTRICAL		
COMPLIANCE (SUPPLY) VOLTAGE RANGE [2]	+20 to +30	VDC
EXCITATION CURRENT RANGE	2 to 20	mA
OUTPUT IMPEDANCE, NOM.	200	OHMS
OUTPUT BIAS VOLTAGE	+11 to +13	VDC
DISCHARGE TIME CONSTANT	0.9 to 2.0	SEC.
OUTPUT SIGNAL POLARITY FOR ACCELERATION TOWARD TOP	POSITIVE GOING	
POWER/SIGNAL GROUND to CASE ISOLATION, MIN	10	GIGAOHMS

SUPPLIED ACCESSORIES:

(1) Model 6523, 1/4-28 captive, socket head cap screw

[1] MEASURED AT 100 Hz, 1 G RMS. A CALIBRATION CERTIFICATE TRACEABLE TO **NIST** IS SUPPLIED WITH EACH INSTRUMENT.

[2] THE USE OF DYTRAN LIVM CURRENT SOURCE POWER UNITS IS RECOMMENDED. **DO NOT CONNECT THIS INSTRUMENT TO A SOURCE OF DC VOLTAGE WITHOUT CURRENT LIMITING PROTECTION, 20 mA MAX.** TO DO SO WILL DESTROY THE INTERNAL AMPLIFIER AND VOID THE WARRANTY.

REV	ECN	DESCRIPTION	BY/DATE	CHK	APPR
A	6577	ADDED 3166M5 TO USED ON BLOCK, ADDED MARKING	JS 03/01/10		

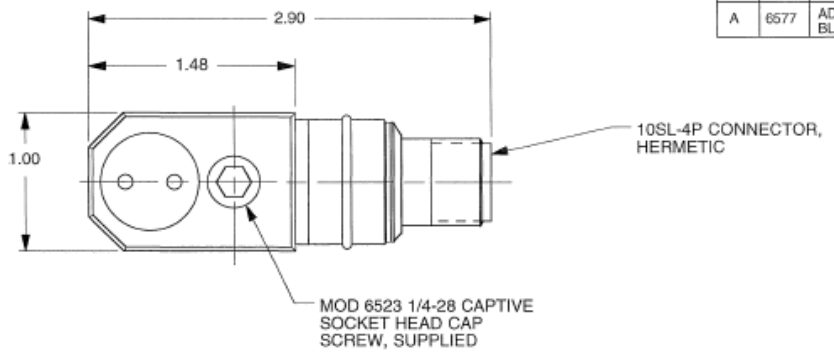

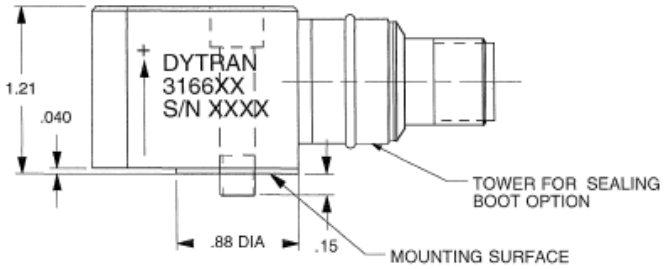

CONNECTOR PINOUT:
PIN A: SIG/PWR
PIN B: GND RETURN

1) POWER GROUND IS INSULATED FROM CASE BY >10 MEGOHMS.
2) SEAL: HERMETIC.

EXCEPT AS OTHERWISE NOTED
ALL DIMENSIONS IN INCHES
TOLERANCE: .XXX = ± .005 .XX= ± .01
SURFACE FINISH EXCEPT AS NOTED √
BREAK EDGES TO DEBURR RADIUS OR CHAMFER
△ THESE DIAS Ⓜ TO .005 T.I.R.
FILLETS - MAX RAD.

DYTRAN INSTRUMENTS, INC. CHATSWORTH, CA.

MASTER
ONLY IF IN RED

SCALE 1X	REV -	DATE -	ECN -		
DATE 7-29-02	PART NO. MODELS 3166B, B1& B2				
DRAWN N.C.	CHECKED R.A.	MAT'L -			
APPROVED Ag S.	NEXT ASSEMBLY	USED ON 3166B, 3166B1, 3166M5			

TITLE: **OUTLINE/INSTALLATION DRAWING, MODELS 3166B, 3166B1 & 3166B2**

DWG NO. **127-3166B**

SHEET 1 OF 1

Model Number	PERFORMANCE SPECIFICATIONS	DOC NO
3055D1		PS3055D1
	IEPE ACCELEROMETER	REVE, ECN 13045, 10/08/15

- HERMETICALLY SEALED
- BASE ISOLATED
- IDEAL LOW FREQUENCY RESPONSE

		ENGLISH		SI	
PHYSICAL					
Weight		0.35	oz	10	grams
Connector	Type	10-32		10-32	
Mounting Provision	Tapped Hole	10-32 X .150 ↓		10-32 X .150 ↓	
Material, Housing/Connector		Titanium		Titanium	
Sensing Element		Ceramic		Ceramic	
Element Style		Planar Shear		Planar Shear	
PERFORMANCE					
Sensitivity, ± 5% [1]		10	mV/g	1	mV/m/s²
Range for ± 5 Volts Output		500	g	4905	m/s²
Frequency Response, ± 5%		1 to 5000	Hz	1 to 5000	Hz
Frequency Response, ± 10%		1 to 10000	Hz	1 to 10000	Hz
Resonant Frequency		> 36	kHz	> 36	kHz
Broad Band Resolution		0.0030	Grms	0.029	m/s² rms
Spectral Noise	1Hz	340	µGrms/√(Hz)	3335	m/s² rms/√(Hz)
	10Hz	130	µGrms/√(Hz)	1275	m/s² rms/√(Hz)
	100Hz	36	µGrms/√(Hz)	353	m/s² rms/√(Hz)
	1000Hz	21	µGrms/√(Hz)	206	m/s² rms/√(Hz)
	10000Hz	12	µGrms/√(Hz)	117.7	m/s² rms/√(Hz)
Linearity [2]		± 1	% F.S.	± 1	% F.S.
Maximum Transverse sensitivity		5	%	5	%
Strain Sensitivity @ 250µε		0.002	g/µε	0.02	m/s²/µε
ENVIRONMENTAL					
Maximum Vibration		600	Gpeak	5886	m/s² peak
Maximum Shock		5000	Gpeak	49050	m/s² peak
Temperature Range (<3% Sensitivity Deviation)		+50 to +100	°F	10 to 38	°C
Temperature Range		-67 to +250	°F	-55 to 121	°C
Seal		Hermetic		Hermetic	
ELECTRICAL					
Supply Current Range [3]		2 to 20	mA	2 to 20	mA
Compliance Voltage Range		18 to +30	Volts	18 to +30	Volts
Output Impedance, Typ		100	Ω	100	Ω
Bias Voltage		11 to 13	VDC	11 to 13	VDC
Discharge Time Constant		0.5 to 1.5	Sec	0.5 to 1.5	Sec
Electrical Isolation		10	GΩ, min	10	GΩ, min

This family also includes:

Model	Sensitivity (mV/g)	Frequency Response (Hz)	Time Constant (Sec)	Operating Temp (°F)
3055D2	100	1 to 10000	0.5 to 1.5	-67 to +250
3055D3	500	1 to 10000	0.5 to 1.5	-67 to +225
3055D4	50	1 to 10000	0.5 to 1.5	-67 to +250
3055D5	20	1 to 10000	0.5 to 1.5	-67 to +250
3055D6	200	1 to 10000	0.5 to 1.5	-67 to +225

Refer to the performance specifications of the products in this family for detailed description

Supplied Accessories:

1) Accredited calibration certificate (ISO 17025)
2) Model 6200 mounting stud, qty 1

Notes:

[1] Measured at 100Hz, 1 Grms per ISARP37.2.
[2] Measure using zero-based straight line method, % of F.S. or any lesser range.
[3] Do not apply power to this system without current limiting, 20 mA MAX. To do so will destroy the IC charge amplifier.
[4] In the interest of constant product improvement, we reserve the right to change specifications without notice.

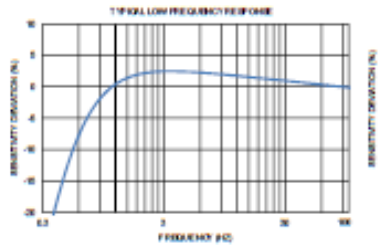

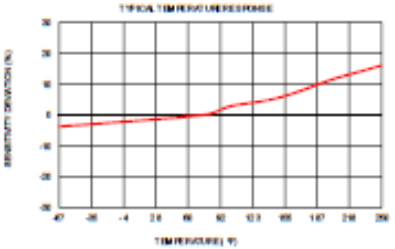

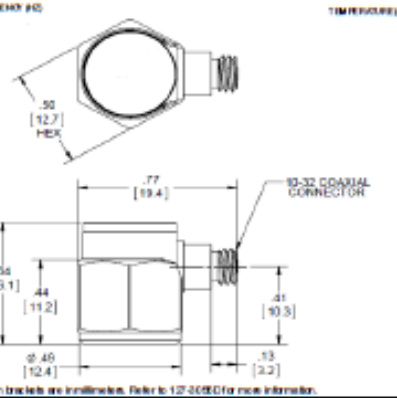

Units on the line drawing are in inches, units in brackets are in millimeters. Refer to 127-2055D for more information.

21592 Marilla Street, Chatsworth, California 91311 Phone: 818.700.7818 Fax:818.700.7880 www.dytran.com
For permission to reprint this content, please contact info@dytran.com

PROPRIETARY AND CONFIDENTIAL

THE INFORMATION CONTAINED IN THIS DRAWING IS THE SOLE PROPERTY OF DYTRAN INSTRUMENTS INC. ANY REPRODUCTION IN PART OR AS A WHOLE WITHOUT THE WRITTEN PERMISSION OF DYTRAN INSTRUMENTS INC. IS PROHIBITED

MODEL	SENSITIVITY
3055D1	10 mV/g
3055D2	100 mV/g
3055D3	500 mV/g
3055D4	50 mV/g
3055D5	20 mV/G
3055D6	200 mV/g

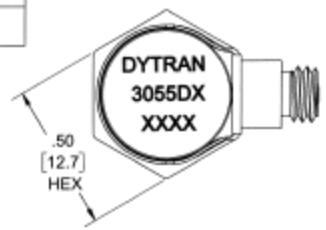

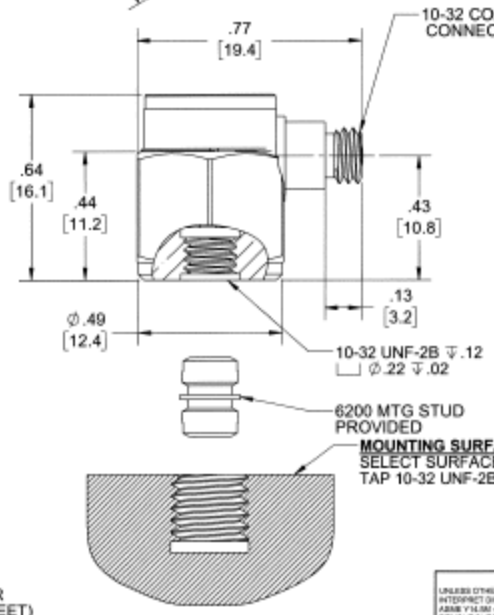

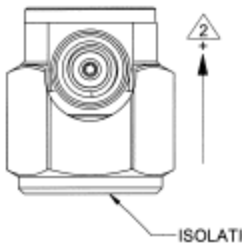

REVISIONS					
REV.	ECN	DESCRIPTION	BY/DATE	CHK	APPR
A	11394	INITIAL RELEASE	RA, 11/05/14	EM	DV
B	14310	ZONE B3 10-32 UNF WAS: 10-32 UNC	RA, 06/28/18		

4 MATES WITH DYTRAN 6010AXX OR 6011AXX CABLE (XX=LENGTH IS FEET)

3. WEIGHT: 10 GRAMS, MAX.

2 ARROW INDICATES ACCELERATION DIRECTION FOR POSITIVE OUTPUT.

1. MATERIAL: TITANIUM ALLOY

NOTES: UNLESS OTHERWISE SPECIFIED

UNLESS OTHERWISE SPECIFIED: INTERPRET DIM & TOL PER ASME Y14.5M - 1994. REMOVE BURRS. CO-INTERSHIM INTERNAL THDS 90° TO MAJOR DIA. CHAM EXT THDS 45° TO MINOR DIA. THD LENGTHS AND DEPTHS ARE FOR MIN FULL THDS. DIMENSIONS APPLY AFTER FINISHING. ALL MACHINED SURFACES: TOTAL RUNOUT WITHIN .005. BREAK SHARP EDGES .005 TO .010. MACHINED FILLET RADII .005 TO .015. WELDING SYMBOLS PER AWS A2.4. ABBREVIATIONS PER MIL-STD-12.

UNLESS OTHERWISE SPECIFIED: DIMENSIONS ARE IN INCHES. DECIMALS TOLERANCES ARE: .XX ±.01 .XXX ±.005 ANGLES ±1°

APPROVALS		DATE
DRAWN	RA	05/29/14
DESIGN	RA	01/23/14
CHK	EM	12/17/14
APP	DV	12/17/14

DO NOT SCALE DRAWING

DYTRAN INSTRUMENT, INC. Chatsworth, CA

MASTER

ONLY IF IN RED

TITLE: OUTLINE/INSTALLATION, ACCEL, ISOLATED, 10 MV/G, SIDE 10-32 CONN

SIZE	CAGE CODE	DWG NO	REV
B	2W033	127-3055D	B

SCALE: 3:1 PART NO: SHEET 1 OF 1

Model Number	PERFORMANCE SPECIFICATIONS	DOC NO
3056D1	IEPE ACCELEROMETER	PS3056D1
		REVISION: D (12/15/15)

- HERMETICALLY SEALED
- BASE ISOLATED

		ENGLISH		SI	
PHYSICAL					
Weight		0.35	oz	10	grams
Connector	Type	10-32		10-32	
Mounting Provision	Tapped Hole	10-32 X .150 ↓		10-32 X .150 ↓	
Material, Housing/Connector		Titanium		Titanium	
Sensing Element		Ceramic		Ceramic	
Element Style		Planar Shear		Planar Shear	
PERFORMANCE					
Sensitivity, ±5% [1]		10	mV/G	1.0	mV/m/s²
Range for ± 5 Volts Output		500	G peak	4905	m/s²
Frequency Response, ±10%		1 to 10,000	Hz	1 to 10,000	Hz
Resonant Frequency		> 36	kHz	> 36	kHz
Broad Band Resolution		0.0040	G rms	0.0392	m/s² rms
Linearity [2]		±1	% F.S.	±1	% F.S.
Maximum Transverse Sensitivity		5	%	5	%
Strain Sensitivity @ 250με		0.001	G/με	0.01	m/s²/με
ENVIRONMENTAL					
Maximum Vibration		600	G peak	5886	m/s² peak
Maximum Shock		3000	G peak	29430	m/s² peak
Temperature Range		-67 to 250	°F	-55 to 121	°C
Seal		HERMETIC		HERMETIC	
ELECTRICAL					
Supply Current Range [3]		2 to 20	mA	2 to 20	mA
Compliance Voltage Range		+18 to +30	Volts	+18 to +30	Volts
Output Impedence, Typ		100	Ω	100	Ω
Bias Voltage		+9 to +13	VDC	+9 to +13	VDC
Discharge Time Constant		.5 to 1.5	Sec	.5 to 1.5	Sec
Electrical Isolation		10	GΩ, min	10	GΩ, min

This family also includes:

Model	Sensitivity (mV/g)	Frequency Response (Hz)	Time Constant (Sec)	Operating Temp (°F)
3056D2	100	1 to 10000	0.5 to 1.5	-67 to +250
3056D3	500	1 to 10000	0.5 to 1.5	-67 to +225
3056D4	20	1 to 10000	0.5 to 1.5	-67 to +250
3056D5	50	1 to 10000	0.5 to 1.5	-67 to +250
3056D6	200	1 to 10000	0.5 to 1.5	-67 to +225
3056D7	1	1 to 10000	0.5 to 1.5	-67 to +250
3056D8	5	1 to 10000	0.5 to 1.5	-67 to +250

Refer to the performance specifications of the products in this family for detailed description

Supplied Accessories:

1) Accredited calibration certificate (ISO 17025)

Notes:

[1] Measured at 100Hz, 1 Grms per ISA RP 37.2.

[2] Measured using zero-based straight line method, % of F.S. or any lesser range.

[3] Do not apply power to this system without current limiting, 20 mA MAX. To do so will destroy the IC charge amplifier.

[4] In the interest of constant product improvement, we reserve the right to change specifications without notice.

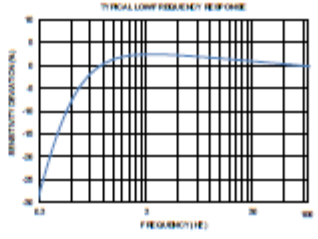

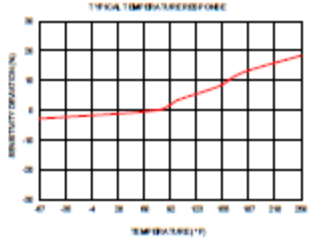

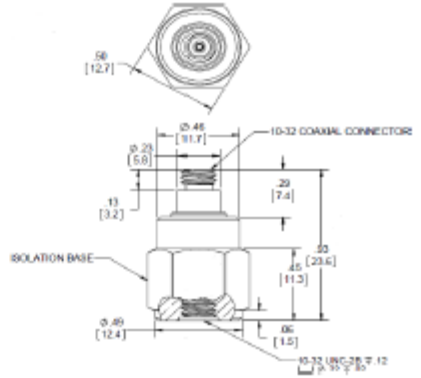

Units on the line drawing are in inches, units in brackets are in millimeters. Refer to GT-3056D for more information.

21592 Marilla Street, Chatsworth, California 91311 Phone: 818.700.7818 Fax:818.700.7880 www.dytran.com

For permission to reprint this content, please contact info@dytran.com

PROPRIETARY AND CONFIDENTIAL

THE INFORMATION CONTAINED IN THIS DRAWING IS THE SOLE PROPERTY OF DYTRAN INSTRUMENTS INC. ANY REPRODUCTION IN PART OR AS A WHOLE WITHOUT THE WRITTEN PERMISSION OF DYTRAN INSTRUMENTS INC. IS PROHIBITED

MODEL	SENSITIVITY
3056D1	10 mV/g
3056D2	100 mV/g
3056D3	500 mV/g
3056D4	20 mV/g
3056D5	50 mV/g
3056D6	200 mV/g
3056D7	1 mV/g
3056D8	5 mV/g

DWG NO 127-3056D SH 1 REV D

REVISIONS

REV.	ECN	DESCRIPTION	BY/DATE	CHK	APPR
A	11394	INITIAL RELEASE	RA, 11/06/14	EM	DV
B	11943	REVISED MARKING LOCATION, ADDED VIEW A-A	RA, 05/05/15	MH	LN
C	11983	3056D7 WAS: 5 mV/g, ADDED: 3056D8	LA 05/28/15	DV	MH
D	14310	ZONE B3 10-32 UNF WAS: 10-32 UNC	RA, 06/28/18		

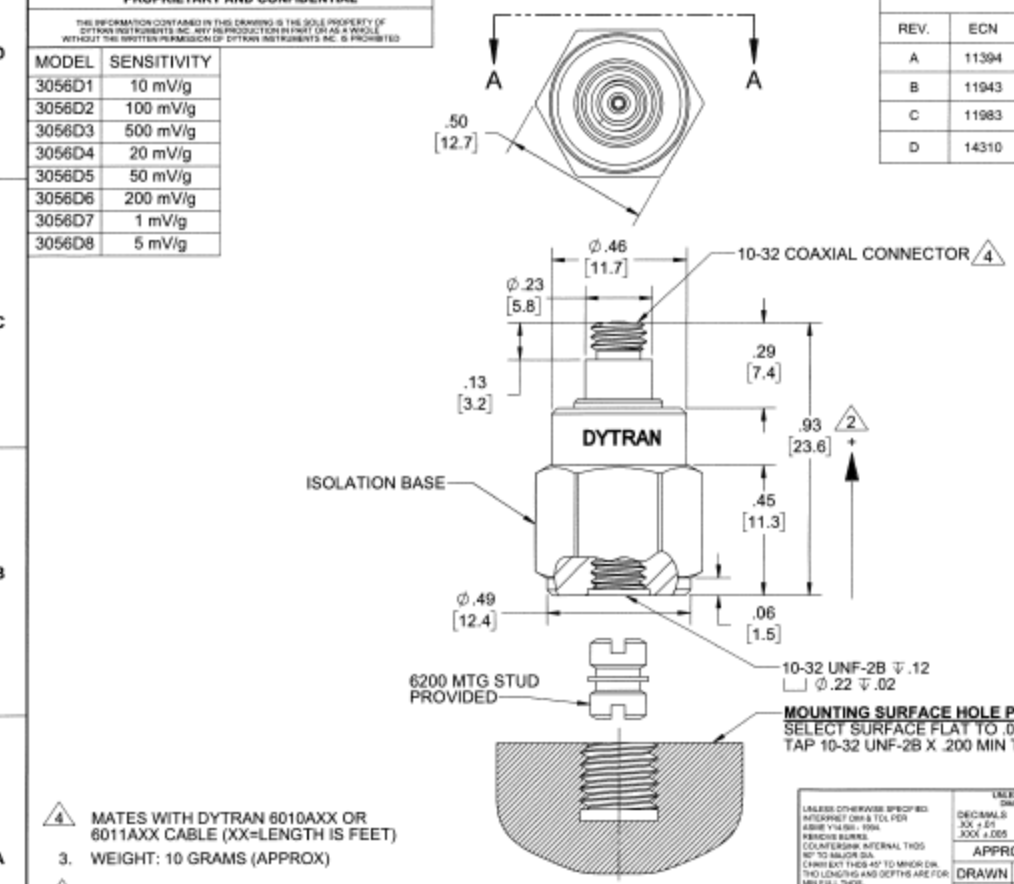

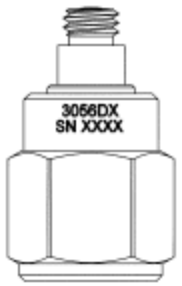

VIEW A-A
ROTATED 180°CW

4 MATES WITH DYTRAN 6010AXX OR 6011AXX CABLE (XX=LENGTH IS FEET)

3. WEIGHT: 10 GRAMS (APPROX)

2 ARROW INDICATES ACCELERATION DIRECTION FOR POSITIVE OUTPUT.

1. MATERIAL: TITANIUM ALLOY

NOTES: UNLESS OTHERWISE SPECIFIED

UNLESS OTHERWISE SPECIFIED DIMENSIONS ARE IN INCHES. TOLERANCES ARE: DECIMALS XX ±.01 XXX ±.005 ANGLES ±1°

APPROVALS		DATE
DRAWN	RA	10/29/14
DESIGN	RT	08/28/14
CHK	EM	12/12/14
APP	DV	12/17/14

DO NOT SCALE DRAWING

DYTRAN INSTRUMENTS, INC. Chatsworth, CA

MASTER ONLY IF IN RED

TITLE: OUTLINE/INSTALLATION, MODEL 3056D

SIZE	CAGE CODE	DWG NO	REV
B	2W033	127-3056D	D

SCALE: 3:1 | PART NO: 3056D | SHEET 1 OF 1

Dytran Instruments, Inc.
21592 Marilla St. Chatsworth, CA 91311 Ph: 818-700-7818
Fax 818-700-7880, www.dytran.com email: info@dytran.com

CALIBRATION CERTIFICATE

CUSTOMER:	*MONTANA TECH*		**STATION:** 9	**REPORT #:**	**26430**
PO #:	*CC-DC2819*	**SO#:** *197771*	**TEMP (°C):** 24	**PROCEDURE:**	**TP-3002**
MODEL:	*3055D3T*	**S/N:** *26430*	**TYPE[1]:** 1	**AS RECEIVED:**	**AS RETURNED:**

INPUT	FREQUENCY	Sens
g's	Hz	mV/g
1.00	2	515.99
1.00	20	491.06
1.00	30	490.51
1.00	50	490.60
1.00	**100**	**486.95**
1.00	300	483.62
1.00	500	481.26
1.00	1000	478.11
1.00	3000	475.73
1.00	5000	472.23
1.00	8000	494.97
1.00	10000	501.21
BIAS	**VDC**	11.90
TRANSVERSE SENS. (%):		0.70
DISCHARGE T.C. (SEC.):		0.90

CALIBRATION EQUIPMENT

DII#	DESCRIPTION	CAL. DUE DATE
1776	DAQ	8/18/2019
1289	ACCELEROMETER	2/23/2019

CALIBRATION NOTES:
1451.4 v1.0 UNLOCKED

* [1] CALIBRATION TYPE CODE:
1-NEW UNIT 2-RE-CALIBRATION
* [2] IF APPLICABLE
* [3] UNCERTAINTY STATEMENT APPLIES TO CALIBRATED PARAMETERS ONLY
* [4] THIS CALIBRATION WAS PERFORMED IN ACCORDANCE WITH ANSI/NCSL Z540-1-1994, ISO 10012-1, ISO/IEC17025

* AS RECEIVED/AS RETURN CODES:
1 = IN TOLERANCE, NO ADJUSTMENTS
2 = IN TOLERANCE, BUT ADJUSTED
3 = OUT OF TOLERANCE < 5%
4 = OUT OF TOLERANCE > 5%
5 = REPAIR REQUIRED
6 = REPAIRED AND CALIBRATED
7 = UNIT NON-REPAIRABLE, RECOMMEND REPLACEMENT
8 = UNIT SERVICEABLE WITH CURRENT CALIBRATION DATA

* ESTIMATED UNCERTAINTY OF CALIBRATION [3]
SENSITIVITY OVER FREQUENCY: 1-20HZ-2.1%,20-100HZ-1.9%, 100-2,500HZ-1.5%,2,500-10,000HZ-2.6% ,
SENSITIVITY AT TEMPERATURE: 4.3%
TRANSVERSE SENSITIVITY: 3.6%,
ACOUSTIC PRESSURE: 130dB 7.6%, 140dB 2.7%, 150dB 1.4%, 160dB 1.3%,
STATIC FORCE:10-500LBF-1.0%,500-1,000LBF-1.3%,1,000-10,000LBF-1.0%,10,000-100,000LBF-1.2%,
DEAD WEIGHT: 0.7%,
DROP -SHOCK:3.0%,
STATIC PRESSURE: 0-100PSI-2.4%, 100-10,000PSI-1.0%,
LINEARITY: 100-HZ-1.9%,500HZ-1.6%,1,000HZ-2.9%
DC -VOLTAGE: 0.1%
COVERAGE FACTOR K=2,
CONFIDENCE LEVEL 95%

* THIS CERTIFICATE SHALL NOT BE REPRODUCED EXCEPT IN FULL, WITHOUT THE WRITTEN PERMISSION FROM DYTRAN INSTRUMENTS, INC.

Cal. Tech.: DAVID NUTE

TEST DATE: 2/11/2019

FREQUENCY RESPONSE (IF APPLICABLE)

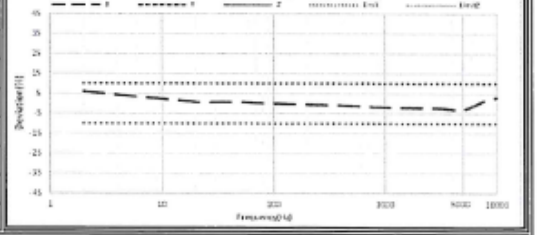

-----END OF REPORT-----

Ken Supin

Dytran Instruments, Inc.
21592 Marilla St. Chatsworth, CA 91311 Ph: 818-700-7818 Fax 818-700-7880
www.dytran.com email: info@dytran.com

ACCREDITED Calibration Laboratory CERT#2672.01

CALIBRATION CERTIFICATE
LIVM ACCELEROMETER

CUSTOMER:	*SERVO HYDRAULIC SOLUTIONS LLC*			**TEST REPORT #:**	*5822*
PURCHASE ORDER #:	*CC-D.WELLER*	**SALES ORDER #:**	*172988*	**PROCEDURE:**	*TP3002*
MODEL:	*3166B1*	**SERIAL #:**	*5822*	**RANGE, F.S. (g's):**	*+/- 10*
NEW UNIT	X	**RE-CALIBRATION [1]**		**AS RECEIVED CODE**	**AS RETURNED CODE**
TEMPERATURE (°C):	*22*			**HUMIDITY (%):**	*42*
SENSITIVITY MEASURED AT 1G RMS, 100 Hz (mV/g) [2]:	*493.8*			**DISCHARGE T.C. (sec):**	*0.90*
REMARKS:					

TEST EQUIPMENT LIST - CALIBRATION STATION # 9

DII #	MANUFACTURER	MODEL	SERIAL #	DESCRIPTION	CAL DATE	DUE DATE
1224	*NATIONAL INST.*	*PCI-4461*	*14D69AA*	*DATA ACQUISITION CARD*	*11/10/14*	*11/10/15*
1867	*DYTRAN INST.*	*3010M14*	*1772*	*ACCELEROMETER*	*06/08/15*	*06/08/16*

[1] AS RECEIVED / AS RETURNED CODES:
1 = IN TOLERANCE, NO ADJUSTMENTS
2 = IN TOLERANCE, BUT ADJUSTED
3 = OUT OF TOLERANCE < 5%
4 = OUT OF TOLERANCE > 5%
5 = REPAIR REQUIRED
6 = REPAIRED AND CALIBRATED
7 = UNIT NON-REPAIRABLE, RECOMMEND REPLACEMENT
8 = UNIT SERVICEABLE WITH CURRENT CALIBRATION DATA

[2] THE REFERENCE SENSITIVITY IS MEASURED AT 100 Hz, 1G RMS.

[3] THIS CALIBRATION WAS PERFORMED IN ACCORDANCE WITH ANSI/NCSL Z540-1-1994, ISO 10012-1, ISO/IEC17025 USING THE BACK-TO-BACK COMPARISON METHOD PER ISA RP37.2 AND IS TRACEABLE TO THE NIST THROUGH TEST REPORT # 1772 DUE 06/08/16.

ESTIMATED UNCERTAINTY OF CALIBRATION: 1.6% FROM 20-100 Hz, 1.4% FROM 100-2500 Hz, 2.8% FROM 2.5kHz-10 kHz. APPLIES TO FREQUENCY RESPONSE ONLY.

THIS CERTIFICATE SHALL NOT BE REPRODUCED EXCEPT IN FULL, WITHOUT THE WRITTEN PERMISSION FROM DYTRAN INSTRUMENTS, INC.

CALIBRATION TECHNICIAN: *DAVID NUTE* CAL 1

TEST DATE : *08/06/15*

RECOMMENDED RECALL DATE : *08/06/16*

Dytran Instruments, Inc.
21592 Marilla St. Chatsworth, CA 91311 Ph: 818-700-7818 Fax 818-700-7880
www.dytran.com email: info@dytran.com

CALIBRATION CERTIFICATE
LIVM ACCELEROMETER

CUSTOMER:	*SERVO HYDRAULIC SOLUTIONS LLC*			**TEST REPORT #:**	*5821*
PURCHASE ORDER #:	*CC-D.WELLER*	**SALES ORDER #:**	*172988*	**PROCEDURE:**	*TP3002*
MODEL:	*3166B1*	**SERIAL #:**	*5821*	**RANGE, F.S. (g's):**	*+/- 10*
NEW UNIT	X	**RE-CALIBRATION [1]**		**AS RECEIVED CODE**	**AS RETURNED CODE**
TEMPERATURE (°C):	*22*			**HUMIDITY (%):**	*42*
SENSITIVITY MEASURED AT 1G RMS, 100 Hz (mV/g) [2]:	*503.08*			**DISCHARGE T.C. (sec):**	*0.90*
REMARKS:					

TEST EQUIPMENT LIST - CALIBRATION STATION # 9

DII #	MANUFACTURER	MODEL	SERIAL #	DESCRIPTION	CAL DATE	DUE DATE
1224	*NATIONAL INST.*	*PCI-4461*	*14D69AA*	*DATA ACQUISITION CARD*	*11/10/14*	*11/10/15*
1867	*DYTRAN INST.*	*3010M14*	*1772*	*ACCELEROMETER*	*06/08/15*	*06/08/16*

[1] AS RECEIVED / AS RETURNED CODES:
1 = IN TOLERANCE, NO ADJUSTMENTS
2 = IN TOLERANCE, BUT ADJUSTED
3 = OUT OF TOLERANCE < 5%
4 = OUT OF TOLERANCE > 5%
5 = REPAIR REQUIRED
6 = REPAIRED AND CALIBRATED
7 = UNIT NON-REPAIRABLE, RECOMMEND REPLACEMENT
8 = UNIT SERVICEABLE WITH CURRENT CALIBRATION DATA

[2] THE REFERENCE SENSITIVITY IS MEASURED AT 100 Hz, 1G RMS.

[3] THIS CALIBRATION WAS PERFORMED IN ACCORDANCE WITH ANSI/NCSL Z540-1-1994, ISO 10012-1, ISO/IEC17025 USING THE BACK-TO-BACK COMPARISON METHOD PER ISA RP37.2 AND IS TRACEABLE TO THE NIST THROUGH TEST REPORT # 1772 DUE 06/08/16.

ESTIMATED UNCERTAINTY OF CALIBRATION: 1.6% FROM 20-100 Hz, 1.4% FROM 100-2500 Hz, 2.8% FROM 2.5kHz-10 kHz. APPLIES TO FREQUENCY RESPONSE ONLY.

THIS CERTIFICATE SHALL NOT BE REPRODUCED EXCEPT IN FULL, WITHOUT THE WRITTEN PERMISSION FROM DYTRAN INSTRUMENTS, INC.

CALIBRATION TECHNICIAN: *DAVID NUTE*

TEST DATE : *08/06/15*

RECOMMENDED RECALL DATE : *08/06/16*

Dytran Instruments, Inc.
21592 Marilla St. Chatsworth, CA 91311 Ph: 818-700-7818 Fax 818-700-7880
www.dytran.com email: info@dytran.com

CALIBRATION CERTIFICATE
LIVM ACCELEROMETER

CUSTOMER:	*SERVO HYDRAULIC SOLUTIONS LLC*			**TEST REPORT #:**	*5820*
PURCHASE ORDER #:	*CC-D.WELLER*	**SALES ORDER #:**	*172988*	**PROCEDURE:**	*TP3002*
MODEL:	*3166B1*	**SERIAL #:**	*5820*	**RANGE, F.S. (g's):**	*+/- 10*
NEW UNIT	X	**RE-CALIBRATION [1]**		**AS RECEIVED CODE**	**AS RETURNED CODE**
TEMPERATURE (°C):	*22*			**HUMIDITY (%):**	*42*
SENSITIVITY MEASURED AT 1G RMS, 100 Hz (mV/g) [2]:	*495.97*			**DISCHARGE T.C. (sec):**	*1.00*
REMARKS:					

TEST EQUIPMENT LIST - CALIBRATION STATION # 9

DII #	MANUFACTURER	MODEL	SERIAL #	DESCRIPTION	CAL DATE	DUE DATE
1224	*NATIONAL INST.*	*PCI-4461*	*14D69AA*	*DATA ACQUISITION CARD*	*11/10/14*	*11/10/15*
1867	*DYTRAN INST.*	*3010M14*	*1772*	*ACCELEROMETER*	*06/08/15*	*06/08/16*

[1] AS RECEIVED / AS RETURNED CODES:
1 = IN TOLERANCE, NO ADJUSTMENTS
2 = IN TOLERANCE, BUT ADJUSTED
3 = OUT OF TOLERANCE < 5%
4 = OUT OF TOLERANCE > 5%
5 = REPAIR REQUIRED
6 = REPAIRED AND CALIBRATED
7 = UNIT NON-REPAIRABLE, RECOMMEND REPLACEMENT
8 = UNIT SERVICEABLE WITH CURRENT CALIBRATION DATA

[2] THE REFERENCE SENSITIVITY IS MEASURED AT 100 Hz, 1G RMS.

[3] THIS CALIBRATION WAS PERFORMED IN ACCORDANCE WITH ANSI/NCSL Z540-1-1994, ISO 10012-1, ISO/IEC17025 USING THE BACK-TO-BACK COMPARISON METHOD PER ISA RP37.2 AND IS TRACEABLE TO THE NIST THROUGH TEST REPORT # 1772 DUE 06/08/16.

ESTIMATED UNCERTAINTY OF CALIBRATION: 1.6% FROM 20-100 Hz, 1.4% FROM 100-2500 Hz, 2.8% FROM 2.5kHz-10 kHz. APPLIES TO FREQUENCY RESPONSE ONLY.

THIS CERTIFICATE SHALL NOT BE REPRODUCED EXCEPT IN FULL, WITHOUT THE WRITTEN PERMISSION FROM DYTRAN INSTRUMENTS, INC.

CALIBRATION TECHNICIAN: *DAVID NUTE*

TEST DATE : *08/06/15*

RECOMMENDED RECALL DATE : *08/06/16*

Dytran Instruments, Inc.
21592 Marilla St. Chatsworth, CA 91311 Ph: 818-700-7818 Fax 818-700-7880
www.dytran.com email: info@dytran.com

ACCREDITED
Calibration Laboratory
CERT#2671.01

CALIBRATION CERTIFICATE
LIVM ACCELEROMETER

CUSTOMER:	*SERVO HYDRAULIC SOLUTIONS LLC*			**TEST REPORT #:**	*5765*
PURCHASE ORDER #:	*CC-D.WELLER*	**SALES ORDER #:**	*172988*	**PROCEDURE:**	*TP3002*
MODEL:	*3166B1*	**SERIAL #:**	*5765*	**RANGE, F.S. (g's):**	*+/- 10*
NEW UNIT	X	**RE-CALIBRATION [1]**		**AS RECEIVED CODE**	**AS RETURNED CODE**
TEMPERATURE (°C):	*22*			**HUMIDITY (%):**	*42*
SENSITIVITY MEASURED AT 1G RMS, 100 Hz (mV/g) [2]:	*487.3*			**DISCHARGE T.C. (sec):**	*1.70*
REMARKS:					

TEST EQUIPMENT LIST - CALIBRATION STATION # 9

DII #	MANUFACTURER	MODEL	SERIAL #	DESCRIPTION	CAL DATE	DUE DATE
1224	*NATIONAL INST.*	*PCI-4461*	*14D69AA*	*DATA ACQUISITION CARD*	*11/10/14*	*11/10/15*
1867	*DYTRAN INST.*	*3010M14*	*1772*	*ACCELEROMETER*	*06/08/15*	*06/08/16*

[1] AS RECEIVED / AS RETURNED CODES:
1 = IN TOLERANCE, NO ADJUSTMENTS
2 = IN TOLERANCE, BUT ADJUSTED
3 = OUT OF TOLERANCE < 5%
4 = OUT OF TOLERANCE > 5%
5 = REPAIR REQUIRED
6 = REPAIRED AND CALIBRATED
7 = UNIT NON-REPAIRABLE, RECOMMEND REPLACEMENT
8 = UNIT SERVICEABLE WITH CURRENT CALIBRATION DATA

[2] THE REFERENCE SENSITIVITY IS MEASURED AT 100 Hz, 1G RMS.

[3] THIS CALIBRATION WAS PERFORMED IN ACCORDANCE WITH ANSI/NCSL Z540-1-1994, ISO 10012-1, ISO/IEC17025 USING THE BACK-TO-BACK COMPARISON METHOD PER ISA RP37.2 AND IS TRACEABLE TO THE NIST THROUGH TEST REPORT # 1772 DUE 06/08/16.

ESTIMATED UNCERTAINTY OF CALIBRATION: 1.6% FROM 20-100 Hz, 1.4% FROM 100-2500 Hz, 2.8% FROM 2.5kHz-10 kHz. APPLIES TO FREQUENCY RESPONSE ONLY.

THIS CERTIFICATE SHALL NOT BE REPRODUCED EXCEPT IN FULL, WITHOUT THE WRITTEN PERMISSION FROM DYTRAN INSTRUMENTS, INC.

CALIBRATION TECHNICIAN: *DAVID NUTE*

TEST DATE : *08/06/15*

RECOMMENDED RECALL DATE : *08/06/16*

Shaker_Model_for thesis.xmcd 6/18/2019, 4:37 PM
F:__MTECH THESIS\Shake Table\Calibration\MathCAD\

Shake Table Model

Created 11/15/2018 by Peter Lucon File Name: Shaker_Model_r00.xmcd

Modified 06//2018 by Peter Lucon Current File Name: Shaker_Model_r00.xmcd

Description: The program calculates the angles for the 4 bar linkage (offset crank) given a driven angle.

System Variables:

Length of the Base Member 'L1': $L_1 := (26in - 14 \cdot in) = 12 \cdot in$

Length of the Left Member 'L2': $L_2 := 14 \cdot in$

Length of the Coupler Linkage 'L3': $L_3 := 29 \cdot in$

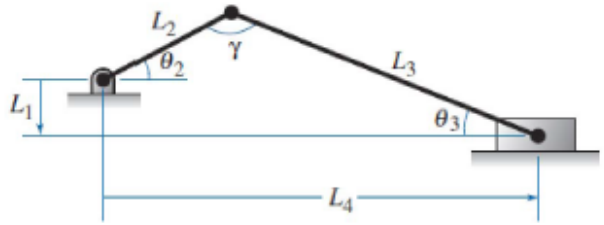

Driving Angle by the Motor 'Theta2': $\theta_2 := -75deg$

Single Solution Given above Angle:

Theta 3: $\theta_3 := \left(asin\left(\frac{L_1 + L_2 \cdot sin(\theta_2)}{L_3}\right)\right) = -3.01 \cdot deg$

Positive Displacement is

Encoder +/- 10V = +/- 22 deg of motion

Length of the Right Linkage 'L4': $L_4 := L_2 \cdot cos(\theta_2) + L_3 \cdot cos(\theta_3) = 32.583 \cdot in$

1400 N*m torque spec.

Angle Between R_{CD} and R_{CB} $\gamma := 180deg - (\theta_2 + \theta_3) = 258.01 \cdot deg$

$\frac{.25}{10} \cdot 22 = 0.55$

MontanaTech

Graphical Solution Given 0-360 degree Angle for Theta2:

Speed of Driven Component: $\omega_A := 100\,rpm$

Time for the Analysis: $t := 0s, 0.001s .. \frac{2\cdot\pi}{\omega_A}$

$\theta_{max} := 22deg$

$\theta_{mean} := -75deg$ $\theta_{min} := -\theta_{max} + \theta_{mean}$

Define Theta 2 over 0 - 360 deg

$\theta_2 := \theta_{min} + 2\cdot\pi, 2\cdot\pi + \theta_{min} + 0.001deg .. 2\cdot\pi + \theta_{min} + 2\theta_{max}$

$\theta_{min} = -97\cdot deg$

$\theta_{mean} = -75\cdot deg$

$\theta_{min} + 2\cdot\pi = 263\cdot deg$

Theta 3: $\theta_{3i}(\theta_2) := \left(\operatorname{asin}\left(\frac{L_1 + L_2\cdot\sin(\theta_2)}{L_3}\right)\right)$

$L_{4i}(\theta_2) := L_2\cdot\cos(\theta_2) + L_3\cdot\cos(\theta_{3i}(\theta_2))$

$\gamma_i(\theta_2) := 180deg - (\theta_2 + \theta_{3i}(\theta_2))$

Shaker_Model_for thesis.xmcd 6/18/2019, 4:37 PM
F:__MTECH THESIS\Shake Table\Calibration\MathCAD\

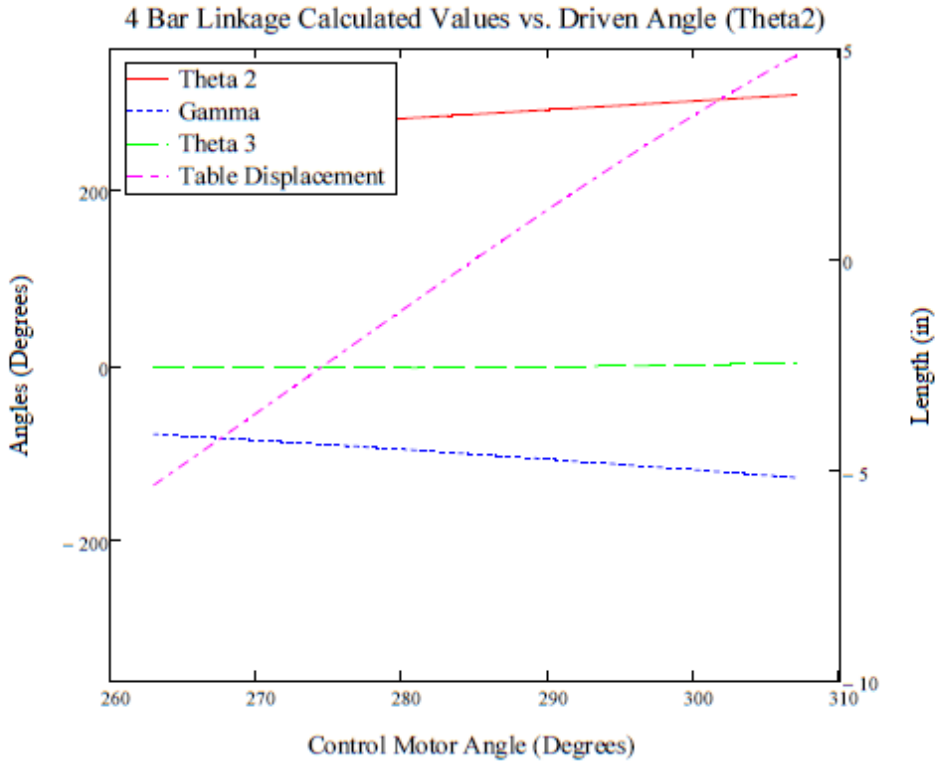

$\theta_2 =$

263	deg
263.001	
263.002	
263.003	
263.004	
263.005	
263.006	
263.007	
263.008	
263.009	
263.01	
263.011	
263.012	
263.013	
263.014	
...	

Shaker_Model_for thesis.xmcd
F:__MTECH THESIS\Shake Table\Calibration\MathCAD\

6/18/2019, 4:37 PM

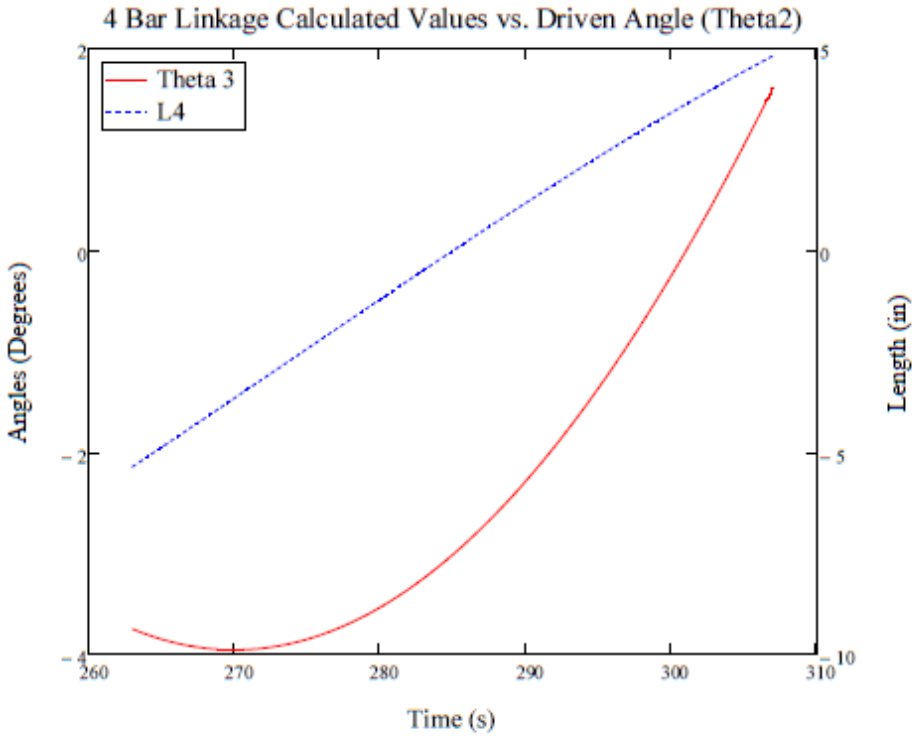

$L_{4i}(\theta_2) - L_{4i}(\theta_{mean}) =$ in

-5.352
-5.351
-5.351
-5.351
-5.351
-5.35
-5.35
-5.35
-5.35
-5.349
-5.349
-5.349
-5.349
-5.349
-5.348
...

MontanaTech

10.2. MATLAB Script

```
%%  shakeDataBatchProc.m
%   By: Thad Haines
%   Program Purpose:    Batch process shake table data, exporting clean
%                       data and optionally making plots

%   History:
%   03/28/19    13:15   init
%   03/29/19    10:09   verified 'b' version of functions (for old
MATLAB)
%   03/31/19    10:41   Addition of sub2 - unfiltered data, optional
xlim

%% init MATLAB
clear; format compact; clc; close all;

%% Test of single file
rawName = 'MatLAB test data01_20190329_14-58-13.csv'
% clean data and export xls
cleanName = shakeDataCleanSmooth( rawName );

%% Plot data
% Plot smoothed data with raw data
shakeDataPlotSub(cleanName)

% Plots of unfiltered data
shakeDataPlotSub2(cleanName)
shakeDataPlotSub2(cleanName, [0, 3]) % optional xlimit entry

% Plot raw data
shakeDataPlotSubRaw(rawName)
```

File: shakeDataCleanSmoothb

```
function [ cleanName ] = shakeDataCleanSmoothb( fileName )
%shakeDataCleanSmooth Reads raw shake table data and exports clean and
%smooth data. Returns name of cleaned file.
% Parse first 5 Columns from Raw Data when LED < 3.5
% Includes removing data from begining and end of raw data, making new
time
fprintf('Reading %s...\n',fileName)
% Read in of raw data
rawData = xlsread(fileName);

fprintf('Data Read Okay. Parsing Data...')
% Separation of desired data columns
t = rawData(:,1);
Vout = rawData(:,2);
LED = rawData(:,3);
g1 = rawData(:,4);
g2 = rawData(:,5);

% Data timestep
```

```
ts = (t(2)-t(1));

% First Index when LED < 3.5 V
dataStart = find(LED<3.5, 1);
dataEnd = find(LED(dataStart:end)>3.5,1);

% Handle MATLAB indexing from 1
dataEnd = dataStart+dataEnd - 2;

% collect cleanData
cleanData(:,1) = t(dataStart:dataEnd);
% Create new time starting for clean data
cleanData(:,2) = (0:length(cleanData(:,1))-1)*ts;
cleanData(:,3) = Vout(dataStart:dataEnd);

fprintf(' Smoothing Data...')
% Handle raw and smoothed accel data
cleanData(:,4) = g1(dataStart:dataEnd);
cleanData(:,5) = smooth(cleanData(:,4),'moving',50);
cleanData(:,6) = g2(dataStart:dataEnd);
cleanData(:,7) = smooth(cleanData(:,6),'moving',50);

% Column header definition - May change if desired
col_header={'Old Time [sec]','Time [sec]','Vout [V]',...
    'g1 raw [g]','g1 smooth [g]','g2 raw [g]','g2 smooth [g]'};

fprintf(' Writing Clean Data...\n')
cleanName = strjoin({fileName(1:(end-3)), 'clean.xls'},'');
xlswrite(cleanName,col_header);
xlswrite(cleanName,cleanData,1,'A2')
fprintf('Clean Data Saved as: %s\n', cleanName)
end
```

FILE: shakeDataPlot

```
function [  ] = shakeDataPlot( cleanName )
%shakeDataPlot Creates Plots from clean data file

grey = [.7 .7 .7];

cleanData = xlsread(cleanName);

fprintf('Plotting data from: %s\n', cleanName)
t = cleanData(:,2);
Vout = cleanData(:,3);
g1 = cleanData(:,4);
g1S = cleanData(:,5);
g2 = cleanData(:,6);
g2S = cleanData(:,7);

figure
plot(t,Vout,'k','linewidth',2)
title('Voltage Input')
xlabel('Time [sec]')
```

```
ylabel('Voltage [V]')
grid on

figure
plot(t,g1,'color',grey)
hold on
plot(t,g1S,'k','linewidth',1)
legend('g1','g1 Smoothed')
title('Accelerometer g1')
xlabel('Time [sec]')
ylabel('g [g]')
grid on

figure
plot(t,g2,'color',grey)
hold on
plot(t,g2S,'k','linewidth',1)
legend('g2','g2 Smoothed')
title('Accelerometer g2')
xlabel('Time [sec]')
ylabel('g [g]')
grid on
end
```

FILE: shakeDataPlotSub2

```
function [  ] = shakeDataPlotSub2( cleanName, optionalXlimtit )
%shakeDataPlotSub Creates Figure with subplots from clean data file
% plots only un-processed data, provides optional X plot limits

bfz= 10; % font Size
lw = 1.3;
grey = [.7 .7 .7];
cleanData = xlsread(cleanName);


fprintf('Plotting data from: %s\n', cleanName)
t = cleanData(:,2);
Vout = cleanData(:,3);
g1 = cleanData(:,4);
g2 = cleanData(:,6);

if nargin > 1
    xlimit = optionalXlimtit;
else
    xlimit = [t(1) t(end)];
end

figure
subplot(3,1,1)
plot(t,Vout,'k','linewidth',lw)
title('Voltage Input')
%xlabel('Time [sec]')
ylabel('Voltage [V]')
grid on
```

```
set(gca, 'fontsize',bfz)
xlim(xlimit)

subplot(3,1,2)
plot(t,g1,'k','linewidth',lw)
hold on
title('Accelerometer g1 - Table')
%xlabel('Time [sec]')
ylabel('g [g]')
grid on
set(gca, 'fontsize',bfz)
xlim(xlimit)

subplot(3,1,3)
plot(t,g2,'k','linewidth',lw)
title('Accelerometer g2 -Block')
xlabel('Time [sec]')
ylabel('g [g]')
grid on
set(gca, 'fontsize',bfz)
xlim(xlimit)
end
```

FILE: shakeDataPlotSubRawb

```
function [  ] = shakeDataPlotSubRawb( rawName )
%shakeDataPlotSub Creates Figure with subplots from raw data file
fz= 13; % font Size
grey = [.7 .7 .7];

rawData = xlsread(rawName);

fprintf('Plotting data from: %s\n', rawName)
t = rawData(:,1);
Vout = rawData(:,2);
LED = rawData(:,3);
g1 = rawData(:,4);
g1S = smooth(rawData(:,4),'moving',50);% for old MATLAB
%g1S = smoothdata(rawData(:,4),'movmean',50); % For new MATLAB
g2 = rawData(:,5);
g2S = smooth(rawData(:,5),'moving',50); % for old MATLAB
%g2S = smoothdata(rawData(:,5),'movmean',50); % For new MATLAB

figure
subplot(3,1,1)
plot(t,Vout,'k','linewidth',2)
hold on
plot(t,LED,'m','linewidth',2)
title('Voltages')
xlabel('Time [sec]')
ylabel('Voltage [V]')
legend('Output Voltage','LED')
grid on
set(gca, 'fontsize',fz)
```

```
subplot(3,1,2)
plot(t,g1,'color',grey,'linewidth',2)
hold on
plot(t,g1S,'k','linewidth',1)
legend('g1','g1 Smoothed')
title('Accelerometer g1 - Table')
xlabel('Time [sec]')
ylabel('g [g]')
set(gca, 'fontsize',fz)
grid on

subplot(3,1,3)
plot(t,g2,'color',grey,'linewidth',2)
hold on
plot(t,g2S,'k','linewidth',1)
legend('g2','g2 Smoothed')
title('Accelerometer g2 - Block')
xlabel('Time [sec]')
ylabel('g [g]')
set(gca, 'fontsize',fz)
grid on
end
```

11. Appendix D: Experimental Results Summary

The following is a brief description on how to read Tables VI, VII, and VIII:

# of Runs:	Sequential total number of runs
Block #:	Block number: 2, 3, or 4
Input Profile:	Vibration profile used for testing, first number is voltage and second number is frequency
Scaling:	Scaling of original vibration profile. This increases the initial voltage (i.e. 1 V scaled at 1.5 is 1.5 V)
Friction Angle (deg):	Friction angle between block and shake table
Acceleration of Ramp up (g):	On real-time plots (screen grab from LabVIEW software), this value is the first inflection point (negative)
Acceleration of Slowdown (g):	On real-time plots (screen grab from LabVIEW software), this value is the second inflection point (positive)
Data:	Shows if DAQ .csv datafile was saved (Y/N)
Plot Pic?:	Shows if a screen grab of the real-time LabVIEW plots was saved (Y/N)
Video?:	Shows if a high-speed camera video was saved (Y/N/SM*) *slow motion video recorded with iPhone
Trial #:	Trial number with same testing configuration
Observations:	Comments from testing and reviewing data collected

Table VI: Observations during Block 2 testing

# of Runs	Block #	Input Profile	Scaling	Friction Angle (deg)	Acceleration of Ramp up (g)	Acceleration of Slowdown (g)	Data	Plot Pic ?	Video?	Trial #	Observations
1	2	1V_3Hz	1.0	20	-0.16	0.18	Y	Y	Y	1	stable
2	2	1V_3Hz	1.5	20	-0.20	0.23	Y	Y	Y	1	stable
3	2	1V_3Hz	2.0	20	-0.25	0.33	Y	Y	Y	1	slight right, then mostly left, no definitive lift
4				20	-0.24	0.33	Y	Y	Y	2	slight right, then mostly left, no definitive lift
5				20	-0.24	0.33	Y	Y	Y	3	slight right, then mostly left, no definitive lift
6	2	1V_3Hz	2.5	20	-0.28	0.41	Y	Y	Y	1	slight lift and slide right, then more distinct lift left (better than trial 2)
7				20	-0.28	0.41	Y	Y	Y	2	more sliding right than lift, then mostly slide back left, no definitive lift
8				20	-0.27	0.40	Y	Y	Y	3	similar to trial 2, more slide than lift, no definitive lift
9	2	1V_3Hz	2.6	20	-0.29	0.43	Y	Y	Y	1	more slide right than lift, then mostly left, no definitive lift
10				20	-0.30	0.44	Y	Y	Y	2	more sliding right than lift
11	2	1V_3Hz	2.7	20	-0.30	0.45	Y	Y	Y	1	small lift mostly slide right, more distinct lift beginning but still slides back left, no definitive lift/topple
12				20	-0.31	0.45	Y	Y	Y	2	small lift mostly slide right, more distinct lift beginning but still slides back left, no definitive lift/topple
13	2	1V_3Hz	2.8	20	-0.30	0.47	Y	Y	Y	1	slide right with slight lift, then mostly slide back left with slightly larger lift, beginning of lift/topple?
14				20	-0.31	0.49	Y	Y	Y	2	slight lift to slide right, larger lift and slide back left than 2.7, still mostly more slide than lift/topple
15				20	-0.31	0.48	Y	Y	Y	3	slide right with slight lift, then mostly slide back left with minor lift, more obvious slide back than lift/topple

# of Runs	Block #	Input Profile	Scaling	Friction Angle (deg)	Acceleration of Ramp up (g)	Acceleration of Slowdown (g)	Data	Plot Pic ?	Video?	Trial #	Observations
16	2	1V_3Hz	2.9	20	-0.32	0.50	Y	Y	Y	1	mostly slide right with minimal lift, slide back left with a little more lift, still appears to be sliding more than lift/topple
17				20	-0.31	0.50	Y	Y	Y	2	mostly slide right with minimal lift, slide back left with a little more lift, still appears to be sliding more than lift/topple
18	2	1V_3Hz	3.0	20	-0.33	0.50	Y	Y	Y	1	larger lift than any before with sliding right and distinct initiation of lift/topple left.
19				20	-0.31	0.50	Y	Y	Y	2	smaller lift than trial 1, with slide right and mostly lift and slide back left.
20				20	-0.34	0.49	Y	Y	Y	3	mostly sliding both direction, no definitive initiation of lift/topple
21				20	-0.31	0.49	Y	Y	Y	4	mostly sliding both direction, no definitive initiation of lift/topple
22	2	1V_3Hz	3.1	20	-0.33	0.50	Y	Y	Y	1	mostly sliding both direction, no definitive initiation of lift/topple
23				20	-0.32	0.50	Y	Y	Y	2	mostly sliding both direction, no definitive initiation of lift/topple
24				20	-0.33	0.49	Y	Y	Y	3	mostly sliding both direction, no definitive initiation of lift/topple
25	2	1V_3Hz	3.2	20	-0.33	0.51	Y	Y	Y	1	some noise in good accelerometer, ramp up accel could be -0.33/-0.32. mostly sliding both direction, no definitive initiation of lift/topple
26				20	-0.32	0.51	Y	Y	Y	2	mostly sliding both direction, no definitive initiation of lift/topple
27				20	-0.32	0.48	Y	Y	Y	3	mostly sliding both direction, no definitive initiation of lift/topple

# of Runs	Block #	Input Profile	Scaling	Friction Angle (deg)	Acceleration of Ramp up (g)	Acceleration of Slowdown (g)	Data	Plot Pic ?	Video?	Trial #	Observations
28	2	1V_3Hz	3.3	20	-0.33	0.51	Y	Y	Y	1	mostly sliding both direction, no definitive initiation of lift/topple
29				20	-0.33	0.50	Y	Y	Y	2	same as above
30				20	-0.34	0.49	Y	Y	Y	3	some noise, could be -0.34/-0.35. mostly sliding in both directions, no definitive lift/topple
31	2	1V_3Hz	3.5	20	-0.34	0.53	Y	Y	Y	1	mostly sliding both direction, directly to stable with minimal wobble, no definitive initiation of lift/topple
32				20	-0.34	0.52	Y	Y	Y	2	noise in accelerometers, could be -0.34/-0.35, mostly sliding both directions to stable with minimal wobble, no definitive lift/topple
33	2	1V_3Hz	4.0	20	-0.40	0.60	Y	Y	Y	1	negligible lift, mostly slide right and larger lift left initiating a topple
34				20	-0.39	0.59	Y	Y	Y	2	mostly sliding and beginning to spin
35	2	1V_3Hz	4.5	20	-0.45	0.65	Y	Y	Y	1	looking more stable than before, mostly sliding and a bit of wobble
36	2	1V_3Hz	5.0	20	-0.49	0.73	Y	Y	Y	1	same as above
37	2	4.5V_3Hz	0.46	20	-0.30	0.68	Y	Y	Y	1	negligible lift and mostly slide right with minimal lift and mostly slide left, looked stable
38	2	4.5V_3Hz	0.48	20	-0.31	0.71	Y	Y	Y	1	noise, slight lift mostly slide right, larger lift and slide back left
39				20	-0.31	0.71	Y	Y	Y	2	tail end of noise, negligible lift and slide right, with minimal lift and mostly slide back left
40				20	-0.31	0.70	Y	Y	Y	3	beginning of noise, negligible lift and mostly slide right with some potential lifting to topple going left*
41				20	-0.35	0.67	Y	Y	Y	4	negligible lift mostly slide right, with small lift left but mostly slide, didn't appear to topple

# of Runs	Block #	Input Profile	Scaling	Friction Angle (deg)	Acceleration of Ramp up (g)	Acceleration of Slowdown (g)	Data	Plot Pic ?	Video?	Trial #	Observations
42	2	4.5V_3Hz	0.50	20	-0.32	0.74	Y	Y	Y	1	dark yellow plot with noise (ignore), negligible lift right mostly slide, and small lift left with mostly slide and some spin
43				20	-0.33	0.74	Y	Y	Y	2	clear plot, mostly slide right to left, stable
44				20	-0.32	0.74	Y	Y	Y	3	mostly slide right to left, wobble and stable
45	2	4.5V_3Hz	0.52	20	-0.34	0.78	Y	Y	Y	1	clear plot, negligible lift mostly slide right with some lift left, but mostly slide and spin
46				20	-0.33	0.79	Y	Y	Y	2	same as above
47				20	-0.33	0.78	Y	Y	Y	3	mostly slide and wobble, looked stable
48	2	4.5V_3Hz	0.55	20	-0.35	0.81	Y	Y	Y	1	negligible lift mostly slide right with some lift left, but mostly slide and spin
49	2	1V_3Hz	1.5	46	-0.18	0.23	Y	Y	Y	1	stable
50	2	1V_3Hz	2.5	46	-0.26	0.38	Y	Y	Y	1	small lift right then lift left, but no definitive lift leading to topple
51				46	-0.27	0.39	Y	Y	Y	2	same as above
52	2	1V_3Hz	2.6	46	-0.27	0.40	Y	Y	Y	1	small lift right then lift left, but no definitive lift leading to topple
53				46	-0.28	0.41	Y	Y	Y	2	same as above
54	2	1V_3Hz	2.7	46	-0.30	0.40	Y	Y	Y	1	small lift right then distinct lift left, but not definitive lift to topple. Scale 2.8 looks much better.
55				46	-0.29	0.40	Y	Y	Y	2	small lift right then distinct lift left, but not definitive lift to topple
56	2	1V_3Hz	2.8	46	-0.31	0.44	Y	Y	Y	1	small lift right and distinct lift left potentially leading to toppling
57				46	-0.31	0.43	Y	Y	Y	2	same as above
58				46	-0.31	0.43	Y	Y	Y	3	same as trial 1
59	2	1V_3Hz	3.0	46	-0.32	0.46	Y	Y	Y	1	distinct lifting leading to toppling

Table VII: Observations during Block 3 testing

# of Runs	Block #	Input Profile	Scaling	Friction Angle (deg)	Acceleration of Ramp up (g)	Acceleration of Slowdown (g)	Data	Plot Pic ?	Video?	Trial #	Observations
1	3	1V_3Hz	1	20	-0.16	0.18	Y	Y	Y	1	relatively stable, some wobbling, maybe starting right to left
2				20	-0.15	0.18	Y	Y	N	2	no observation made
3				20	-0.15	0.18	Y	Y	Y	3	relatively stable, some wobbling
4	3	1V_3Hz	1.5	20	-0.20	0.23	Y	Y	Y	1	relatively stable, with slight right movement first, then left
5				20	-0.21	0.23	Y	Y	Y	2	relatively stable, with slight left movement first, then slight right, then mostly left
6				20	-0.21	0.23	Y	Y	Y	3	relatively stable, with slight right movement first, then left
7	3	1V_3Hz	1.6	20	-0.21	0.23	Y	Y	Y	1	relatively stable, with slight right movement first, then left
8				20	-0.22	0.23	Y	Y	Y	2	relatively stable, with slight right movement first, then left
9				20	-0.21	0.23	N	Y	N	3	no observation made
10				20	-0.21	0.22	Y	Y	N	4	no observation made
11				20	-0.21	0.22	Y	Y	Y	5	relatively stable, with slight right movement first, then left
12	3	1V_3Hz	1.7	20	-0.22	0.25	Y	Y	Y	1	slight right, then mostly left
13				20	-0.23	0.26	Y	Y	Y	2	slight right, then mostly left
14				20	-0.23	0.26	Y	Y	Y	3	slight right, then mostly left
15				20	-0.23	0.25	Y	Y	N	4	no observation made
16				20	-0.22	0.25	Y	Y	Y	5	slight right, then mostly left

# of Runs	Block #	Input Profile	Scaling	Friction Angle (deg)	Acceleration of Ramp up (g)	Acceleration of Slowdown (g)	Data	Plot Pic ?	Video?	Trial #	Observations
17	3	1V_3Hz	1.8	20	-0.23	0.28	Y	Y	Y	1	distinct slight right, then mostly left
18				20	-0.23	0.29	N	Y	N	2	no observation made
19				20	-0.23	0.29	Y	Y	Y	3	distinct slight right, then mostly left with some sliding southwest corner
20				20	-0.24	0.29	Y	Y	Y	4	distinct slight right, then mostly left
21				20	-0.24	0.28	Y	Y	N	5	no observation made
22	3	1V_3Hz	1.9	20	-0.23	0.31	Y	Y	Y	1	distinct right, then mostly left
23				20	-0.24	0.32	Y	Y	Y	2	distinct right, then mostly left with some sliding towards southwest corner
24				20	-0.23	0.31	Y	Y	N	3	no observation made
25				20	-0.23	0.31	Y	Y	Y	4	distinct right, then mostly left with some sliding towards south (in loading direction)
26				20	-0.23	0.31	Y	Y	Y	5	distinct slight right, then mostly left with some sliding southwest corner
27	3	1V_3Hz	2.0	20	-0.24	0.32	Y	Y	Y	1	small right movement, then mostly left
28				20	-0.24	0.33	Y	Y	Y	2	small right movement, then mostly left with negligible sliding left
29				20	-0.25	0.33	Y	Y	Y	3	small right movement, then mostly left with negligible sliding left
30	3	1V_3Hz	2.5	20	-0.27	0.4	Y	Y	Y	1	distinct right first, then left
31	3	4.5V_3Hz	0.25	20	-0.21	0.37	N	Y	N	1	memory full, didn't save data, only plot
32				20	-0.19	0.35	Y	Y	Y	2	noise in data, negligible lift right and small lift left, no definitive topple
33				20	-0.20	0.36	Y	Y	Y	3	noise in data, negligible lift right and small lift left, no definitive topple, LED flashes
34				20	-0.19	0.35	Y	Y	Y	4	negligible lift right and small lift left, no definitive topple

# of Runs	Block #	Input Profile	Scaling	Friction Angle (deg)	Acceleration of Ramp up (g)	Acceleration of Slowdown (g)	Data	Plot Pic ?	Video?	Trial #	Observations
35	3	4.5V_3Hz	0.28	20	-0.20	0.35	Y	Y	Y	1	noise in data, negligible lift right, small lift left, no definitive topple
36	3	4.5V_3Hz	0.29	20	-0.22	0.37	Y	Y	Y	1	noise in data, could be -0.22/-0.23, slight lift right, more lift left, possible initial topple
37				20	-0.22	0.38	Y	Y	Y	2	same as above
38				20	-0.22	0.38	Y	Y	Y	3	noise in data, could be -0.22/-0.23, slight lift right, more lift left, possible initial topple
39	3	4.5V_3Hz	0.3	20	-0.23	0.40	Y	Y	Y	1	slight lift right and distinct initiation of lift/topple left
40				20	-0.23	0.40	Y	Y	Y	2	some noise in data, maybe -0.22, negligible lift right with distinct lift left, maybe initiating topple
41				20	-0.23	0.40	Y	Y	Y	3	clean data, negligible lift right with distinct lift left, maybe initiating topple
42	3	4.5V_3Hz	0.31	20	-0.23	0.41	Y	Y	Y	1	slight lift right and distinct lift left, maybe initiating topple
43	3	4.5V_3Hz	0.5	20	-0.33	0.75	Y	Y	Y	1	distinct lift right to large lift and then topple left
44	3	1V_3Hz	1.7	46	-0.23	0.25	Y	Y	Y	1	slight lift right, larger lift left, potential for initial lift to topple?
45				46	-0.22	0.24	Y	Y	Y	2	smaller lift left than trial 1
46	3	1V_3Hz	1.8	46	-0.23	0.27	Y	Y	Y	1	slight lift right, large lift right, but not definitive lifting to topple
47				46	-0.23	0.27	Y	Y	Y	2	same as above
48	3	1V_3Hz	2.0	46	-0.24	0.31	Y	Y	Y	1	slight lift right to larger lift left, more distinct lifting to toppling behavior
49				46	-0.23	0.31	Y	Y	Y	2	slight lift right to larger lift left, more distinct lifting to toppling behavior
50	3	1V_3Hz	2.2	46	-0.26	0.34	Y	Y	Y	1	distinct lifting to toppling
51				46	-0.25	0.33	Y	Y	Y	2	distinct lifting to toppling

Table VIII: Observations during Block 4 testing

# of Runs	Block #	Input Profile	Scaling	Friction Angle (deg)	Acceleration of Ramp up (g)	Acceleration of Slowdown (g)	Data	Plot Pic ?	Video?	Trial #	Observations
1	4	1V_3Hz	1	20			N	N	N	1	stable
2				20	-0.15	0.20	N	Y	SM*	2	stable, noise captured in plot. Potential noise in both peaks
3				20	-0.15	0.18	N	Y	SM	3	stable, noise captured in plot
4	4	1V_3Hz	1.3	20			N	N	SM	1	slight wobble, no rotation, mostly left
5				20	-0.18	0.22	N	Y	N	2	no observation made
6				20	-0.18	0.21	Y	Y	Y	3	negligible initial motion right then more visible movement left
7				20	-0.19	0.21	Y	Y	Y	4	negligible initial motion right (maybe due to rounded corner?) then more visible movement left. Noise in ramp up acceleration, so the reading might be a little high.
8				20	-0.18	0.22	Y	Y	Y	5	negligible initial motion right (maybe due to rounded corner?) then more visible movement left.
9	4	1V_3Hz	1.4	20	-0.20	0.22	Y	Y	Y	1	negligible initial motion right (rounded corner?), mostly left
10				20	-0.20	0.23	N	Y	SM	2	negligible initial motion right (rounded corner?), mostly left
11				20	-0.20	0.23	Y	Y	Y	3	negligible initial motion right (rounded corner?), mostly left
12				20	-0.21	0.23	Y	Y	N	4	no observation made
13				20			Y	N	Y	5	negligible initial motion right (rounded corner?), mostly left, plus some wobbling

* SM = slow motion video

# of Runs	Block #	Input Profile	Scaling	Friction Angle (deg)	Acceleration of Ramp up (g)	Acceleration of Slowdown (g)	Data	Plot Pic ?	Video?	Trial #	Observations
14	4	1V_3Hz	1.5	20			N	N	N	1	slight wobble, no rotation, mostly left
15				20	-0.19	0.23	N	Y	N	2	slight wobble, no rotation, mostly left. Noise in ramp up?
16				20	-0.21	0.23	N	Y	N	3	slight wobble, no rotation, mostly left
17				20			N	N	SM	4	slight wobble, no rotation, mostly left
18				20	-0.21	0.23	Y	Y	Y	5	negligible initial motion right then more visible movement left
19				20	-0.21	0.23	Y	Y	Y	6	negligible initial motion right then more visible movement left
20				20	-0.20	0.22	Y	Y	Y	7	negligible initial motion right (maybe due to rounded corner?) then more visible movement left
21	4	1V_3Hz	1.6	20	-0.22	0.23	Y	Y	Y	1	Potential negligible initial motion right (maybe due to rounded corner?) then more visible movement left.
22				20	-0.22	0.24	N	Y	SM	2	same as above
23				20	-0.21	0.23	Y	Y	Y	3	right movement looks distinct, mostly left movement
24				20	-0.22	0.23	Y	Y	N	4	no observation made
25				20	-0.21	0.23	Y	Y	Y	5	Potential negligible initial motion right (maybe due to rounded corner?) then more visible movement left.
26	4	1V_3Hz	1.7	20			N	N	N	1	Distinct left motion
27				20	-0.22	0.25	Y	Y	Y	2	Potential negligible initial motion right (maybe due to rounded corner?) then more visible movement left.
28				20	-0.22	0.26	N	Y	SM	3	same as above.
29	4	1V_3Hz	2	20	-0.25	0.33	N	Y	SM	1	Slow motion vid shows distinct movement right, then left. May not be affected by rounded corner anymore.
30				20	-0.23	0.33	Y	Y	Y	2	Distinct full right motion first and then mostly left.
31				20	-0.24	0.32	Y	Y	SM	3	Distinct full right motion first and then mostly left.

# of Runs	Block #	Input Profile	Scaling	Friction Angle (deg)	Acceleration of Ramp up (g)	Acceleration of Slowdown (g)	Data	Plot Pic ?	Video?	Trial #	Observations
32	4	4.5V_3Hz	0.19	20	-0.16	0.28	Y	Y	Y	1	noise in data, slight lift right, bigger lift left, but overall wobble and stable
33				20	-0.16	0.27	Y	Y	Y	2	clean data, wobble, stable
34	4	4.5V_3Hz	0.21	20	-0.17	0.32	Y	Y	Y	1	negligible lift right to more distinct lift left, potential definitive lift/topple?
35				20	-0.17	0.29	Y	Y	Y	2	less definitive lift/topple than trial 1
36				20	-0.18	0.32	Y	Y	Y	3	some noise, potential for initiation of toppling
37	4	4.5V_3Hz	0.23	20	-0.18	0.34	Y	Y	Y	1	noise, good lift right, distinct lift/topple behavior
38				20	-0.17	0.34	Y	Y	Y	2	little noise, less distinct than trial 1
39				20	-0.18	0.34	Y	Y	Y	3	slight lift right, and good lift/topple behavior left, between trials 1 and 2
40	4	4.5V_3Hz	0.25	20	-0.19	0.36	Y	Y	Y	1	a lot of noise, -0.19/-0.20, good lift right, distinct lift/topple left
41				20	-0.19	0.35	Y	Y	Y	2	clean plot, good lift right, distinct lift/topple left
42				20	-0.19	0.35	Y	Y	Y	3	clean plot, consistent with first 2 trials
43	4	1V_3Hz	1.5	46	-0.20	0.22	Y	Y	Y	1	stable
44	4	1V_3Hz	1.7	46	-0.20	0.23	Y	Y	Y	1	negligible lift right and slight lift left, no toppling
45				46	-0.20	0.24	Y	Y	Y	2	negligible lift right and slight lift left, no toppling
46	4	1V_3Hz	1.8	46	-0.23	0.28	Y	Y	Y	1	negligible lift right and slight lift left, no toppling
47				46	-0.24	0.27	Y	Y	Y	2	negligible lift right and slight lift left, no toppling
48	4	1V_3Hz	1.9	46	-0.22	0.28	Y	Y	Y	1	lift right and distinct lift left leading to toppling
49				46	-0.23	0.29	Y	Y	Y	2	lift right and distinct lift left leading to toppling
50	4	1V_3Hz	2.0	46	-0.23	0.30	Y	Y	Y	1	lift right and distinct lift left leading to toppling
51				46	-0.23	0.32	Y	Y	Y	2	lift right and distinct lift left leading to toppling

12. Appendix E: Numerical Modeling Codes: UDEC & FISH functions

A general modular code was developed for three blocks of varying dimensions and densities tested with two loading scenarios. The modeling procedure consists of 3 steps and includes data for all 3 blocks tested: step 1. Building the block model and defining material and joint properties; step 2. Setting up data recording with FISH function (FindBlocks); and step 3. Organizing data into one datafile with FISH functions (make_array). In step 3, the first loading scenario contains two methods of applying the load to the top block. Scenario 1a applies the load as a horizontal force and Scenario 1b applies the force as a horizontal component of gravity. Scenario 2 involves applying a force to the "shake table" block. Any commands that involve dimensions or refer to centroid locations of the three blocks will require changing dimensions; commands that require changes are highlighted with bold font. All FISH functions are included in section 12.2.

12.1. UDEC Model Setup

```
; Project Title:
; Block density (wood, calculated based on Block 2): p = 470kg/m3
; Block density (wood, calculated based on Block 3): p = 488kg/m3
; Block density (wood, calculated based on Block 4): p = 475kg/m3
; Shake Table density (aluminum): p = 2700kg/m3
; Shake Table dimensions: L_1.52m x UW_1m x T_0.305m
; Block # 2 size: 0.25m x 0.081m (9.81in x 3.19in)
; Block # 3 size: 0.34m x 0.083m (13.56in x 3.25in)
; Block # 4 size: 0.45m x 0.083m (17.75in x 3.25in)
; Joint Model: joint area contact - Coulomb slip
; Units: SI: m-pa-kg-s

; --- STEP 1: GENERATING BLOCKS AND JOINT MODEL PROPERTIES ---
round 0.001
block (1, 0.9) (1,1.35) (2, 1.35) (2,0.9) ; Block 2
block (1, 0.9) (1,1.44) (2, 1.44) (2,0.9) ; Block 3
block (1, 0.9) (1,1.55) (2, 1.55) (2,0.9) ; Block 4

;Joint area contact - Coulomb slip
;First define constitutive model, then define joint properties
```

;Joint properties (local properties) FRICTION = 20
set jcondf joint model area jkn=1e11 jks=1e11 jfric=20
; Block 2
;lower horizontal joint on plane
crack (1, 1)(2,1)
;left block
crack (1, 1.1) (1.46, 1.1)
;joint crack
crack (1.46, 1.1) (1.54, 1.1)
;right block
crack (1.54, 1.1) (2, 1.1)
;left vertical crack
crack (1.46, 1.1) (1.46, 1.35)
;right vertical crack
crack (1.54, 1.1) (1.54, 1.35)

; Block 3
;lower horizontal joint on plane
crack (1, 1)(2,1)
;left block
crack (1, 1.1) (1.46, 1.1)
;joint crack
crack (1.46, 1.1) (1.54, 1.1)
;right block
crack (1.54, 1.1) (2, 1.1)
;left vertical crack
crack (1.46, 1.1) (1.46, 1.44)
;right vertical crack
crack (1.54, 1.1) (1.54, 1.44)

; Block 4
;lower horizontal joint on plane
crack (1, 1)(2,1)
;left block
crack (1, 1.1) (1.46, 1.1)
;joint crack
crack (1.46, 1.1) (1.54, 1.1)
;right block
crack (1.54, 1.1) (2, 1.1)
;left vertical crack
crack (1.46, 1.1) (1.46, 1.55)
;right vertical crack
crack (1.54, 1.1) (1.54, 1.55)

;"atblock" refers to block which contains coordinates x1 y1 (centroid)
del atblock (1.2, 1.3)

```
del atblock (1.8, 1.3)
; contacts are not deleted
set delc off
; ----- end -----

; --- MATERIAL AND JOINT PROPERTIES ----
;Properties for rigid blocks, density needed (kg/m3)
;Use actual block dimensions and mass to calculate density
;Wood block density calculated to 470 kg/m3 (V=0.081x0.083x0.25m, W=787g)
prop mat=1 d=470 ; choose appropriate density listed at the beginning of this code

;Change both horizontal block properties to aluminum (p = 2700kg/m3)
prop mat=2 d=2700
change mat 2 range yrange (0.9, 1.1)

;Change joint properties between 2 horizontal blocks, FRICTION = 0
;Contact between top and shake table block remain as local properties, friction = 20
change jmat 2 range yrange (0.95, 1.05)
prop jmat 2 jkn=1e11 jks=1e11 jfric=0

;Plot block, mat prop, and mat joint to verify change in properties
;Use "print block" in console to get the properties of each block within UDEC
; ----- end -----

;Fix bottom block (added for simplicity in modeling)
fix range yrange (0.9, 1.0)

set gravity = 0.0 -9.81

;cycle model to equilibrium
Solve

; --- STEP 2: HISTORY SETUP ---
;Rigid bodies only record velocity at centroids, but do not have a history command
;Need to develop FISH function to retrieve centroid data for rigid bodies
;Below are FISH functions to save histories of velocity components at block centroid

;"block" refers to the top block
;"table" refers to the block beneath the top block
;Bottom most block used for easier modeling
```

```
def FindBlocks
        iab_block = b_near(1.5,1.23)
        iab_table = b_near(1.5,1.05)

        iab_block = b_near(1.5,1.27)
        iab_table = b_near(1.5,1.05)

        iab_block = b_near(1.5,1.325)
        iab_table = b_near(1.5,1.05)

end
FindBlocks

;Need to copy "block.fin" from Itasca folder to working folder for this to work
call block.fin

def centroid_xvel_block
        centroid_xvel_block = b_xvel(iab_block)
end
def centroid_yvel_block
        centroid_yvel_block = b_yvel(iab_block)
end
def centroid_rvel_block
        centroid_rvel_block = b_rvel(iab_block)
end

def centroid_xvel_table
        centroid_xvel_table = b_xvel(iab_table)
end
def centroid_yvel_table
        centroid_yvel_table = b_yvel(iab_table)
end
def centroid_rvel_table
        centroid_rvel_table = b_rvel(iab_table)
end

;Histories recorded and labeled in sequential order (1, 2, 3, etc)
history centroid_xvel_block
history centroid_yvel_block
history centroid_rvel_block

history centroid_xvel_table
history centroid_yvel_table
history centroid_rvel_table
```

```
        ; --- STEP 3A (Scenario 1a): LOADING TOP BLOCK ---
        ; adding damping will keep the top block from moving away from the lower block while
cycling
        damping local = 0.1

        ;fix shake table block so that only centroid loading occurs
        fix range yrange (1.0, 1.1)

        ;apply loading conditions (positive force for positive displacement)
        load xload 100 range yrange (1.22, 1.24) ; Block 2
        load xload 100 range yrange (1.26, 1.28) ; Block 3
        load xload 100 range yrange (1.324, 1.326) ; Block 4

        cycle  time 0.5

        ; -- STEP 3B (Scenario 1b): LOADING TOP BLOCK WITH GRAVITY COMMAND --
        ; adding damping will keep the top block from moving away from the lower block while
cycling
        damping local = 0.1

        ;fix shake table block so that only centroid loading occurs
        fix range yrange (1.0, 1.1)

        ;apply load with horizontal gravity component. UDEC automatically applies force at
centroid
        set gravity = 1.70 -9.81

        cycle  time 0.5

        ; --- STEP 3C (Scenario 2): LOADING BOTTOM BLOCK ---
        ;Adding damping will keep the top block from moving away from the lower block while
cycling
        damping local = 0.1

        ;Apply loading conditions (negative force for positive displacement)
        load xload -100 range yrange (1.0, 1.1)
        cycle  time 0.5

        ;Plot velocity vectors to see movement

        ; --- STEP 4: HISTORY WRITING ---
        ;NEW CODE: Write histories
        Hist write 1 vs. time skip 10 table 1
        Hist write 2 vs. time skip 10 table 2
        Hist write 3 vs. time skip 10 table 3
        Hist write 4 vs. time skip 10 table 4
```

```
Hist write 5 vs. time skip 10 table 5
Hist write 6 vs. time skip 10 table 6

;Creating one file with multiple data sets
Def make_array
  array lister(1)
end
make_array


Def out_tab
  n = table_size(1)
  ff = 'UDEC Data_Block # Bott or Top loading_ADD TRIAL RUN HERE.his'
;Filename, adjust as needed
  oo = open( ff , 1 , 1)


  ;header lines in file
  lister(1) = 'Trial # CHANGE NUMBER IN EXCEL FILE'
  oo = write(lister,1)
  lister(1) = 'columns: time hist1 hist2 hist3 hist4 hist5 hist6'
  oo = write(lister,1)


  ;Lines of data. Unclear what maximum length of the line is
  loop i (1,n)
   line = string(xtable(1,i))
   line = line+' '+string(ytable(1,i))
   line = line+' '+string(ytable(2,i))
   line = line+' '+string(ytable(3,i))
   line = line+' '+string(ytable(4,i))
   line = line+' '+string(ytable(5,i))
   line = line+' '+string(ytable(6,i))
   lister(1) = line
   oo = write(lister,1)
  end_loop
  oo = close
end
out_tab
```

12.2. FISH Functions

FISH Function Name: *FindBlocks*
Function described below tells UDEC to record velocity information and where to collect from.

```
def FindBlocks
        iab_block = b_near(1.5,1.23)
        iab_table = b_near(1.5,1.05)

        iab_block = b_near(1.5,1.27)
        iab_table = b_near(1.5,1.05)

        iab_block = b_near(1.5,1.325)
        iab_table = b_near(1.5,1.05)

end
FindBlocks

;Need to copy "block.fin" from Itasca folder to working folder for this to work
call block.fin

def centroid_xvel_block
        centroid_xvel_block = b_xvel(iab_block)
end
def centroid_yvel_block
        centroid_yvel_block = b_yvel(iab_block)
end
def centroid_rvel_block
        centroid_rvel_block = b_rvel(iab_block)
end

def centroid_xvel_table
        centroid_xvel_table = b_xvel(iab_table)
end
def centroid_yvel_table
        centroid_yvel_table = b_yvel(iab_table)
end
def centroid_rvel_table
        centroid_rvel_table = b_rvel(iab_table)
end

;Histories recorded and labeled in sequential order (1, 2, 3, etc)
history centroid_xvel_block
history centroid_yvel_block
history centroid_rvel_block
```

```
history centroid_xvel_table
history centroid_yvel_table
history centroid_rvel_table
```

FISH Function Name: *make_array*

Function described below arranges data collected from *FindBlocks* function and organizes it in a spreadsheet.

```
Def make_array
  array lister(1)
end
make_array


Def out_tab
  n = table_size(1)
  ff = 'UDEC Data_Block # Bott or Top loading_ADD TRIAL RUN HERE.his'
;Filename, adjust as needed
  oo = open( ff , 1 , 1)


  ;header lines in file
  lister(1) = 'Trial # CHANGE NUMBER IN EXCEL FILE'
  oo = write(lister,1)
  lister(1) = 'columns: time hist1 hist2 hist3 hist4 hist5 hist6'
  oo = write(lister,1)


  ;Lines of data. Unclear what maximum length of the line is
  loop i (1,n)
   line = string(xtable(1,i))
   line = line+' '+string(ytable(1,i))
   line = line+' '+string(ytable(2,i))
   line = line+' '+string(ytable(3,i))
   line = line+' '+string(ytable(4,i))
   line = line+' '+string(ytable(5,i))
   line = line+' '+string(ytable(6,i))
   lister(1) = line
   oo = write(lister,1)
  end_loop
  oo = close
end
out_tab
```

13. Appendix F: Shake Table Standard Operation Procedure (SOP)

SOP #	Shake Table 001	Revision #	A
Author	Sara Y. Magallón	Date	5/31/2019
Geological Engineering Department SOP Title: **Shake Table Manual**	Contacts: Professor Mary MacLaughlin mmaclaughlin@mtech.edu Geological Engineering MG 213B Steve Berry (Lab Technician) sberry@mtech.edu MG 004		

Revisions	Changes Made and Reasons for Changes	Initials	Date

SOP Table of Contents

1.0 SCOPE **2**

2.0 DEFINITIONS **2**

3.0 PRINCIPLES AND APPLICATIONS **4**

4.0 MATERIALS **4**

5.0 SAFETY **5**

6.0 EQUIPMENT AND CALIBRATION **7**

7.0 PROCEDURE **8**

8.0 RECORDING DATA **11**

9.0 UNCERTAINTY **13**

10.0 REFERENCES **13**

1.0 Scope

This document is a written procedure detailing the operation of the **Shake Table** located in the Mining and Geology Building, room 002 (MG002) on the Montana Tech campus.

Figure 1 – Shake Table setup in MG 002

2.0 Definitions

2.1 **Shake Table:** A device for single-axis shaking of scaled structural models, slopes or building components with a wide range of simulated ground motions, including reproductions of recorded earthquakes time-histories. To produce the shaking, the machine responds to a computer program, which inputs the shaking data and uses accelerometers to collect the output of the Shake Table. Data from the table returns to the computer allowing for further analysis.

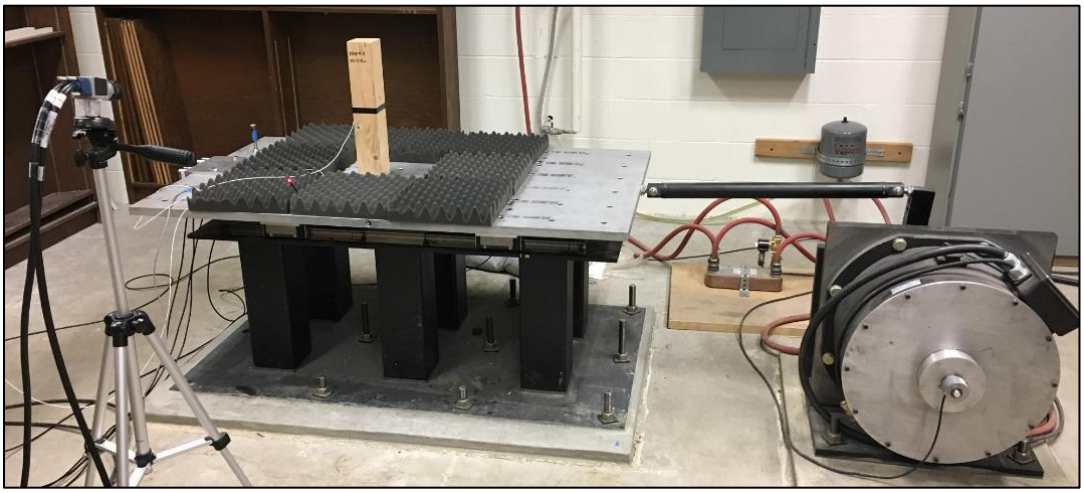

Figure 2 – Experiment setup on Shake Table

2.2 **MT Earthquake Main.vi:** A data acquisition application created with LabVIEW that automates experiments on a large vibration stage. *MT Earthquake Main.vi* acquires analog data on up to 32 channels, outputs an arbitrary waveform on one analog out

(AO) channel to the vibration system, and acquires images at 340 fps on a Basler camera. The design's core functionality involves configuring data acquisition and analog out, outputting and acquiring data, logging data to disk, and displaying data.

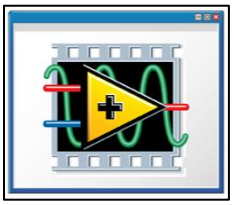

Figure 3 – Software Icon

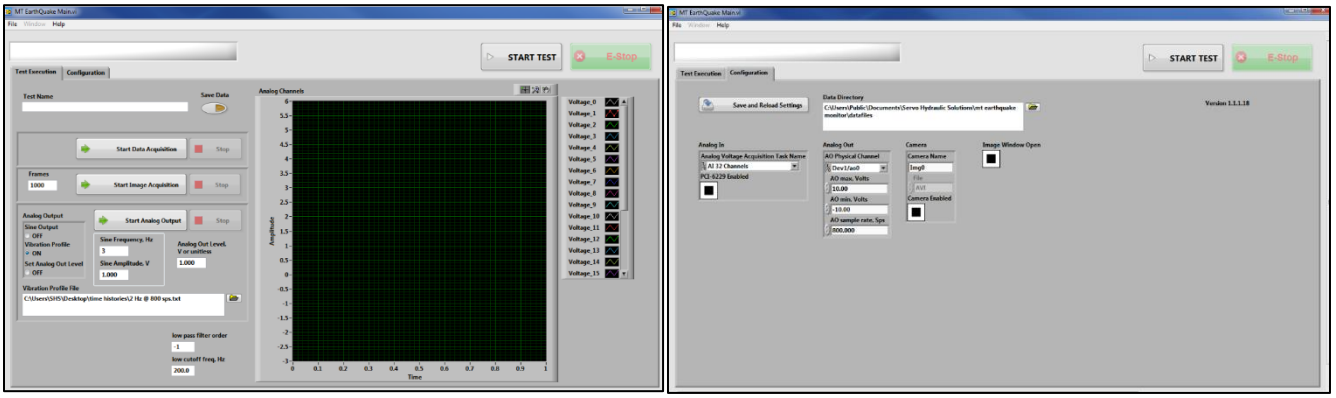

Figure 4 – Software user interface;
EQ Monitoring main screen (left) and configuration setup (right)

2.3 **DAQ System (Data Acquisition System):** The process of measuring an electrical or physical phenomenon such as voltage, current, temperature, pressure, or sound with a computer. A DAQ system consists of sensors, DAQ measurement software, and a computer with programmable software. The DAQ system associated with the Shake Table acquires data at 800 sps.

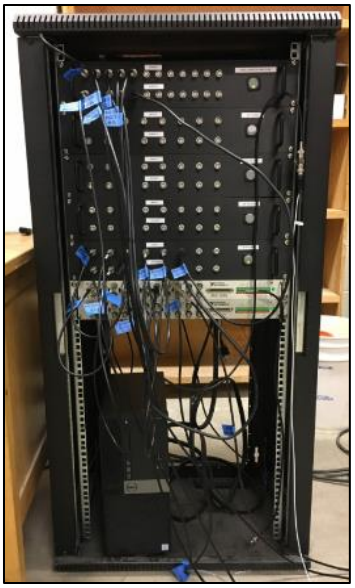

Figure 5 – DAQ system with BNC cables

2.4 **Accelerometer:** An instrument for measuring acceleration [G]. The accelerometers used in this system are piezoelectric from Dytran Instruments, Inc (https://www.dytran.com/).

3.0 Principles and Applications

3.1 Principles Section for SOP's: The basic principles of interest in the procedures include:

3.1.1 Physically starting the Shake Table,

3.1.2 Opening the *MT Earthquake Main.vi* software, and

3.1.3 Properly performing one of three available experiments with the Shake Table software.

3.2 Application Section for SOP's

3.2.1 The Shake Table can be used to replicate real-time histories of earthquakes or apply simple sinusoidal functions to determine the behavior of blocks or various structures placed on the table. In order to determine the movement of the blocks on the table, accelerometers are applied and data is collected through the DAQ system.

3.2.2 Currently, the Shake Table is only able to apply single-axis motion, but has the capability to apply bi-directional motions.

4.0 Materials

4.1 Materials Sections

4.1.1 The breaker and control panels used to turn on the Shake Table are towards the west.

4.1.2 The DAQ system and computer containing all of the hard-and software necessary for the operation of the Shake Table is located towards the southeast.

4.1.3 Accelerometers:

4.1.3.1. Dytran series 3202A2 (industrial accelerometer, 100mV/g sensitivity): https://www.dytran.com/Model-3202A-Industrial-Accelerometer-P1628/

4.1.3.2. Dytran series 3166B1 (industrial accelerometer, 500mV/g sensitivity): https://www.dytran.com/product-details.php?cid=&pid=414

4.1.3.3. Dytran series 3055D3T (general purpose accelerometer, 500mV/g sensitivity): https://www.dytran.com/Model-3055D1-General-Purpose-Accelerometer-P3230/

Figure 6 – Dytran accelerometers series 3202, 3166, and 3055 (left to right)

4.1.4 Basler acA2000 – 340kc high-speed camera

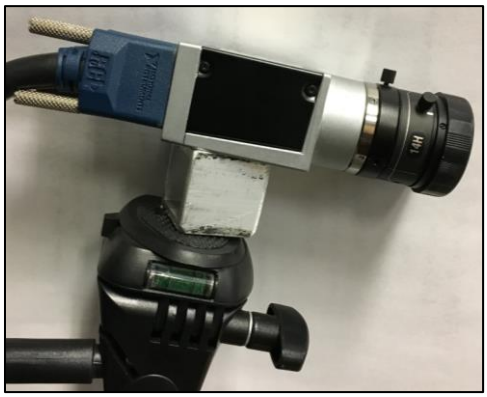

Figure 7 – High-speed camera on tripod mount

4.1.5 Prefabricated, multi-length BNC cables (black)

Figure 8 – BNC cables

4.1.6 Foam padding, egg crate style, black, 8 – 12x12 inch squares

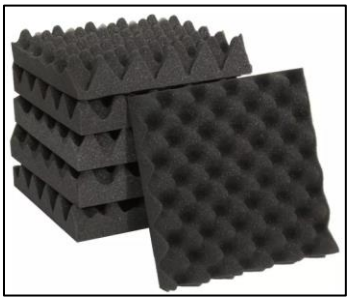

Figure 9 – Foam padding

5.0 Safety

5.1 Procedure Safety

5.1.1 Operation of the Shake Table is limited to trained personnel only.

5.1.2 Before operating the Shake Table, the surrounding area must be clear. Personnel, equipment, cables, or other objects near the moving table must be moved out of the way.

5.1.3 Perform a trial run without any objects on the Shake Table. Before starting the *MT Earthquake Main.vi* software, ensure the input parameters, vibration

profile, or scaling factors are correct to avoid chaotic motions, which can affect the performance of the Shake Table.

5.1.4 During operation of the Shake Table, the 3ft x 5ft table moves in the north-south direction. Be aware of moving parts as they can be dangerous.

5.1.5 Do not attempt to touch the table or grab any equipment on the table while it is in motion.

5.1.6 In the case of an emergency, safely stop the experiment using the stop button on the software, the E-stop on the control panel, or the red emergency stop button on the control box in the northwest corner of the room.

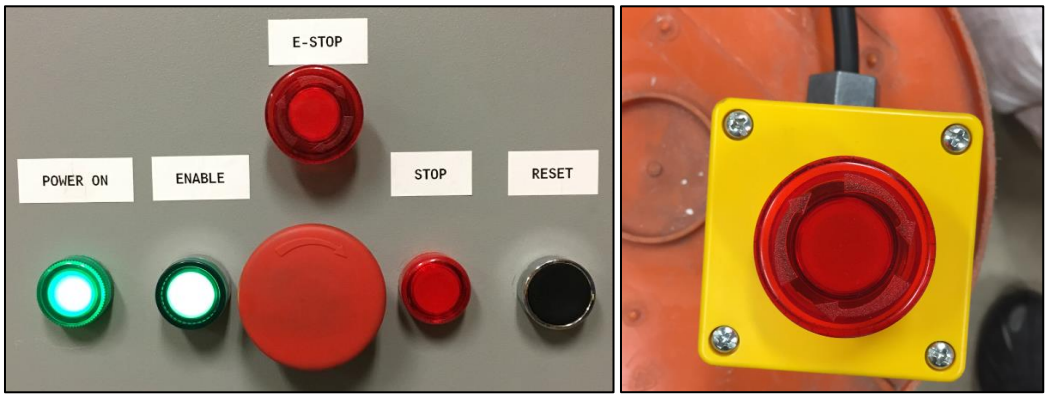

Figure 10 – Control panel buttons (left) and emergency button with 17-ft-long cable (right)

5.1.6.1. Emergency Evacuation Assembly Area 3 (west of ELC).

Figure 11 – Emergency evacuation plan

6.0 Equipment and Calibration

6.1 Equipment – Shake Table

6.1.1 3ft x 5ft x 1in thick aluminum table

6.1.2 Steel foundation with greased rollers attached to concrete block located in building crawl space

6.1.2.1. Consult with lab technician how frequently they should be greased

6.1.3 Dytran accelerometers (refer to Figure 6)

6.2 Equipment – Software: *MT Earthquake Main.vi*

6.2.1 NI PCI-6229 data acquisition board

6.2.2 NI PCIe-1433 framegrabber board

6.2.3 Basler acA2000-340kc high speed camera

6.2.4 Cabling and other external equipment as required

6.2.5 Windows 7 PC

6.2.6 NI Vision Acquisition System

6.2.7 NI Vision Module

6.3 Calibration

6.3.1 Shake Table does not have a calibration certificate from manufacturer.

6.3.1.1. Professor Peter Lucon and graduate student, Sara Magallón, conducted in-house calibration experiments (refer to excel file named: "*Shake Table Voltage to Displacement Calibration_PL_SM*" created 11/2018 and MathCAD file named: "*Shaker_Model_r01*" created 11/2018).

6.3.1.2. Calibrations have not been verified.

6.3.2 *MT Earthquake Main.vi* software does not have calibration certificate from programmer.

6.3.2.1. LabVIEW code is not available for verification of code and low/high-pass filters applied to the DAQ.

6.3.2.2. Refer to word document named "*MT Earthquake Monitor Software Design Doc"* by Chris Clark, created 4/2016 for additional information regarding the computer software.

6.3.3 Dytran accelerometers are calibrated in accordance with ISO/IEC 17025, ANSI/NCSL Z540-1-1944, ISO 10012-1 and are NIST traceable. Calibration certificates are available.

6.3.3.1. Accelerometers with S/N's 5765, 5820, and 26430 have additional low frequency calibrations, down to 2Hz.

6.3.3.2. Accelerometers do not need to be calibrated again unless they are dropped or damaged.

7.0 Procedure

7.1 Procedural Steps in the SOP

7.1.1 Turn on computer

7.1.2 Activate Shake Table by moving switch labeled “135” in Breaker Panel from left (off) to right (on)

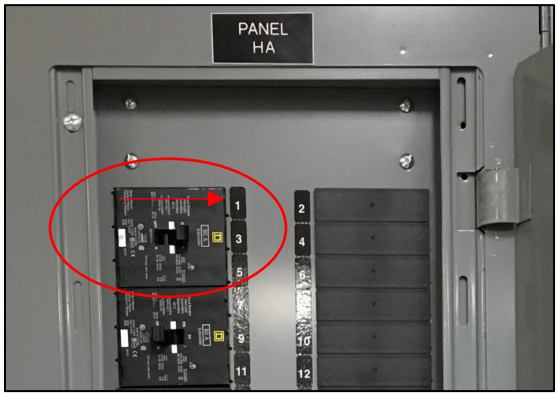

Figure 12 – Breaker panel

7.1.3 Wait about 30 seconds, then press green “Enable” button on Control Panel. A slight buzzing sound will be heard once the table has properly been activated.

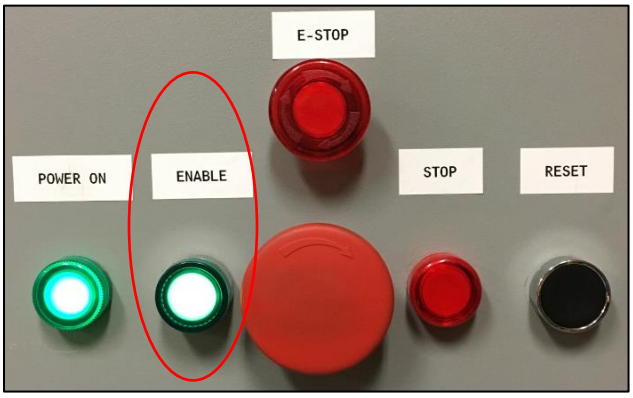

Figure 13 – Control panel

7.1.4 On PC, locate the “Earthquake Monitor_11” icon on desktop to open the Shake Table software. Older versions of the program can be found in the following location: C:\Program Files\MT EarthQuake Monitor

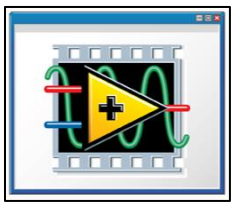

Figure 14 – Software icon

7.1.5 Two screens will open

7.1.5.1. Main screen. Hovering over various parameters may activate pop-up text explaining what it does.

Figure 15 – Main screen of software

1. Test Name: choose desired test name.
2. Frames: default 340 frames per second
3. Low pass filter order: a digital filter that indicates how steep the filter is. A value of 2 is shallow, a value of 6 is steep. There will be a smaller phase shift with shallow filters. By default use -1 which turns off the filter and is typically used with sine functions (modify when using real-time histories).
4. Low cutoff freq. Hz: digital filter, default 200, especially when using sine functions (modified when using real-time histories)
5. Sine Output: can choose input function without needing a time history
   a. Click to turn ON, then use white box parameters to develop sine wave
   b. Sine Frequency, Hz: integers only, starting at 1.
   c. Sine Amplitude, V: max +/- 10V (max displacement of table)
6. Vibration Profile:
   a. Click to turn ON, this requires the use of a "Vibration Profile File" (either one created by user or a real-time history).
   b. Vibration Profile File: navigate through this to find the profile to be implemented. ONLY ".txt" files will work with the "Vibration Profile". Make sure to convert excel files into ".txt" format.
7. Set Analog Out Level: click to turn ON, use "Analog Out Level, V" (section 8.) to manually input desired voltage. Will hold that voltage until changed.
   a. If table does not return to starting position, use this shortcut by adding 0V to return to starting position.

8. Analog Out Level, V or unitless: when using the “Set Analog Out Level” function, this will operate in voltage. When using the “Vibration Profile” function, this is a unitless scaling factor (i.e. if input vibration profile is a 1V step function, applying 2 in this box will double the voltage and create a 2V profile).
9. Save Data: click to activate yellow light, which indicates that data will be saved.
10. Start Data Acquisition: manually turn on data acquisition, will show DAQ channels on plot.
11. Start Image Acquisition: manually start camera recording.
12. Start Analog Output: manually start “Analog Output” profile
13. Start Test: starts 10 through 12 at the same time*
14. E-Stop: manually stop program
15. Voltage_#: data channels previously programmed using the NI MAX. These channels show the input function and accelerometer data. To turn off, right click and deselect “Plot Visible”.
16. X-axis: shows time
17. Y-axis: auto adjusts, shows amplitude in V and acceleration in G’s. Can lock scale from readjusting by right clicking on the y-axis and deselecting “Autoscale Y”.

* ”Start Test” does not technically start everything at the same time. Timestamp on data collected is different from timestamp on images.

7.1.5.2. Configuration screen

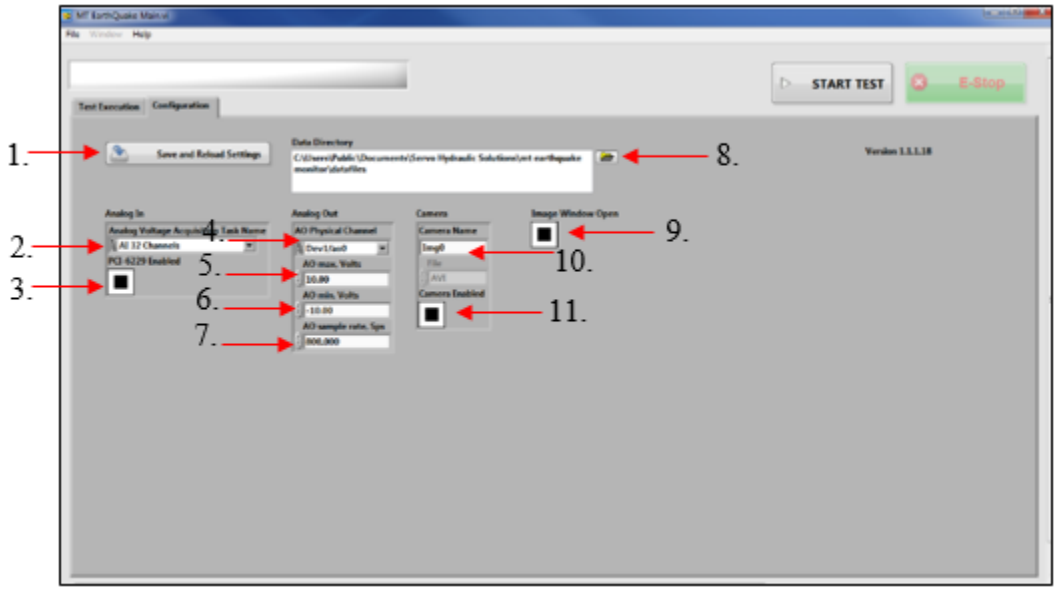

Figure 16 – Configuration screen of software

1. Save and Reload Settings: if changes are made to anything on this screen, MAKE SURE to click this button to SAVE settings. Settings will remain the same after closing program and are only changed after this button is clicked.
2. Analog Voltage Acquisition Task Name: default “AI 32 Channels”
3. PCI-6229 Enabled: default ON (with black square) to activate NI card in computer
4. AO Physical Channel: default “Dev1/ao0”
5. AO max, Volts: default 10.00, max capacity of Shake Table
6. AO min, Volts: default -10.00, min capacity of Shake Table

7. AO sample rate, Sps: default 800 samples per second
8. Data Directory: where to place data files after completing experiments.
9. Image Window Open: default ON (with black square) will open second window (white) which will show the camera recording during test.
10. Camera Name: default "Img0"
11. Camera Enabled: default OFF (no black square). The image processing takes a while so it is best to keep the camera off until the user is ready to perform a full test. When user is ready to perform full test, click on the camera box to enable (with black square) AND click "Save and Reload Settings".

7.1.6 After desired settings have been applied, profile is set, and data saving is selected, the user is ready to run the experiment.

7.1.6.1. Before running the experiment with data saving, camera enabled, and structures on the table, it is recommended that the profile be run first with a clear table and camera off to ensure the profile settings appear correct and quicker data processing.

7.1.7 When trial run is completed and real experiment is ready to execute, press "Start Test" and allow the profile to run in completion before doing anything else.

7.1.8 This concludes the experimental portion of the shake table. Data recording is explained in section 8. Once all experiments have been completed, ensure the table is at its starting position, if not use "Set Analog Out Level" shortcut (see section 7.1.5.1, part 7a).

7.1.9 To turn off Shake Table, close out of the software and turn off breaker "135" in breaker panel.

8.0 Recording Data

8.1 After completion of the procedures, a data set is recorded. The data set consists of 5 files: test name here.avi, .csv, .tdms, .tdms_index, and .avi_ (see Figure 17).

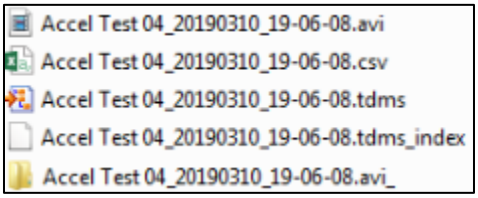

Figure 17 – Files recorded with each experiment

8.2 The default location of the data is: *C:\Users\Public\Documents\Servo Hydraulic Solutions\MT Earthquake Monitor\DataFiles*

8.2.1 Remember, the user can change the location of where data is stored, see section 7.1.5.2, step 8: "Data Directory".

8.3 File ".avi"

8.3.1 The ".avi" file is a video that is constructed from the individual pictures taken by the high-speed camera. It is a slow-motion video. After performing an experiment, most of the processing time is due to the construction of this video.

8.3.2 As previously mentioned in section 7.1.5.2, step 11, keep camera disabled until user is ready to record full test because processing time is delayed while pictures are generated and merged to complete this video.

Figure 18 – Example of video file

8.4 File ".csv"

8.4.1 An excel data file is created containing information that includes a time stamp, voltage of the input profile, and multiple columns corresponding to the various channels on the DAQ system that have accelerometers associated to them (see Figure 19). Data is recorded on all channels because noise is recorded even when the channel is not setup to receive data. Therefore, only use channels that have been properly calibrated for the attached device.

timestamp	Output To Table	LED Light	Accel 5822	Block Accel 26430	Accel 5820	Accel 5821	Accel 5765
seconds	Volts		g's	g's	g	g	g
0	0	3.9667	-0.0327	-0.0211	-0.0039	0.0014	-0.0016
0.001	0.0003	3.9667	-0.0229	-0.0175	-0.0006	0.0091	0.0014
0.002	-0.0004	3.9664	-0.0327	-0.0175	0.001	0.002	0.0017
0.003	-0.0004	3.9664	-0.0294	-0.0171	-0.0016	0.0046	-0.0006
0.004	-0.0004	3.9664	-0.0356	-0.0185	-0.0042	-0.0012	-0.0033
0.005	-0.0004	3.9667	-0.0343	-0.0221	-0.0075	-0.0064	-0.0069
0.006	-0.0007	3.9664	-0.0435	-0.0231	-0.0098	-0.0077	-0.0089

Figure 19 – Example of excel data set

8.5 File ".tdms"

8.5.1 A TDMS file is a data file saved in the National Instruments (NI) Technical Data Management Streaming (TDMS) format. It contains simulation or measurement data recorded by National Instruments software, such as LabVIEW and DIAdem.

8.5.2 To open these types of files: Use 'Open with>>Excel Importer' or double-click from Windows Explorer to open a TDM/TDMS file in Excel. Use VBA and the TDM Excel Add-In COM-API to automate loading of TDM and TDMS files into Excel (National Instruments 2019, 11.1.2).

8.6 File ".tdms_index"

8.6.1 TDMS files also automatically generate a complimentary *.tdms_index file. This file provides consolidated information on all the attributes and pointers in the bulk data file that drastically speeds up read access to the data on larger

data sets. This index file is not required for storage or distribution and automatically regenerates (National Instruments 2019, 11.1.3).

8.7 Folder ".avi_"

8.7.1 The ".avi_" folder is where all the high-speed camera photos are stored. They are titled with a timestamp, as shown in Figure 20. These are the images that are merged to make the slow-motion video.

8.7.1.1. Be aware that the timestamp of these images DO NOT match the timestamp in the excel file.

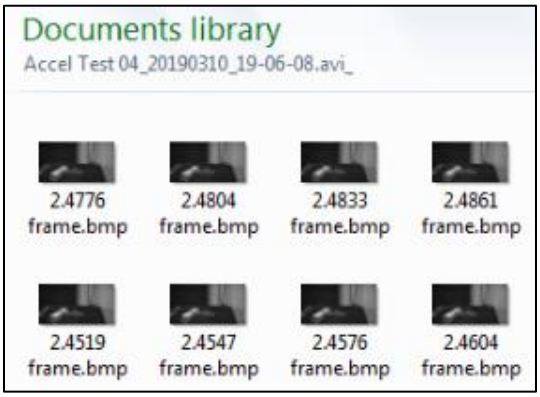

Figure 20 – Example of high-speed camera photos

9.0 Uncertainty

9.1 The Shake Table does not have proper calibration certificates from the manufacturer. All calibrations were performed in-house as best as possible. The calibrations available ONLY apply to the CURRENT setup. If any changes are made to the Shake Table system, then calibrations will no longer be valid.

9.2 The uncertainty of the Shake Table cannot be quantified. The user must be aware that all values obtained from the table should be reviewed before using in further research.

10.0 References

10.1 Reference Lists

10.1.1 Chris Clark. Bolder Software LLC. "Earthquake Monitor System Software Design". October 20, 2016.

10.1.2 National Instruments, http://www.ni.com/example/27944/en/, site accessed 5/2019.

10.1.3 National Instruments, http://www.ni.com/product-documentation/3727/en/, site accessed 5/2019.

SIGNATURE PAGE

This is to certify that the thesis prepared by Sara Magallón entitled "Investigation of the Toppling of Rectangular Rigid Blocks Using a Shake Table and Distinct Element Models" has been examined and approved for acceptance by the Department of Geoscience, Montana Technological University, on this 19th day of July, 2019.

Mary MacLaughlin, PhD, Professor
Department of Geoscience
Chair, Examination Committee

Larry Smith, PhD, Department Head
Department of Geoscience
Member, Examination Committee

Peter Lucon, PhD, Interim Department Head
Department of Mechanical Engineering
Member, Examination Committee